MOLECULAR AND SUPRAMOLECULAR SURFACE MODIFICATION TOOLS FOR HIGHLY SENSITIVE AMPEROMETRIC AND ELECTROCHEMILUMINESCENT BIOSENSORS.

Mabel Torréns del Valle

Dipòsit Legal: T 148-2015

UNIVERSITAT ROVIRA I VIRGILI
MOLECULAR AND SUPRAMOLECULAR SURFACE MODIFICATION TOOLS FOR HIGHLY SENSITIVE AMPEROMETRIC AND ELECTROCHEMILUMINESCENT BIOSENSORS.
Mabel Torréns del Valle
Dipòsit Legal: T 148-2015

Mabel Torréns del Valle

MOLECULAR AND SUPRAMOLECULAR SURFACE MODIFICATION TOOLS FOR HIGHLY SENSITIVE AMPEROMETRIC AND ELECTROCHEMILUMINESCENT BIOSENSORS

DOCTORAL THESIS

Departament d'Enginyeria Química

UNIVERSITAT ROVIRA I VIRGILI

Tarragona
2014

UNIVERSITAT ROVIRA I VIRGILI
MOLECULAR AND SUPRAMOLECULAR SURFACE MODIFICATION TOOLS FOR HIGHLY SENSITIVE AMPEROMETRIC AND ELECTROCHEMILUMINESCENT BIOSENSORS.
Mabel Torréns del Valle
Dipòsit Legal: T 148-2015

Mabel Torréns del Valle

MOLECULAR AND SUPRAMOLECULAR SURFACE MODIFICATION TOOLS FOR HIGHLY SENSITIVE AMPEROMETRIC AND ELECTROCHEMILUMINESCENT BIOSENSORS

DOCTORAL THESIS

Supervised by: Dr. Mayreli Ortiz and Ciara K. O´Sullivan

Departament d'Enginyeria Química

UNIVERSITAT ROVIRA I VIRGILI

Tarragona
2014

UNIVERSITAT ROVIRA I VIRGILI
MOLECULAR AND SUPRAMOLECULAR SURFACE MODIFICATION TOOLS FOR HIGHLY SENSITIVE AMPEROMETRIC AND ELECTROCHEMILUMINESCENT BIOSENSORS.
Mabel Torréns del Valle
Dipòsit Legal: T 148-2015

UNIVERSITAT ROVIRA I VIRGILI

Department of Chemical Engineering
Universitat Rovira i Virgili
Av. Països Catalans 26
43007 Tarragona, Spain
Tel: 977 55 96 58
Fax: 977 55 96 67

I STATE that the present study, entitled "Molecular and supramolecular surface modification tools for highly sensitive amperometric and electrochemiluminescent biosensors", presented by Mabel Torréns del Valle for the award of the degree of Doctor, has been carried out under my supervision at the Department of Chemical Engineering of this university, and that it fulfils all the requirements to be eligible for the International Doctorate Award.

Tarragona, 25th November 2014

Doctoral Thesis Supervisor/s

Dr. Ciara O'Sullivan

Dr. Mayreli Ortiz

UNIVERSITAT ROVIRA I VIRGILI
MOLECULAR AND SUPRAMOLECULAR SURFACE MODIFICATION TOOLS FOR HIGHLY SENSITIVE AMPEROMETRIC AND ELECTROCHEMILUMINESCENT BIOSENSORS.
Mabel Torréns del Valle
Dipòsit Legal: T 148-2015

UNIVERSITAT ROVIRA I VIRGILI
MOLECULAR AND SUPRAMOLECULAR SURFACE MODIFICATION TOOLS FOR HIGHLY SENSITIVE AMPEROMETRIC AND ELECTROCHEMILUMINESCENT BIOSENSORS.
Mabel Torréns del Valle
Dipòsit Legal: T 148-2015

A mi hijo, quien me inspira y me fortalece

Acknowledgments

My first and special acknowledgments should go to Dr. Mayreli Ortiz, my supervisor and friend. For her invaluable help, guidance and all her patience and love during these years. I would not have been able to complete this work without her support. For sharing all her acknowledgement with me and teaching me the value of the science every day, thanks.

My sincere gratitude to my supervisor Prof. Ciara K. O´Sullivan for accepting me in the NBG group, for encouraging me to ask the FI and for her guidance during these years.

I want also to give special thank to Prof. Alex Fragoso, for taking care of me and my work like a supervisor, for be a friend and be my English dictionary, for introducing me in his cyclodextrin world.

I want to express my gratitude to prof. Valerio Beni for agreeing to be my scientific tutor during my short stay in Linkoping and overall, for his time and support. Also, to Prof. Anthony Turner for accepting me in his research group at the Department of Physics, Chemistry and Biology (IFM), Linkoping, and for his advices during the meetings in this stay. I also always remember the support and cooperation I received from Dr. Martin Wing Cheung, Dr. Mikhail Vagin and Dr. Anders Elfwing, thanks to all of you.

I am very grateful for the FI scholarship from Generalitat de Cataluña and Multisense-Chip project, which generously provided the funds for the execution of this project.

I am very grateful to Dr. Ewelina Wajs and Dr. Vijayalakshmi Gunasekaran, these unconditionally friends that help me in all moments to finish this project.

I have also received valuable input from the all members of the NBG group specially, Mary Carmen, Sira, Tete, Bárbara, Vasso, Betul and Mary Luz. Also my gratitute to Dr. Thomas Esterle and Dr. Bruno Teixeria for their “nano-time” and support.

UNIVERSITAT ROVIRA I VIRGILI
MOLECULAR AND SUPRAMOLECULAR SURFACE MODIFICATION TOOLS FOR HIGHLY SENSITIVE AMPEROMETRIC AND ELECTROCHEMILUMINESCENT BIOSENSORS.
Mabel Torréns del Valle
Dipòsit Legal: T 148-2015

A special acknowledgements to all my Master-PhD colleagues specially Dr. Diana Garibo and Dr. Ahmed Medi who help me a lot during these last years. And, of course, our Prof. Xavier Rius, for motivating me to continue in the research field of biosensor.

Also thanks to all members of microscopy, especially to Merce Moncusí and Mariana Stefanova for dedicating a lot of their time to help me to achieve nice AFM pictures.

I should thanks Nuria Juanpere and Merche Maurin for their constant help and their so efficiently work.

In addition I would like to thanks to my great friend Dr. Neyvis Almora for her constant help during this year and the great suggestions to improve this manuscript.

Special thanks to Prof. José Luis Mola, Prof. Pedro J. Ortiz, Prof. Edilso Reguera and Prof. Martha Giamberini and my collages and friends Dr. Pedro Ortiz, Dr. Enrique Ruiz, Dr. Luis Maqueira.

I am very grateful to Dr. Ana Lilian Montero and MSc. Alejandro Álvarez, my dear friends who taught me to enjoy the purest science.

A mi tía Rosa por animarme a continuar con este proyecto y contagiarme con su entusiasmo y a Anita por su apoyo en momentos decisivos.

Agradezco a mis amados padres que me enseñaron a disfrutar del conocimiento y cada día me motivan a seguir superándome, igualmente por apoyarme y animarme en mis peores momentos. A mi hermano, por cuidarme.

Finally, I would like to thank to my husband José Luis who spent long nights checking this manuscript and sharing me ideas to improve it, who supports me and takes care of our baby in so lovely way, allowing me to focus and finish my thesis without worries, for his unconditional love.

TABLE OF CONTENTS

SUMMARY

The aim of the present Thesis is to develop different platforms based on supramolecular and covalent interactions for stable immobilisation of DNA as recognition element in order to improve the biosensor performance.

The **Chapter 1** contains a general introduction which includes a brief information of genosensors and different DNA immobilisation methods, including host-guest supramolecular interactions and covalent bonding. In addition, an overview of detection techniques used in this thesis such as amperometry and electrochemiluminescence is presented.

In **Chapter 2** the development of an enzyme linked oligonucleotide assay for the detection of a human leukocyte antigen allele associated with celiac disease based on cyclodextrin-modified polymeric surfaces is described. The surface of maleimide-pre-coated plates was modified with a layer of thiolated cyclodextrin polymer and used for the supramolecular capture of adamantane or ferrocene modified carboxymethylcellulose polymers bearing DNA probes. The assay was optimised in terms of incubation time, temperature and surface chemistry and applied to the highly sensitive and selective detection of HLA sequences. A real sample analysed using this platform showed a good correspondence with traditional maleimide activated plates.

A novel genosensor platform based on supramolecular interactions is reported in **Chapter 3**. It has been developed based on the self-assembly of bifunctionalised polymer bearing adamantane and DNA onto cyclodextrin surfaces. The surface chemistry can undergo a controlled regeneration, as revealed by SPR and impedance spectroscopy, has an excellent detection limit of 0.08 nM and demonstrated high selectivity, clearly differentiating between complementary and non-complementary DNA sequences. The performance of the developed genosensor was validated by applying it to the detection of DNA in a real patient sample that had been previously genotyped.

Chapter 4 describes a novel route for the immobilisation of an electron transfer mediator on electrode surfaces based on the interfacial complexation of a bifunctionalised carboxymethylcellulose polymer backbone bearing ferrocene units and a DNA probe on a cyclodextrin-functionalised surface. The interfacial self-assembly has been studied using

surface plasmon resonance and electrochemical techniques and the applicability of the modified surface for the construction of an amperometric genosensor was explored for the detection of a celiac disease associated allele. The supramolecular strategy simplifies the operation of the biosensor, only requiring the addition of enzyme substrate and the proximity of the mediator to the electrode surface greatly improves the detection limits attained (10 pM) with respect to a similar supramolecular system based on electrochemically inactive adamantane/CD inclusion complexes (80 pM) and requiring addition of the mediator in solution. In addition, the use of the hydrophilic CMC backbone contributes to the elimination of non-specific interactions and to an optimal spacing of the immobilised DNA probes.

Looking for more stable surfaces, a controlled, rapid and potentiostat-free method is reported in **Chapter 5** for grafting the diazonium salt (3,5-bis(4-diazophenoxy)benzoic acid tetrafluoroborate, DCOOH) on gold and carbon substrates, based on a Zn-mediated chemical dediazonation. The highly stable thin layer organic platforms obtained were characterized by cyclic voltammetry, AFM, impedance, XP and Raman spectroscopies. A dediazonation mechanism based on radical formation is proposed. Finally DCOOH was proved as a linker to an aminated electroactive probe.

This new method for grafting diazonium salts on gold and carbon surfaces was tested for tethering DNA capture probe. In **Chapter 6** the viability of using the Zn-mediated diazonium grafted surfaces for preparing surfaces for amperometric biosensors is tested. The DNA probe was linked to the grafted organic layer through a amide bond formation and a sandwich type amperometric detection was achieved. The genosensor developed using the new approach, demonstrated to have higher sensitivity and lower limit of detection in comparison with those prepared using traditional electrografting, which could be related with the more controlled manner of producing the desired thin layer in our approach.

Finally in **Chapter 7** a carbon electrode tethered ruthenium(II)-tris-bipyridine-DNA probe linked to the surface through a thin layer of diazonium salt grafted by controlled Zn mediated strategy has been tested as DNA sensor using electrochemiluminescence.

Overall, this work has contributed to the development of novel biosensing platforms exploiting supramolecular host-guest interaction and covalent binding for transducer activation. These systems showed very high performances which allow the development of new alternatives for the sensitive detection of biomolecules.

LIST OF PUBLICATIONS.

1) M. Ortiz, **M. Torréns**, N. Alakulppi, L. Strömbom, A. Fragoso, C. K. O'Sullivan. *Amperometric supramolecular genosensor self-assembled on cyclodextrin-modified surfaces.* Electrochem Comm, 2011, 13, 578-581.

2) M. Ortiz, **M. Torréns**, N. Canela, A. Fragoso, and C. K. O'Sullivan. *Supramolecular confinement of polymeric electron transfer mediator on gold surface for picomolar detection of DNA.* Soft Matter , 2011, 7, 10925-10932.

3) M. Ortiz, **M. Torréns**, A. Fragoso, and C. K. O'Sullivan. *Highly sensitive colorimetric enzyme-linked oligonucleotide assay based on cyclodextrin-modified polymeric surfaces.* Anal .Bioanal. Chem, 2012, 403, 195-202.

4) **M. Torréns**, M. Ortiz, A. P. F. Turner, V. Beni, and C. K. O'Sullivan. *Controlled Zn-mediated grafting of thin layers of bipodal diazonium salt on gold and carbon substrates.* Chem. Eur. J. , 2014. DOI: 10.1002/chem.201405121

5) **M. Torréns**, M. Ortiz, A. P. F. Turner, V. Beni, and C. K. O'Sullivan. *Amperometric detection of Francisella tularensis genomic sequence on Zn-mediated diazonium modified substrates*. (submitted) 2014.

6) **M. Torréns**, M. Ortiz, D. Bejarano and C. K. O'Sullivan. *Electrochemiluminescent DNA sensor based on controlled Zn-mediated grafting of diazonium precursors.* (submitted) 2014.

LIST OF FIGURE CAPTIONS

CHAPTER 1

CHAPTER 2

CHAPTER 4

CHAPTER 5

CHAPTER 7

LIST OF ABBREVIATIONS

- A: Adenine
- Ada: Adamantane
- AFM: Atomic Force Microscopy
- C: Cytosine
- CDs: Cyclodextrin
- CV: Cyclic voltammetry
- DNA: Deoxyribonucleic acid
- DPV: Differential pulse voltammetry
- dsDNA: Double strand DNA
- EC: Electrochemistry
- ECL: Electrochemiluminescence
- EDC: N-Ethyl-N'-3 Dimethylaminopropyl Carbodiimide
- EIS: Electrochemical impedance spectroscopy
- Fc: Ferrocene
- FTIR: Fourier transform infrared spectroscopy
- G: Guanine.
- i: Current peak
- LOD: Limit of detection
- MALDI-TOF: Matrix-Assisted Laser Desorption/Ionisation-Time-Of-Flight
- NHS: N-hydroxy succinimide
- NMR: Nuclear magnetic resonance
- PBS: Phosphate buffer saline
- PCR: Polymerase chain reaction
- Pt: Platinum wire, counter electrode
- Rct: Charge transfer resistance
- RU: Resonance unites.
- Rubpy: Ruthenium (II) tris-bipyridine N-hydroxysuccinimide
- SAM: Self assembly monolayer
- SPR: Surface plasmon resonance
- ssDNA: Single strand DNA
- T: Thymine
- Tm: Melting temperature.
- TMB: Tetramethylbenzidine
- TPA: Tripropylamine
- XPS: X-ray photoelectron spectroscopy

CHAPTER 1

GENERAL INTRODUCTION

CHAPTER 1

GENERAL INTRODUCTION

1.1 PRINCIPLE OF BIOSENSOR

Since 1987, when the first personal glucose-meter was commercialised,[1] the quality of life of diabetic patients changed radically. As a consequence of the construction of this sensor and the subsequent updates, patients have the possibility of a continuous control of the glucose level with a more adequate and personalised management of the disease.[2]

The Era of biosensors began in 1962 when Clark revealed the possibility of the construction of an electrochemical sensor using glucose oxidase enclosed in a membrane.[3,4] Since this first report many biosensor definitions have been used[5] and in 1992 the IUPAC gave a general definition of biosensor as *"a device that uses specific biochemical reactions mediated by isolated enzymes, immunosystems, tissues, organelles or whole cells to detect chemical compounds usually by electrical, thermal or optical signals"*.[6] Recently, Turner described them as *"analytical devices incorporating a biological sensing element. They harness the exquisite sensitivity and specificity of biology in conjunction with physicochemical transducers to deliver complex bioanalytical measurements with simple, easy-to-use formats."* [7] **Figure 1.1** is a graphic summary of the concept of biosensor.

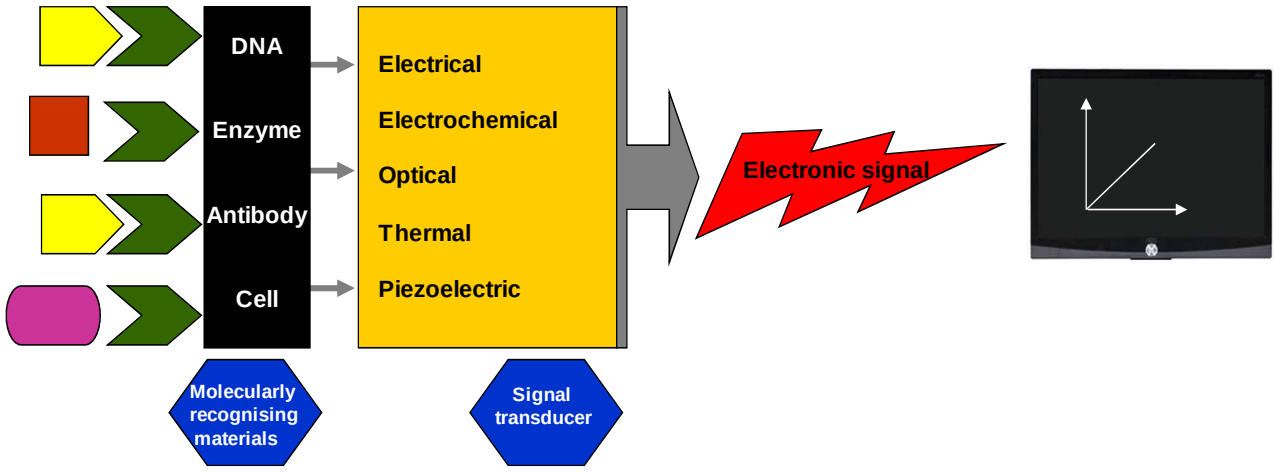

Figure 1.1. Biosensor configuration

The biological sensing elements (bioreceptor) include organelles, tissues, cell receptors, microorganisms, enzymes, antibodies or antigens, nucleic acids, etc.[8] In general a biosensor, which presents one of these two latter bioreceptors, are classified as immunosensors and genosensors, respectively.

In the construction of efficient biosensors the design of a robust sensing platform and the detection method are critical, different immobilisation methods including physical adsorption,[9] host-guest interactions[10] or covalent bonding[11] have been developed coupled with detection techniques such as electrochemical,[12] piezoelectric,[13] gravimetric,[14] optical,[15] depending on the system under study.

Many alternatives for the combination of bioreceptors and detection methods have been published for clinical applications such as the screening or early detection of diseases,[16] for monitoring food production and food poisioning,[17] for the detection of biological warfares including *Bacillus anthracis*[18] or *Francisella tularensis,*[19] and many others.

1.2 GENOSENSORS

When the biorecognition element used in the biosensor is a DNA probe, it is usually called genosensor, and the knowledge about the intrinsic characteristics of DNA is crucial in genosensor development.

The polymeric structure of the DNA molecule, called a polynucleotide is formed by the linking of four monomers (nucleotides). These nucleotides consist of a backbone comprising a unit of deoxyribose sugar, a phosphate group with rhe genetic information provided by the nitrogenated bases, adenine (A), guanine (G), cytosine (C) or thymine (T), with A and G being purine derivatives whilst C and T are pyrimidine derivatives (**Figure 1.2**).

As can be seen in **Figure 1.2,** the formation of the DNA structure is due to the linking of the nucleotides via phosphodiester bonds where the phosphate group is shared between two sugars. The presence of the OH groups in the carbon 3´ and 5´ facilitates the connection of monomers until the formation of a polymer of *n* units.

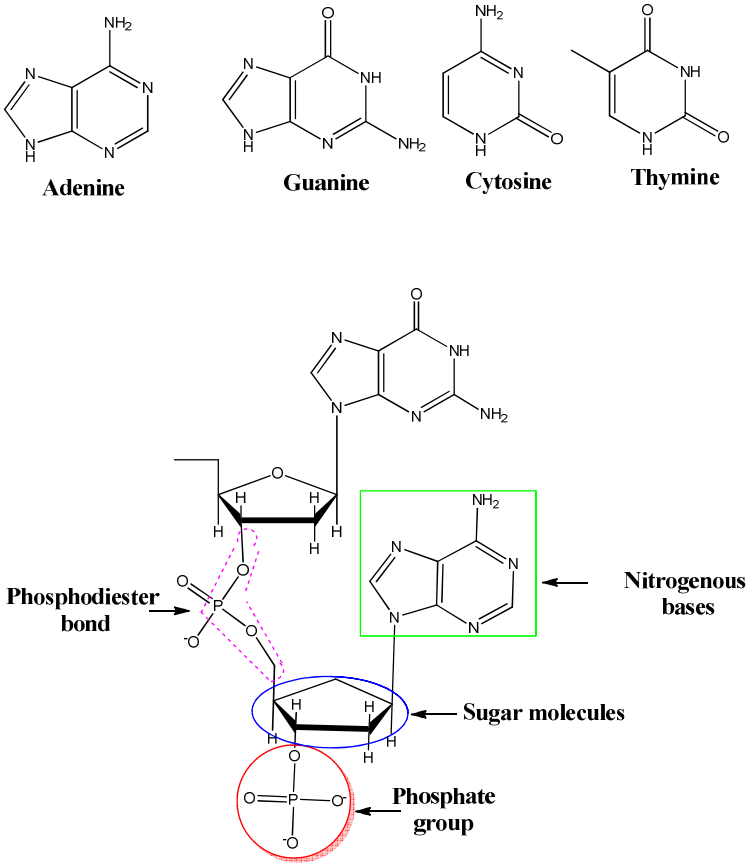

Figure 1.2. Basic components and structure of DNA

The Chargaff ratio exposing the equal percent of A with respect to T and C with respect to G, combined with the X-ray diffraction analysis resulted in the elucidation of the DNA double-helix model in 1953. In this structure two single strands of DNA are bound via hydrogen bonds between the A-T and C-G bases. The high specificity of these interactions is explained by the linking of pyrimidine (one ring) and purine (two rings) presenting lower steric hindrance, avoiding the separation of the helix, and the second factor is the formation of the three and two hydrogen bonds between the C and G and A and T bases respectively. Furthermore the hydrophobic interaction between the neighboring bases provides stability to the double stranded DNA.[20, 21]

From the biological point of view, DNA contains the genetic information of living organisms. The coding part of the information included in the genes, are transcribed and translated to produce RNA molecules and proteins.[20] A mistake in the genes, a mutation, results in diseases such as phenylketonuria, cystic fibrosis, sickle cell anaemia, cardiomyopathy and celiac disease.

DNA detection allows to obtain relevant information about the genetic disorders,[22] genetic modified organisms[23] or the presence of microorganisms.[24] DNA analysis has been greatly facilitated using PCR, a simple method proposed by Mullis,[25] to amplify the quantities of DNA.[26] However PCR requires costly equipment, special reagents and in addition is a multistep technique.[27] Thus, the necessity for a sensitive, rapid, reliable and inexpensive alternative for DNA analysis led to the development of genosensors. As said previously, genosensors are affinity biosensors consisting of a nucleic acid recognition layer (probe) immobilised over a signal transducer. This probe is responsible for the selectivity of the sensor, while the transducer modification strategy influences the sensitivity and eliminates non-specific binding. For this reason the construction of an efficient platform for the immobilisation of the probe has been widely studied and different systems have been reported.[28,29]

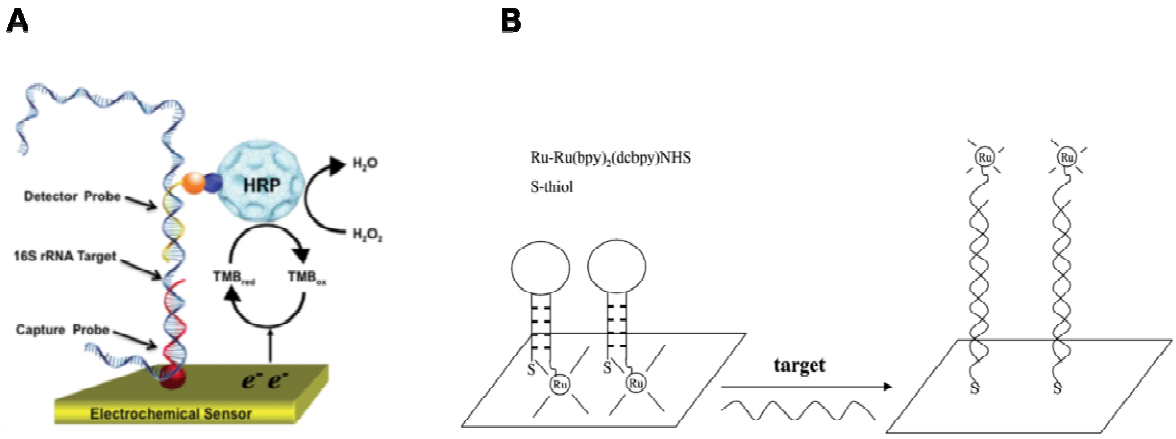

Figure 1.3. Schematic representations of: (A) electrochemical biosensor detection of nucleic acids [31.] and (B) hairpin-DNA probe detection for DNA hybridisation using ECL.[32]

A wide number of reported genosensors exploit the sandwich type detection of a DNA target, which has two regions that can hybridise with a "capture" probe, used for confining to the biosensor surface, and a secondary labelled probe, used for detection (**Figure 1.3**). A widely used label linked to the secondary probe is the enzyme horseradish peroxidase (HRP). Its' wide use is due to efficient electron transfer between the HRP and the electrode, as well as its' commercial availability and high purity.[30] In the case of electrochemiluniscence (ECL), the most common label is the ruthenium(II) *tris*-bipyridine-*N*-hydroxysuccinimide (Rubpy) due to its' strong luminescence, reversible one-electron transfer reaction under non extreme potential and solubility in both, organic and aqueous media.

In addition, the direct detection of DNA target without using any secondary probe can also be achieved using surface plasmon resonance, chronocoulometry and impedance spectroscopy.

DNA immobilisation methods

The relevance of surface engineering for the biosensor development is unquestionable. The adequate modification of the transducer is the first point for guaranteeing subsequent efficiency of the detection.

Different surfaces can be functionalised with a large number of receptor molecules. The coupling on surfaces can exploit not only covalent bonding,[33] for instance, via reversible –S–S– bridge formation, but also metal coordination. The formation of self-assembled monolayers (SAMs) of thiols on gold is one of the more used approaches because of its simplicity and versatility.[34] In SAMs, each chain of alkylthiol is arranged in parallel with the neighbouring chain in the most stable "*trans*" configuration and the stability of Au-S increases in 0.1 eV per carbon atom of the thiol.[33] The formation of SAMs can be optimised by finding the optimal pH and concentration of the thiol and the length of time of its interaction with the surface.[34]

Nowadays, there are commercially available derivatised DNAs suitable for immobilisation on surfaces and the pH used is around 7.4 in water. In the case of DNA sensors, the accessibility of the target to the capture probe immobilised on the surface is crucial and creating the proper spacing between tethered DNA for the further DNA target hybridisation is highly desirable. Two of the more common methods for spacing the DNA molecules in the surface include co-immobilising both the DNA and the spacer-small alkyl thiol molecule in one step, and the two step strategy where firstly the DNA is immobilised and then a short length thiol is used as backfilling.[34]

In addition to SAMs created by Au-S bonding, electrostatic interactions, hydrogen bonding,[35] cyclodextrin host–guest complexation,[36] or the well-known biotin–streptavidin complexes[37] constitute examples of the DNA immobilisation on surfaces. In general, the non-covalent bonding has the advantage of controllable molecular recognition abilities with the possibility for error correction.[38]

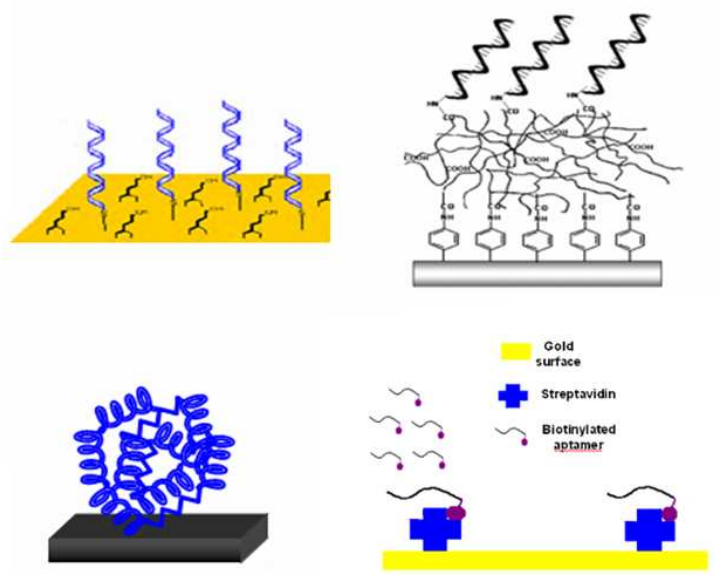

Figure 1.4 Immobilisation methods of biomolecules. [33b, 34e, 37]

Supramolecular Chemistry. Applications of Supramolecular Chemistry for biosensor platform development

The possibilities of supramolecular chemistry as a tool used in the development of nanotechnology may revolutionise our lives in the near future. For example, metal-organic frameworks (MOFs) and porous materials can selectively bind many small molecules by noncovalent forces and have gained attention, for instance, for the separation, storage, and release of gases.[39,40]

Supramolecular interactions[41,42] have recently attracted great interest as surface modification tools.[43,44] These strategies are based on self-assembly and host-guest interactions in order to achieve pre-organisation and improved functional properties of these assemblies. Among many of the existing natural and synthetic macrocyclic structures, cyclodextrins and calixarenes have been the most studied hosts for this purpose (**Figure 1.5**).[43,45]

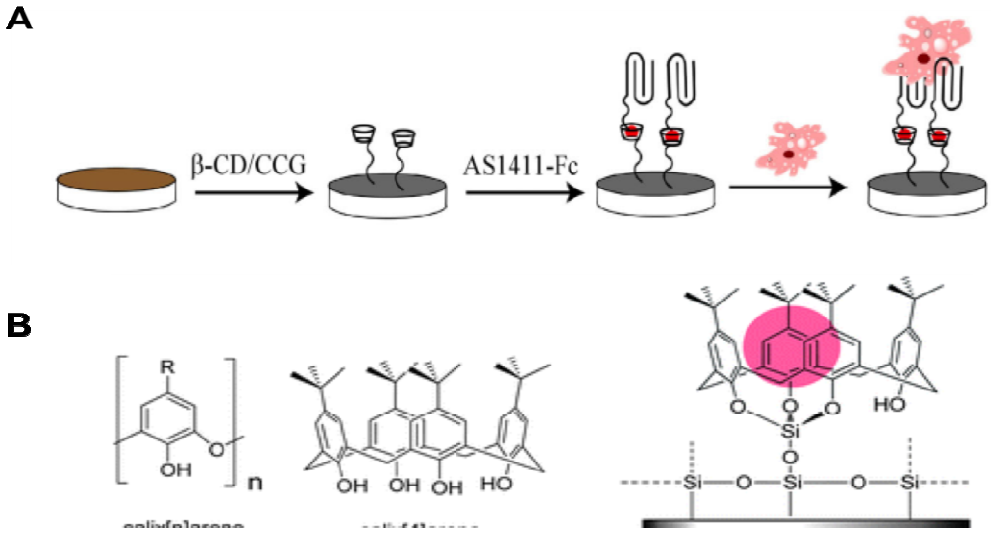

Figure 1.5. Surface modification using (A) CDs [46] and (B) calixarene.[47,48]

Cyclodextrins: Structure and properties

Cyclodextrins (CD) are cyclic oligosaccharides obtained from the degradation of starch and are composed of D-glucopyranose units attached by α-1,4-glucosidic linkage containing 6, 7, or 8 glucose units and are called α-, β-, γ-cyclodextrin, respectively. The cyclodextrin shape is similar to a truncated cone, with a cavity diameter in the range of 0.44 - 0.83 nm (α-CD: 0.49 nm, β-CD: 0.62 nm, γ-CD: 0.83 nm).

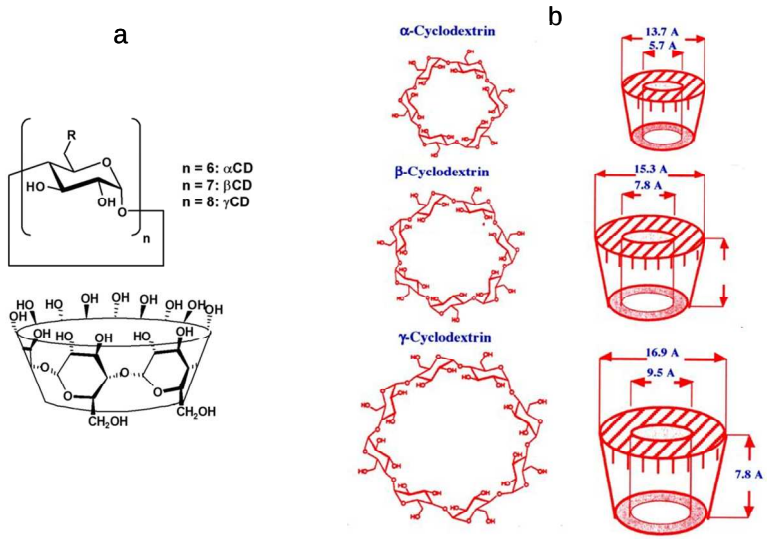

Figure 1.6. Structure of cyclodextrin (a) and molecular structure of α,β and γ CDs (b).[49]

The cavity is lined C-H groups and thus presents a hydrophobic character, which combined with the presence of hydroxyl groups located in the borders of the cavity makes these unique molecules perfect candidates for the formation of inclusion complexes via electrostatic, hydrophobic and van der Waals interactions in an aqueous environment via host-guest interaction.[50,51]

Host-guest interaction is mainly observed in inclusion complex formation, where the host is the cyclodextrin, that presents a large cavity and the guest normally is a molecule able to fit in the CD cavity (**Figure 1.6**). The stability of this complex depends on the shape, volume, polarity, number and character of substituting groups of the guest, as well as the reaction medium, temperature, ionic strength and other factors.[52]

Adamantane and ferrocene are among the more commonly used hosts for βCDs (**Figure 1.6**). The β-cyclodextrin-adamantane inclusion complex, with the highest association constant (10^5-10^6 M^{-1}) has been widely reported for supramolecular constructions.[44] However, the inclusion complexes of βCD with ferrocene also have high values of stability constants ($K = 10^4$ M^{-1}), having the added value or being electroactive, which has been used for interesting electrochemical detection approaches.

Cyclodextrin-based biosensors

Inclusion complexes can be used not only to create interesting tridimensional supramolecular architectures, but also for immobilising the biomolecules on the surface **Figure 1.7**.

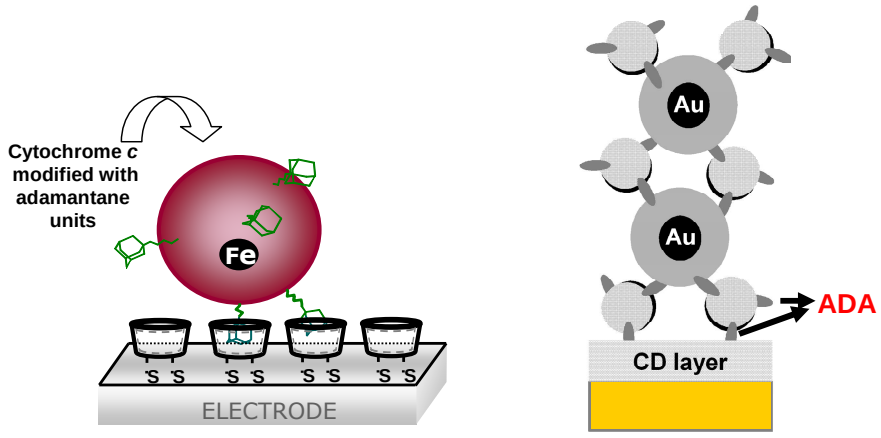

Figure 1.7. Example of platform based on host-guest interaction.[36, 53]

An interesting electrochemical label-free and 'signal-on' method for DNA detection was reported by Aoki et al[54] using a carbon-based inter-digitated array microelectrode chip. DNA probe was functionalised at both ends: β-CD was attached at the 3' end while a ferrocene unit was attached at the 5' terminus. Based on the flexibility of the single strand form, the inclusion of Fc on the β-CD attached on the other end of the probe was proposed, which shifts the Fc/Fc^+ potential to positive values and lowers the current values due to encapsulation in the CD cavity. After hybridisation a signal-on response was obtained due to the rigid structure of the double-strand that breaks the inclusion complex, shifting the redox potential towards a more negative potential (-62 mV) and the observed current at 0.3 V was increased 5.2-fold. On the other hand, Sato et al. proposed a supramolecular system based on a complex formation by ferrocenyl-β-CD and adamantylnaphthalene diimide bound to double stranded DNA.[55]

The inclusion complexation of cyclodextrins has been used to detect DNA. CdSe quantum dots modified by mercapto-β-CD were recently reported for the fluorescent detection of DNA. Firstly, fluorescence of CdSe nanoparticles was quenched by inclusion of phenanthroline inside β-CD cavities. In the presence of double stranded DNA, the included phenanthroline molecule is released from the nanoparticle restoring the fluorescence due to its higher tendency to intercalate in the DNA double helix with a binding constant of 1.33×10^7 M^{-1} which is two orders of magnitude than the binding constant of the β-CD/phenanthroline complex.[56]

Therefore, molecular sensor design is an active field in supramolecular chemistry.[57] Sensing applications rely on exploiting the forces involved in the formation of non-covalent host-guest complexes; the more complementary the binding sites of the host to those of the guest, the higher the binding energy. Molecular recognition is still a challenging topic nowadays, and many efforts have been devoted to the development of supramolecular sensors able to selectively detect analytes of chemical or biological significance. This fascinating field exploits the recognition abilities of supramolecular receptors to yield analytical tools characterized by high sensitivity, specificity, and selectivity.

In the field of biosensors, the improvements in reproducibility, calibration, and manufacturability are still some of the challenges for developing reliable devices,[58] and the

field of supramolecular analytical chemistry opens up new molecular designs and approaches for the use of synthetic receptors in analytical sciences.[40]

Diazonium salts

Diazonium salt are organic compounds in which one or more diazo groups ($-N_2^+$) are linked covalently to alkyl or aryl groups (**Figure 1.8**).[59] Aromatic diazonium salts are more commonly used since they may have other functional groups that supply a linking point for reaction with different molecules or surfaces.

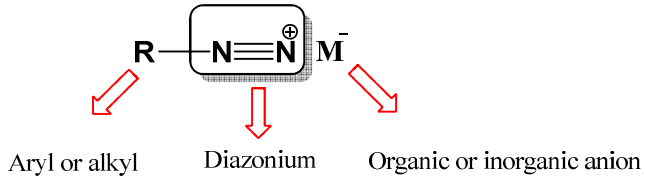

Figure 1.8. General representation of the diazonium salt.

The salts are obtained from the reaction of nitrous acid (HNO_2) with a primary aromatic amine in the presence of mineral acid. It is important to consider that the presence of the nitrous acid is essential to obtain the diazo group ($-N_2^+$) but the instability of this molecule, in many cases, hinders the yield of the reaction. Thus, to avoid the decomposition of HNO_2 and improve the diazonium production, the temperature is adjusted between 0 and 5 ºC and the preparation of the acid is carried out *in situ* by the reaction of a mineral acid and a nitrite salt.

In general 3 molar equivalents of the mineral acid per equivalent of amine are used: one equivalent is using to achieve amine protonation, the second for nitrosonium ion formation and the last one to avoid, in the early stage of the reaction, the coupling of the diazonium with a non-protonated amine. The result is the substitution of the hydrogen of the amine by the nitrosonium ion and the formation of the diazonium salt. (**Figure 1.9**)

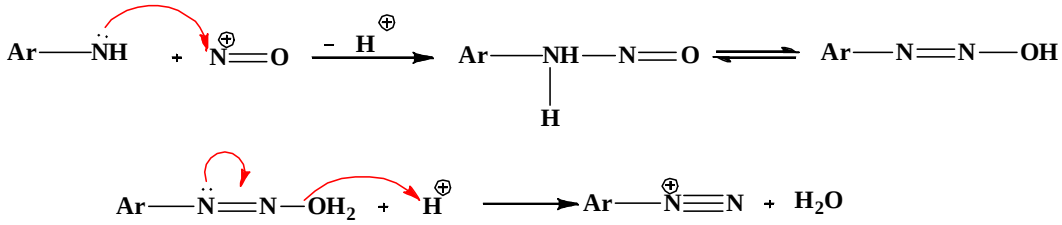

Figure 1.9. Synthesis of diazonium salt.

However the quantities of this ion are adequate for this mechanism only when concentrated acid is used, in the case of strong but diluted acid it has been reported that the diazotation proceeds via amine and N_2O_3 reaction (**Figure 1.10**) [60]

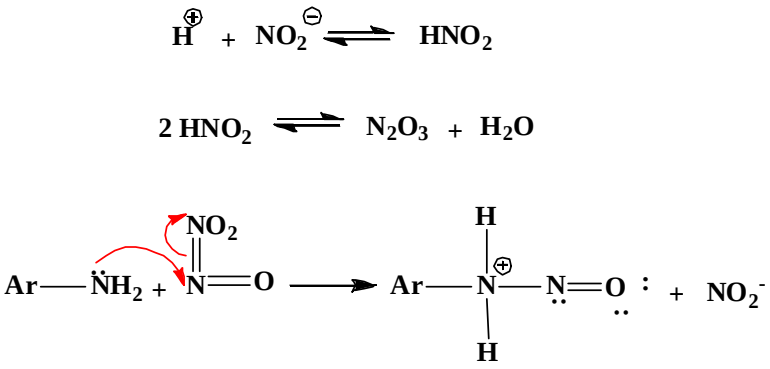

Figure 1.10. Synthesis of diazonium salt using diluted acid.

Regarding stability, the resonance contribution of the aromatic rings makes aryl diazonium more stable with respect to the alkyl ones, which cannot be isolated due to it instability. Although the nature of the aromatic substituents in combination with the counter-anions have significant influence on the isolation of stable diazonium salts.[59] To date the best anions reported are fluoroborate,[61] tosylate[62] or disulfonimide.[63] In addition, if the salt is in solution, the use of aqueous acidic medium or aprotic non-nucleophilic solvents and acidic pH, lower than 3, are the optimum conditions to maintain the diazonium in solution since pH higher or equal to 7 stimulates the formation of the diazohydroxides and diazoates.[64]

The preparation of many diazonium salts is feasible due to the high variety of commercial amines. Many of these diazonium salts are involved in a plethora of reactions and one of them is azo coupling from aromatic amines or phenols due to the electrophilic character of the azo groups, another example are the substitution reactions, where the azo group is replaced by different nucleophiles including F^-, CN^- or Cl^-.[65]

Finally the high stability of the leaving group N_2 also facilitates the formation of aryl radical or carbocations that are able to interact with different surfaces.

Diazonium salt and surface modification

Despite the tendency to modify surfaces using thiol moieties, the poor long term stability due to the easy oxidation of thiol, the narrow working potential window, in the range -1 V to +1 V (vs SCE), and the lower bonding energy of S-Au with respect to the C-C bond has led to the use of diazoniums as an alternative for the development of a stable surface based on covalent bonding.[66] This system offers the advantage of facile preparation, rapid reduction and the possibility of the introduction of different functional groups.[66]

Pinson was the first to detail the electrochemical grafting of diazonium on carbon surfaces.[67] Subsequently, this strategy has been exploited in sensors detection of proteins, cofactors, enzymes, DNA, etc. The steps involved in this process include the reduction of diazonium salt in aprotic or aqueous acidic medium via application of potential of the voltammetric peak of diazonium for a period of time using cyclic voltammetry (CV) or via electrolysis.[68] The reduction potential of diazonium is relatively low due to the stability of the leaving N_2 molecule.

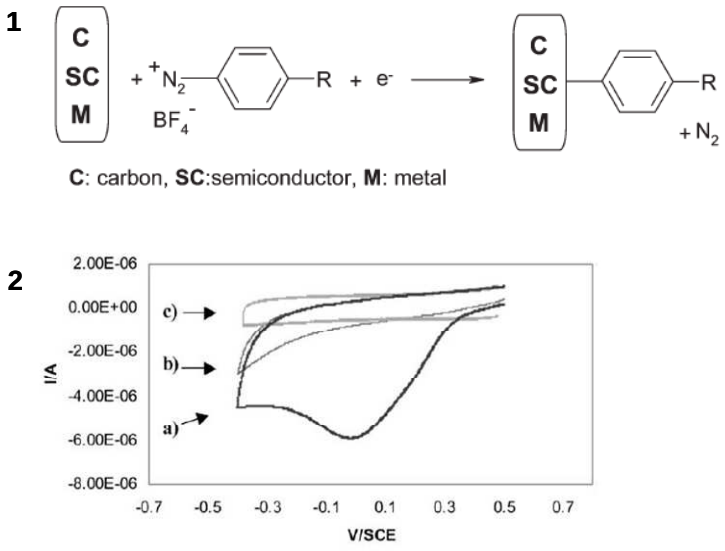

Figure 1.11. Modification of surfaces by electrochemical reduction of diazonium salts (1) and CV of the reduction of diazonium salt, a) first and b) second scan and c) the same electrode in ACN + 0.1 M NBu_4BF_4. (2)[69]

Thus, the typical voltammogram during the electrografting shows an irreversible reduction peak around 0 V attributed to the cleavage of N_2 group that is related with the electron transfer reaction. This one-electron wave almost disappears after the second cycle and it is associated with the almost complete blocking of the electrode surface. The proposed immobilisation mechanism is based on the formation of highly reactive radicals, observed by ESR, which react with the surface but also with the molecules already immobilised. Taking into account the easier reduction of this species, special attention to the potential range chosen is needed, because the modification of surfaces is highly affected when other reduction products are present. As a consequence of the presence of these free radicals the formation of layers with different thickness has been reported, from monolayers to multilayers. This grafted surfaces been widely investigated using different techniques such as electrochemistry, AFM, X-ray reflectivity.[64] The use of reducing agents including hypophosphorous acid or iron powder for reduction of the N_2 group has also been reported for the formation of multilayers. The multilayer formation has been used for the preparation of lithium batteries and the development of supercapacitor electrodes.[69] However, in the case of biosensors this multilayer formation can be a drawback, although some studies reported the presence of pinholes in the layers that allow electron transfer from the surface, it has also been demonstrated that above a certain thickness, is hindered. Hence a monolayer or layers close to monolayer are highly desired to obtain higher electron transferring that can result in a good biosensor performances.[68]

Some interesting alternatives to obtain these structures are the reduction of diazo group controlling the charge consuming during the electrochemical process or via ultrasonic, heating and microwave methods. Furthermore, the immobilisation of diazonium on reductive surface is an attractive and simple method. On these surfaces the grafting process was in agreement with the redox reaction ($E_{OCP}(Zn) < E_{OCP}(Fe) < E_{OCP}(Ni)$) demonstrating that both the metal surface and the diazonium salt are involved in the mechanism.[64]

In addition, spontaneous reduction of nitrogen group is also reported to form monolayers. Moreover parameters as concentration, reaction time or the presence of diazoniums salts with sterical hindered are reported to have influence in the final layers structures.[64] Finally, added to the stability of the diazonium derivatives on surfaces and the possibility to activate it with a great number of functional groups to link biomolecules to the surfaces, this immobilisation strategy can be used to modify carbon or metallic surfaces to construct biosensors.

Detection methods

Some examples of molecular sensors include colorimetric sensors that have the advantage of allowing simple on-site real-time detection without instruments, luminiscence-based sensors which offer significant advantages such as high sensitivity,[70] and electrochemical sensors which provide low detection limits, a wide linear response range, simple instrumentation and good stability and reproducibility.[71] Depending on the sensing mechanism, electrochemical sensors can be classified as potentiometric, conductometric, voltammetric and amperometric.[8]

Amperometric biosensors

Amperometric biosensors belong to a class of the most widespread, numerous and successfully commercialised devices of biomolecular electronics. In amperometry, a constant applied potential value between a working electrode and a reference electrode is applied and the response is recorded in terms of absolute current or current density in the electrochemical cell. This applied potential promotes a redox reaction, which produces a current.[72] The current density, defined as the ratio between current and electrode area, is a function of the presence in the solution of electrochemically active species, whose oxidation or reduction takes place on the surface of a working electrode, proportional to its concentration. During measurement the working electrode may act either as an anode or cathode depending on the nature of the substance measured and the voltage value applied.[73]

Amperometric biosensors can be divided into three main classes:

1- Amperometric mediatorless biosensors - they are based on measurement of concentration of substrates or products directly involved in an enzyme reaction. In the reaction process always some products are generated and some substrates are consumed. If they are electroactive, their concentration can be measured directly. These reactions are usually catalysed by various oxidases, which constitute the most commonly used enzymes in amperometric biosensors. Some examples of oxidases applied in these biosensors are: peroxidases, glucose oxidase, lactate oxidase, choline oxidase, alcohol oxidase, glutamate oxidase, or xantine oxidase, etc.[72]

Several amperometric biosensors are based on monitoring oxygen consumption or detection of hydrogen-peroxide formation. Both are electrochemically active, oxygen can be electrochemically reduced and hydrogen peroxide can be oxidised and the current generated is proportional to the concentration of the enzyme substrate present in the sample.[73] The other enzymes used in amperometric biosensors are dehydrogenases or hydrolytic enzymes.

2- Amperometric mediated biosensors – these devices use mediators (alternative -oxidising agents) as electron carriers. Mediators have the advantage of requiring low applied potentials and therefore the interference of oxygen (in the case of oxidases) and of different interferents on the response decreases dramatically. These mediators are low-molecular weight molecules, which transfer electrons between redox centre of the enzyme and working electrode, for example:

Mediators can be categorised as a natural or artificial electron carriers. For instance, the natural mediators are: cytochrome a_3, b, c_3, ubiquinone, vitamin K_2, flavoproteins or ferredoxin, etc. Yet, the artificial electron carriers may be as follow: ferricyanide (hexacyanoferrate III), 2,6-dichlorophenol, ferrocene, methylene blue, benzyl violet, hydroquinone, catecols etc. From all of them, the ferricyanide and ferrocene are the most common and well – known.

There are two ways to employ a mediator for the measurement, either by adding it to a measuring solution or via immobilisation on the electrode surface. The first method is easier but has less applicability in packed devices. What is more, organic colorants such as methylene blue, phthalocyanide or methyl violet are toxic, unstable to reduction, pH sensitive and often could be autooxidised. For that reason, an optimal and more technologically attractive method is the second way (immobilised mediators). It has also been observed that the mediator solubility can influence the sensor response, for example in the immobilisation process of dimethylferrocene and glucose oxidase. Simply, when the sensor is dipped into the solution, the insoluble mediator stays at the surface. Following application of voltage, the ferrocenium ions are created and being highly soluble in aqueous solutions they leach, thus reducing the mediator volume on the electrode surface, which results in decreasing response.[72] To overcome this disadvantage some conductive polymers modified by mediators can be employed,[72,74] or the introduction of the mediator and enzyme into colloidal graphite emulsion over which the cationic membrane is fixed.[75] The proper mediator has to fulfil following conditions: applied voltage should not exceed the oxygen reduction potential,

reduced mediator should not react with oxygen, electron transfer between the mediator and enzyme should be very fast, mediator should not be influenced by pH, mediator should be non toxic.

3- Amperometric biosensors based on direct electron transfer – these types of sensors are based on direct electron transfer between enzyme and electrode (bioelectrocatalysis). This process is entirely catalytic, where direct electron transfer from the electrode toward the substrate (and vice versa) across active centre of enzyme, undergo without any carriers. In the biocatalysis process, an electron itself is a co-substrate of the reaction; therefore enzyme and electrode reactions cannot be independent from one another.

Indeed, some very important aspects for development of amperometric biosensors include: an electrochemical redox-enzyme activation and subsequent direct electron transfer between the enzyme and electrode. Some reported biosensors have a high sensitivity due to a large current density, which enables electrode miniaturisation. Moreover, a non-specific interfering response is lower because of the effective electric activation of redox-enzyme providing high sensor selectivity and sensitivity.[72]

Luminescence techniques

According to the IUPAC, *"luminescence is the spontaneous emission of radiation from an electronically or vibrationally excited species not in thermal equilibrium with its environment"*.[77] In this optical technique the electromagnetic irradiation generated by previous excited molecules is achieved by using different excitation sources. Based in those points, the luminescence reaction can be classified according to:

- Sonoluminescence: In this phenomenon flashing of light are emitted after the implosion of the cavitation bubbles.[78] (**Figure 1.12)**

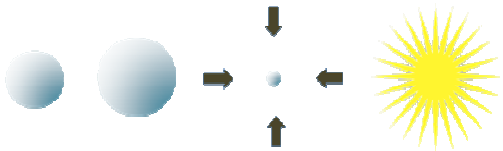

Figure 1.12. Schematic representation of sonoluminiscence.

-Triboluminescence: The light emission is achieved when a chemical bond breaks due to the scratching or fracture of a material. [79]

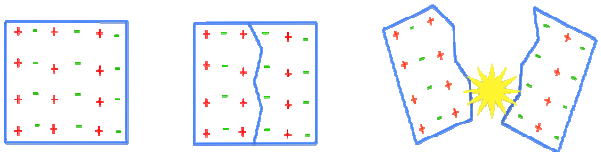

Figure 1.13. Schematic representation of triboluminiscence.

- Bioluminescence (BL): this is a natural process where the light is emitted after chemical reaction catalysed by an enzyme.[80]

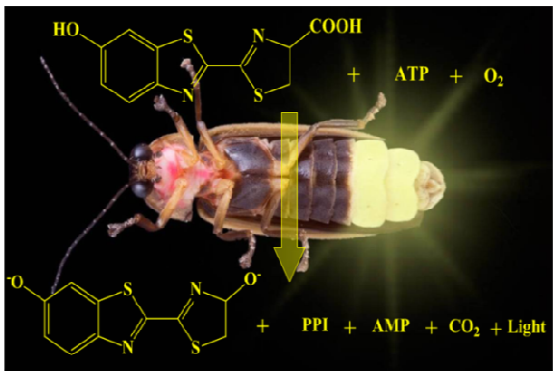

Figure 1.14. Schematic representation of bioluminiscence.

- Chemiluminescence (CL): After a chemical reaction the excited species is generated and light is originated. Typical CL reaction is the formation of excited 3-aminophthalate after reaction of hydrogen peroxide with luminol.[81]

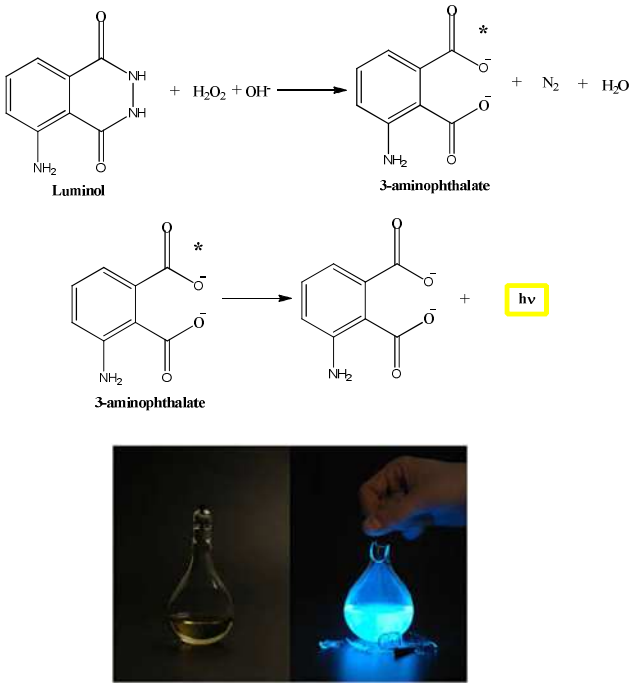

Figure 1.15. Schematic representation of chemiluminescence: the reaction of luminol.

- Electrochemiluminescence (ECL): in this system the light appears after the electron transfer reaction of two species generated on the electrode by the application of potential.[82]

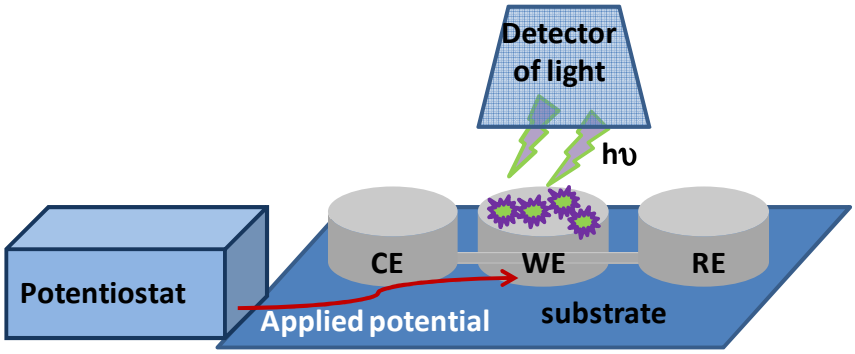

Figure 1.16. Schematic representation of setup for electrochemiluminiscence

Despite the fact that these luminescence techniques are widely useful for detection due to the high sensitivity, the low limit of detection and non-specific background,[83] ECL is a very attractive alternative for biosensor detection due the possibility of control of time and position of emitting light,[84] compatibility with solution-phase and thin-film formats[85] and is dependent of the system chosen, the regeneration of the luminophore after the emission is possible and a new measurement can be carried out.[86]

Fundamentals and advantages of ECL

Some studies in the field of genosensors have been the focus of ECL as detection method. ECL has become a very powerful analytical technique and has been widely used in the areas of, for example, immunoassay, food and water testing, and biowarfare agent detection,[87] highlighting the use of ECL as a powerful tool for ultrasensitive biomolecule detection and quantification.[88]

ECL is a process whereby species generated at electrodes undergo high-energy electron-transfer reactions to form excited states that emit light.[89] This phenomenon was first detected in 1929 when emission of light was observed from luminol at an electrode. However, the first ECL work was not published until the early sixties, when Hercules[90] reported light emission during electrolysis of aromatic hydrocarbons in deoxygenated non aqueous solvents. Since this report, different groups have focused their research on this technique as a tool for analytical applications because it is possible to detect very low concentrations with high sensitivity, a light source is not required for excitation and the instrumentation can be highly simplified for the construction of portable devices. Additionally the measurements are not affected by impurities or scattered light in contrast to fluorescence.[91] The use of ECL has found applications in clinical diagnosis, immunoassays and DNA assays, environmental applications for water testing and biosensors,[92] and can also be coupled to High Performance Liquid Chromatography (HPLC). [93]

ECL mechanism: annihilation and co-reactant

The most common approaches for generating the ECL signal are annihilation and co-reactant pathways. Following the beginning of ECL the first reported system were based on annihilation mechanism. In this process alternate potentials are using to generate oxidized and reduced species that are able to produce the ECL signal by the electron transfer reaction between this two species, that can be identical or not. Depending if the system is energy sufficient or deficient the formation of the excited state is occurs via single annihilation (S-route) or triplet annihilation (T-route) respectively.[88]

The co-reactant mechanism is the second pathway to achieve ECL response. In this mechanism, the intermediate produced from the oxidation or reduction of the co-reactant is able to react with an ECL luminophore and produce the light. ECL measurements can be accomplished with the luminophore and co-reactant in solution or confining the former to the surface for improving the electron transfer for the excitation and subsequently the sensitivity. Furthermore, the use of ruthenium complexes as luminophores and tripropylamine (TPA) as co-reactant in this system is largely described in the literature. Electrochemiluminescence (ECL) of tris(2,2'-bipyridyl)ruthenium(II) ($Ru(bpy)_3^{2+}$) is a well-known detection method that provides high sensitivity with a low background through generation of an optical signal triggered by an electrochemical reaction.[94]

To trigger the optical signal, a sacrificial amine (usually tripropylamine, TPA) is oxidised at the electrode surface generating a radical that reduces the Ru(II) complex to Ru(I) which is further transformed into a Ru(II) excited state that generates the luminescence.

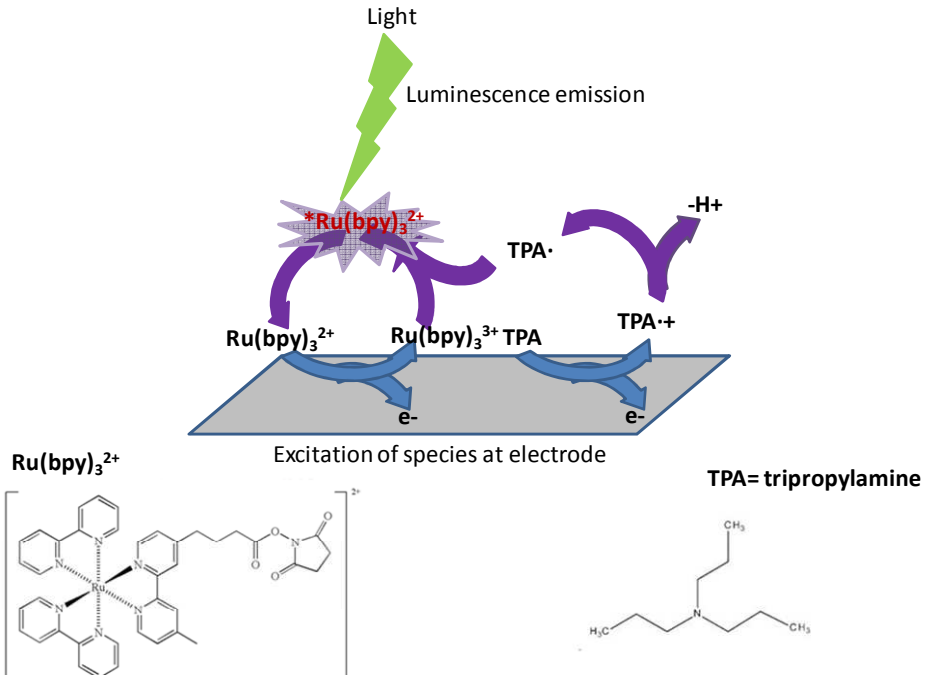

Figure 1.17. Diagram of the ECL mechanism.
(adapted from www.wellstatdiagnostics.com/diagnostics/ecl.html)

Biosensors based in ECL

Landers and co-workers have studied the quenching of ECL by ferrocene (Fc) derivatives.[95] Fc showed more efficient quenching of ECL compared with the known quenchers such as phenol and methylviologen and the proposed mechanism involved bimolecular energy or electron transfer between $Ru(bpy)_3^{2+*}$ and the ferrocenium cation (Fc^+), the oxidized species of Fc. Using Fc as a quencher label on a complementary DNA sequence, an intramolecular ECL quenching in hybridised oligonucleotide strands has been realized, suggesting the potential for application of this system to sequence-specific DNA detection. As the technique of quenching of ECL is considerably simpler and possesses adequate sensitivity, this new approach could open new frontiers in the development of selective and ultrasensitive assays.

For example, the development of a novel genosensors with limit of detection in the fM range was built using a hairpin DNA structure as recognition element and $Ru(bpy)_3^{2+}$-doped silica nanoparticles (Ru-DSNPs) as ECL label and TPA as co-reactant. In this work the

amplification of the signal was attributed to the presence of the new structure designed where the Rubpy is three dimensionally entrapped in the nanoparticles.[96]

Moreover, the interest in ferrocene as a quencher was significantly increased for ECL after the report by Cao et al. detailing the higher efficiency of the quenching effect of the ferrocene over the ruthenium complexes with respect to other quencher molecules.[97] Based on this mechanism, a ECL on-off system based on an aptasensor for adenosine triphosphate detection was developed. In this work a limit of detection of 0.03 pM was achieved using a DNA sandwich structure where the DNA aptamer probe was immobilised on nanoporous gold (NPG)-Rubipy modified glassy carbon electrode. The light emitted by the luminophore decreased by the quencher effect of the Fc linked to the secondary probe in dependence with the adenosine concentration.[98] A similar design using the same luminophore and adenosine aptamer was presented to detect adenosine but on gold surfaces. The off-on system was developed by formation of adenosine/aptamer-Fc complex following previous hybridization of Fc-aptamer/DNA-RuSiNPs on surface. The formations of complex allow the de-hibridisation of Fc-aptamer from the surface and the consequently increase of the ECL signal due to the increase in the distance between Fc and ruthenium derivative.[99]

Since high potentials should be applied to excite the active center, the presence of a robust biorecognition surface is compulsory. The use of diazonium derivatives immobilised on metallic or carbon surfaces is an interesting alternative to be used due to the significant stability reported for the covalent interaction C-C, metal-C. Taking advantage of this stable surface, Piper *et. al.* studied a potential glassy carbon surface for ECL applications.[100]

1.3 THESIS OBJECTIVES

Successful biosensors are commercially available and their acceptance in the market is increasing. Although there are other fields where the biosensors are highly required and their studies are still in the early stage and numerous shortcomings have to be resolved in order to lead the market as a fast, sensitive, a user friendly and cheap prototype. This Thesis is a contribution of the development of different platforms for the improvement of the biosensor performance.

Overall Objective

To develop novel genosensor platforms based on supramolecular and covalent interactions for point-of-care detection of genetic diseases and biological pathogens using amperometric and electrochemiluminescence techniques.

Specific objectives:

The Overall Objective of the Thesis was accomplished through the following specific objectives:

1. To develop stable surface chemistry for development of genosensors exploiting supramolecular chemistry and robust organic platforms.

2. Application of developed surface chemistries for highly sensitive and stable electrochemical genosensors

3. Enhancement of sensor sensitivity and selectivity using electrochemiluminiscent transduction.

1.4 REFERENCES

1. J. Wang, Electroanalysis, **2001**, 13, 983.
2. http://www.idf.org/
3. M. Maccini, A brief story of biosensor technology. Biotechnological Applications of Photosynthetic Proteins: Biochips, Biosensors and Biodevice. **2006**. Edited by Maria Teresa Giardi and Elena V. Piletska. Landes Bioscience.
4. J.D. Newman and A.P. F. Turner. Handbook of Biosensors and Biochips, Chapter 3, **2007**, Edited by Robert S. Marks, David C. Cullen, Isao Karube, Christopher R. Lowe and Howard H. Weetall. John Wiley & Sons, Ltd. ISBN 978-0-470-01905-4.
5. Turner, A.P.F., Karube, I. and Wilson, G.S. Biosensors, fundamentals and applications, **1987**. Oxford University Press.
6. B. Nagel, H. Dellweg and L.M. Gierasch, Pure & Appl. Chem., **1992**, 64,143.
7. A.P.F Turner, Chem. Soc. Rev., **2013**, 42, 3184.
8. R. Monošík, M. Streďanský and E. Šturdík, Acta Chimica Slovaca, **2012**, 5, 109.
9. S. Sumitra Datta, L. R. Christena and Y.R. Yamuna Rani Sriramulu Rajaram, Biotech, **2013**, 3,1.
10. A. Fragoso, B. Sanromà, M. Ortiz and C.K. O'Sullivan Soft Matter, **2009**, 5, 400.
11. A.M. Debela, M. Ortiz, V. Beni and C.K. O'Sullivan, Chem. Eur. J. **2014**, 20, 1.
12. D. Grieshaber, R. MacKenzie, J. Voros and Reimhult, Sensors, **2008**, 8, 1400.
13. L. Su, L. Zou, C.C. Fong, W.L. Wong, F. Wei, K.Y. Wong, R.S. Wu and M. Yang, Biosens Bioelectron, **2013**, 46, 155.
14. D.H. Nam, J.O. Lee, B.I. Sang, K. Won and Y.H. Kim, **2013**, 1, 25.
15. F. Long, A. Zhu and H. Shi, Sensors, **2013**, 13, 13928.

16. H. Joda, V. Beni, D. Curnane, I. Katakis, N. Alakulppi, J. Partanen, J. K. Lind, L. Strömbom and C.K. O'Sullivan, Anal Bioanal Chem., **2012**, 403, 807.

17. P. Arora, A. Sindhu, N. Dilbaghi and A. Chaudhury, Biosensors and Bioelectronics, **2011**, 28, 1.

18. N. Ghosh, G. Gupta, M. Boopathi, V. Pal, A.K. Singh, N. Gopalan and A.K. Goel, Indian J Microbiol, **2013**, 53, 48.

19. M.H.F. Meyer, H.J. Krause, M. Hartmann, P. Miethe, J. Osterd and M. Keusgen, Journal of Magnetism and Magnetic Materials, **2007**, 311, 259.

20. V.A. Bloomfield, D.M. Crothers and I.Jr. Tinoco,. *Nucleic Acid: Structures, Properties and Functions*, **2000**, Herndon, V.A. University Science Books.

21. M. I. Pividori, Nuevos genosensores amperométricos Diseño y construcción, Doctoral Thesis, **2002**, Universitat Autonoma de Barcelona.

22. A. Bonanni, M. J. Esplandiu, M. I. Pividori, S. Alegret, M. del Valle, Anal Bioanal Chem, **2006**, 385, 1195.

23. M.U. Ahmed, M. Saito, M.M. Hossain, S.R. Rao, S. Furui, A. Hino, Y. Takamura, M. Takagia and E. Tamiya, Analyst, **2009**, 134, 966.

24. G. Martínez-Paredes, M.B. González-García and A. Costa-García, SENSOR AND ACTUATORS B, **2010**, 149, 329.

25. http://www.ncbi.nlm.nih.gov/probe/docs/techpcr/.

26. R. Saiki, S. Scharf, F. Faloona, K. Mullis, G. Horn and H. Erlich, Science, **1985**, 230: 1350.

27. A. J. Monsuur, P. I. W. De Bakker, A. Zhernakova, D. Pinto, W. Verduijn, J. Romanos, R. Auricchio, A. Lopez, D.A. Van Heel, J.B.A. Crusius and C. Wijmenga, PLoS ONE, **2008**, 3, e2270.

28. F. R. R. Teles and L. P. Fonseca, Talanta, **2008**, 77, 606.

29. J. J. Gooding, Electroanalysis, **2002**, 14, 1149.

30. X. Zhang, H. Ju, J. Wang, Electrochemical Sensors, Biosensors and their Biomedical Applications, **2008**, Elsevier Inc.

31. R. Mohan, K. E. Mach, M. Bercovici, Y. Pan, L. Dhulipala, P. K. Wong, J. C. Liao, Plosone, **2011**, 6, e26846

32. J. Zhang, H. Qi, Y. Li, J. Yang, Q. Gao, and C. Zhang, Anal. Chem. **2008,** 80, 2888.

33. (a) T. Menanteau, E. Levillain, T. Breton, Chem. Mater.**2013**, 2, 2905; (b) J. Hajdukiewicz, S. Boland, P. Kavanagh, D.l Leech, Biosensors and Bioelectronics, **2010**, 25, 1037.

34. (a) K. I. Rubinstein, A. Vaskevich andJ. Israel, J. Chem., **2010**, 50, 333 ; (b)C. Vericat, M. E. Vela, G. Corthey, E. Pensa, E. Cortes, M. H. Fonticelli, F. Ibanez, G. E. Benitez, P. Carro and R. C. Salvarezza, RSC Adv., **2014**, 4, 27730; (c) J. C. Love, L. A. Estroff, J. K. Kriebel, R. G. Nuzzo and G.M. Whitesides, Chem. Rev. **2005**, 105, 1103; (d) Y. Xue1, X. Li, H. Li and W. Zhang, Nature Communications, **2014**, 5, doi:10.1038/ncomms5348; (e) L. Civit, A. Fragoso, C.K. O'Sullivan, Biosensors and Bioelectronics, **2010**, 26, 1684.

35. W. H. Binder, R. Zirbs, F. Kienberger and P. Hinterdorfer, *Polymers Advanced Techn*., **2006**, 17, 754.

36. A. Fragoso, J. Caballero, E. Almirall, R. Villalonga and R. Cao, Langmuir **2002**, 18, 5051.

37. H. Bai, R.Wang [1], Billy Hargis, H. Lu and Y. Li, Sensors, **2012**, 12, 12506

38. H. J. Schneider, Applications of supramol. Chem., **2012,** Taylor & Francis Group, LLC.

39. S. Keskin and S. Kizilel, Ind. Engin. Chem. Research, **2009**, 50, 1799.

40. R. C. Huxford, J. Della Rocca and W. B. Lin, Curr. Opin. Chem. Biology, **2011**, 14, 262.

41. D. A. Uhlenheuer, K. Petkau and L. Brunsveld, Chem. Soc. Rev. **2010**, 39, 2817.

42. J.-M. Lehn, Supramolecular Chemistry. Concepts and Perspectives, **1995**, Wiley-VCH,

43. O. Crespo-Biel, B.J. Ravoo, D.N. Reinhoudt and J.J. Huskens, Mater. Chem. **2006**, 16, 3997.

44. R. Villalonga, R. Cao and A. Fragoso, Chem. Rev., **2007**, 107, 3088.

45. F. Corbellini, A. Mulder, A. Sartori, M.J.W. Ludden, A. Casnati, R. Ungaro, J. Huskens, M. Crego-Calama and D. N. J. Reinhoudt, Am. Chem. Soc., **2004**, 126, 17050.

46. L. Feng, W. Li, J. Renand and X. Qu, Nano Research, **2014,** DOI 10.1007/s12274-014-05704

47. C. D. Gutsche, B. Dhawan, K. H. No and R. Muthukrishnan, J. Am. Chem. Soc., **1981**, 103, 3782.

48. P. Molenveld, J. F. J. Engbersen and D. N. Reinhoudt, Eur. J. Org. Chem., **1999**, 3269.

49. http://www.chromatography-online.org/Chrial-GC/Contemporary-Chiral-Stationary Phases/Cyclodextrin.html

50. J. Szejtli, Chem. Rev. **1998**, 98, 1743.

51. Y. Chen and Y. Liu, Chem. Soc. Rev., **2010**, 39, 495.

52. L.X. Song, L. Bai, X.M. Xu, J. He and S.Z. Pan, Coordination Chemistry Reviews, **2009**, 253, 1276.

53. A. Fragoso, B. Sanromà, M. Ortiz and C.K. O'Sullivan, Soft Matt., **2009**, 5, 400.

54. H. Aoki, A. Kitajima and H. Tao, Supramol. Chem., **2010**, 22, 455.

55. S. Sato, T. Nojima and S.J. Takenaka, Organomet. Chem., 2004, 689, 4722.

56. Y. Liang, Y. Yu, Y. Cao, X. Hu, J. Wu, W. Wang and D.E. Finlow, Spectrochim. Acta A, **2010**, 75, 1617.

57. A. W. Orr, B. P. Helmke, B. R. Blackman and M. A. Schwartz, Dev. Cell, **2006**, 10, 11.

58. J. Ribas-Arino, M. Shiga and D. Marx, J. Am. Chem. Soc., **2010**, 132, 10609.

59. H. Bonin, E. Fouquet and F. X. Felpin, Adv. Synth. Catal., **2011**, 353, 3063.

60. M. Smith and J. March, March's Advanced Organic Chemistry: Reactions, Mechanisms, and Structure 6th Edition, **2007.**

61. D.T. Flood, Org. Synth. 1943, 2, 295.

62. V. D. Filimonov, M. Trusova, P. Postnikov, E. A. Krasnokutskaya, Y. M. Lee, H. Y. Hwang, H. Kim, K.-W. Chi, Org, Lett., **2008**, 10, 3961.

63. M. Barbero, M. Crisma, I. Degani, R. Fochi, P.Perracino, Synthesis, **1998**, 1171.

64. a) D. Bélanger and J. Pinson, Chem Soc. Rev., **2011**, 40, 3995. b) . M. M. Chehimi. Aryl Diazonium Salts: New Coupling Agents and Surface, Science **2012**, ISBN: 978-3-527-32998-4.

65. B. S. Furniss, A. J. Hannaford, P. W. G. Smith, A. R. Tatchell, Textbook of Practical Organic Chemistry 5th Edition, **1989**.

66. a) J. J. Gooding, Electroanalysis, **2007**, 20, 573. b) J. Haccoun, C. Vautrin, A. Chaussé, A. Adenier, Progress in Organic Coating, **2008**, 63, 18.

67. M. Delamar, R. Hitmi, J. Pinson, J. M. Savant, J. Am. Chem. Soc. **1992**, 114, 5883.

68. J. Pinson, F. Podvorica, Chem. Soc. Rev., **2005**, 34, 429.

69. Z. Xiong, T. Gu, X.Wuang, Langmuir, **2014**, 30, 522.

70. K. J. Belde, S. J. Bull, Thin Solid Films, 2006, **515**, 859.;b) Z. Huang, R. Boulatov, Pure Appl. Chem., 2010, **82**, 931.; c) A. Noy, Surface Interface Anal., 2006, **38**, 1429.

71. M. V. Lee, M. T. Hoffman, K. Barnett, J. M. Geiss, V. S. Smentkovski, M. R. Linford, R. C. Davis, J. Nanoscience Nanotechnology, 2006, **6**, 1639.

72. S. V. Dzyadevych, V. N. Arkhypova, A. P Soldatkin, A. V. El'skaya, C. Martelet, and N. Jaffrezie-Renault, ScienceDirect, **2008**, 29, 171.

73. M. Farré, , L. Kantiani, S. Pérez and D. Barceló, Trends in Analytical Chemistry, **2009**, 28, 170.

74. J. M. Dicks, S. Hattori, I. Karube, A. P. F. Turner and T. Yokozawa, Annales de Biologie Clinique, **1987**, 47, 607.

75. I. Rosen-Margalit, and J. Rishpon, Biosensors and Bioelectronics, **1993,** 8, 315.

76. V. D. Filimonov, M. Trusova, P. Postnikov, E. A. Krasnokutskaya, Y. M. Lee, H. Y. Hwang, H. Kim, K.-W. Chi, Org, Lett., **2008**, 10, 3961.

77. http://goldbook.iupac.org/L03641.html

78. Fifth International Symposium on Cavitation (CAV2003) Osaka, Japan, November 1-4, **2003**. GS-3-002

79. S. Biju, N. Gopakumar, J.-C.G. Bunzli, R. Scopelliti, H. K. Kim, and M. L. P. Reddy, Inorg. Chem., **2013**, 52, 8750.

80. E. Michelini, L. Cevenini, M. M. Calabretta, D. Calabria, A. Roda, Anal. Bioanal. Chem., **2014**, 406, 5531

81. M.M. Vdovenko, V. Papper, R.S. Marks and I.Y. Sakharov, Anal. Methods, **2014**, 6, 8654.

82. M.M. Richter, Chem. Rev., **2004**, 104, 3003.

83. P. Zhou, D. Zhou, L. Tao, Y. Zhu, W. Xu, S. Xu, S. Cui, L. Xu and H. Song, Light: Science & Applications, **2014**, 3, e209; doi:10.1038/lsa.2014.90

84. P. Bertoncello, A. J. Stewart and L. Dennany, Anal. Bioanal Chem, **2014**, 406, 5573

85. R. J. Forster, P. Bertoncello and T. E. Keyes, Annu. Rev. Anal. Chem, **2009**, 2**,** 359.

86. M.N. Khan and J.W. Findlay, Ligand-Binding Assays: Development, Validation, and Implementation in the Drug Development Arena, **2009**. Wiley.

87. W. Miao, Chem. Rev., **2008**, 108, 2506.

88. A. J. Bard, Electrogenerated Chemiluminescence, **2004**, Ed.; Dekker: New York.

89. A. B. Nepomnyashchii, A. J. Bard, J. K. Leland , J. D. Debad, , G. B. Sigal, J. L. Wilbur and J. N. Wohlstadter, Chemiluminescence, Electrogenerated. Encyclopedia of Analytical Chemistry, **2014**, 1.

90. D.M. Hercules, Science, **1964**, 145, 808.

91. J. Li and N. Wu. Biosensor based on nanomaterials and nanodevices, Chapter 9: Nanomaterial- based Electrochemiluminicence Biosensor, **2014**, CRC Press

92. M. Yang, R. Chen and C. Yi. Encyclopedia of Microfluidics and Nanofluidics, Electro Chemo Luminescence (ECL), **2008**, 474.

93. Y. Sun, Z. Zhang and X. Zhang, Spectrochimica Acta Part A: Molecular and Biomolecular Spectroscopy, **2013,** 105, 171.

94. L. Hu and G. Xu, Chem. Soc. Rev., **2010**, 39, 3275.

95. W. Cao, J. P. Ferrance, J. Demas, J. P. Landers, J. Am. Chem. Soc., **2006**, *128*, 7572.

96. Q. Sun, G. Zou, X. Zhang, Electroanalysis, **2011**, 23, 2693.

97. W. J. Cao, X. Liu, E. Yang, E. Wang, Electrophoresis, **2002**, 23, 3683.

98. M. Li, H. Yang, C. Ma, Y. Zhang, S. Ge, J. Yu, M. Yan, Sensors & Actuators: B. Chemical, **2014**, 191, 377.

99. C. Rodríguez-Rodrıíguez, A. Rimola, L. Rodríguez-Santiago, P. Ugliengo, A. Alvarez-Larena, H. Gutiérrez-de-Terán, M. Sodupe and P. González-Duarte, Chem Commun., **2010**, 46, 7

100. D. J. E. Piper, G. J. Barbante, N. Brack, P. J. Pigram, C. F. Hogan, Langmuir **2011**, 27, 474-480.

CHAPTER 2

HIGHLY SENSITIVE COLORIMETRIC ENZYME LINKED OLIGONUCLEOTIDE ASSAY BASED ON CYCLODEXTRIN-MODIFIED POLYMERIC SURFACES

(Anal. Bioanal. Chem, 2012, 403, 195-202)

CHAPTER 2

HIGHLY SENSITIVE COLORIMETRIC ENZYME LINKED OLIGONUCLEOTIDE ASSAY BASED ON CYCLODEXTRIN-MODIFIED POLYMERIC SURFACES

2.1 ABSTRACT

In this chapter, the development of an enzyme-linked oligonucleotide assay for the detection of a human leukocyte antigen allele associated with celiac disease based on cyclodextrin-modified polymeric surfaces is described. The surface of maleimide-pre-coated plates was modified with a layer of thiolated cyclodextrin polymer and used for the supramolecular capture of adamantane or ferrocene-modified carboxy- methylcellulose polymers bearing DNA probes. The assay was optimised in terms of incubation time, temperature, and surface chemistry and applied to the highly sensitive and selective detection of HLA sequences with a limit of detection of 0.7 nM. A real sample analysed using this platform showed an excellent correlation with maleimide-activated plates using thiolated DNA probes.

2.2 INTRODUCTION

Genetic tests are diagnostic tools to detect genes associated with inherited disorders[1,2] and the enzyme-linked-oligo- nucleotide assay (ELONAs) has emerged as an attractive technique for clinical applications.[3] The necessity for a sensitive, rapid, reliable, and inexpensive alternative for DNA analysis has led to the development of this simple, sensitive, robust, and versatile bioanalytical technique that has been used for the colorimetric detection of DNA.[3–5] In this technique, a probe is immobilised on the surface of a microtitre plate[4] and the target DNA is detected in a sandwich-type assay, exploiting a secondary-labelled reporter DNA probe,[3] for example via the use of a fluorescein- labelled oligonucleotide probe and an enzyme-labelled anti- fluorescein antibody.[5]

To immobilise the DNA probe on the surface of microtitre plates, the most extended strategy is the interaction of biotiny- lated probes with streptavidin (or avidin)-coated surfaces.[3, 5–7] This

type of surface preserves the biological activity of the immobilised molecule better than direct passive adsorption and the high biotin–streptavidin affinity constant (Kd ~10^{-14} M) provides a robust system as compared with direct passive adsorption.[8]

However, in spite of the general acceptance of streptavidin-coated microtitre plates, some protein leaching and inter-plate variation between provider sources have been observed.[8]
Another alternative for probe immobilisation is via covalent binding using maleimide-activated plates. These are useful for binding thiol-containing molecules[9] and have been used for the colorimetric or fluorescent detection of biomolecules.

The use of supramolecular interactions for the immobilisation of biomolecules on surfaces is garnering great interest.[10,11] Cyclodextrin-modified gold surfaces have been used to capture biomolecules using biotinylated bifunctional linkers terminating in hydrophobic moieties such as adamantane,[12, 13] or, more recently, using polymeric carriers.[14, 15] In this strategy, host–guest interactions act as linkers to promote immobilisation under mild conditions and have been demonstrated to be a useful platform for the detection of auto-antibodies in serum,[16] or DNA from PCR products.[17] In spite of the robustness of these platforms, the application of host–guest interactions as an immobilisation strategy on microtitre plates has not been reported to date. These plates are fabricated with cheap polymeric materials such as polystyrene allow high throughput genomic and proteomic analysis for many biomedical research and clinical diagnostics applications. In this paper we describe the development of an ELONA-type assay for the detection of a human leukocyte antigen (HLA) allele associated with celiac disease[18] an autoimmune condition of known genetic predisposition[19] The surface of maleimide-precoated microtitre plates was modified with a layer of thiolated cyclodextrin polymer and used for the supramolecular capture of adamantane (ADA) or ferrocene (Fc)-modified carboxymethylcellulose (CMC) polymers bearing DNA probes (**Scheme 1.1**). The assay was optimised in terms of incubation time, temperature and surface chemistry and applied to the highly sensitive and selective detection of HLA-DQ2-associated sequences.

2.3 EXPERIMENTAL SECTION

Materials

All reagents were used as received. CMC (MW 90 kDa), 1- ethyl-3-[3-dimethylaminopropyl]carbodiimide hydrochloride, (EDC), phosphate buffered saline (PBS; dry

powder), and tetrame- thylbenzidine (TMB) liquid substrate system were purchased from Sigma-Aldrich. SYBR Green I was purchased from Invitrogen and prepared at a 1:10,000 dilution in PBS (pH 0 7.4 containing 0.8 M NaCl and 50 mM KCl). All solutions were prepared with Milli-Q water (Millipore Inc., Ω 0 18 MΩ·cm). Maleimide-activated microtitre plates were purchased from Pierce. Thiolated α, β and γ-cyclodextrin polymers (CDPSH)[20] and bifunctionalised CMC polymers modified with ADA or Fc residues and DNA probes (ADA-CMC-DNA and Fc-CMC-DNA)[17] were prepared as previously reported. Synthetic oligonucleotides were purchased from Biomers.net (Ulm, Germany).

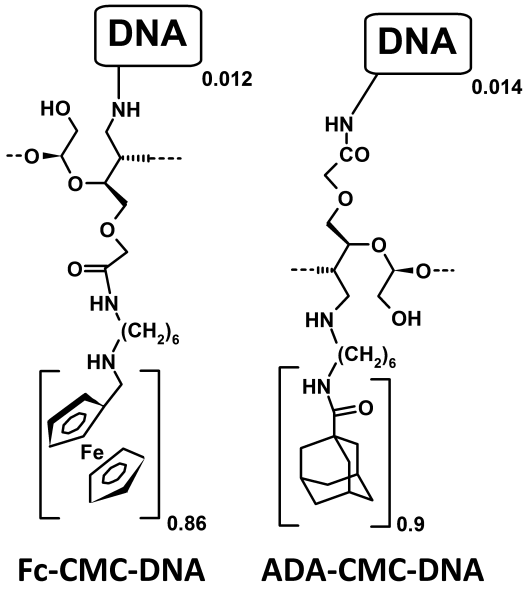

Scheme 2.1. Structure of polymeric carriers

Sequences specific for HLA-DQA1*0201 are shown below:

HLA-DQA1*0201 aminated capture probe linked to ADA-CMC and Fc-CMC polymers: H_2N-C_6-5'-CAA ATC TAA GTC TGT GGA -3'.

HLA-DQA1*0201 thiolated capture probe: HS-C_6-5'-CAA ATC TAA GTC TGT GGA -3'

HLA-DQA1*0201 target: 5'-GAG AGG AAG GAG ACT GTC TGG AAG TTG CCT CTG TTC CAC AGA CTT AGA TTT GAC CCG CAA TTT GCA CTG ACA AAC ATG GCT GTG CTA AAA CAT A-3'.

HLA-DQA1*0201 HRP-labeled probe: 5'-GAC AGT CTC CTT CCT CTC-HRP-3'.

HLA-DQA1*01* (interference 1): 5'-GAG AGG AAG GAG ACT GCC TGG CGG TGG CCT GAG TTC AGC AAA TTT GGA GGT TTT GAC CCG CAG GGT GCA CTG AGA AAC ATG GCT GTG GCA AAA CAC A-3'.

HLA-DQA1*03* (interference 2): 5'-GAG AGG AAG GAG ACT GTC TGG CAG TTG CCT CTG TTC CGC AGA TTT AGA AGA TTT GAC CCG CAA TTT GCA CTG ACA AAC ATC GCT GTG CTA AAA CAT A-3'.

Instrumentation and methods

UV–vis spectra were recorded in a temperature controlled Cary 100 Bio spectrophotometer (Varian) in 1 cm quartz cells. Plate optical densities were recorded in a Wallac Victor2 1420 Multilabel counter from Perkin Elmer.

The fluorescence experiments were performed at 20 °C in a Cary Eclipse spectrofluorimeter equipped with a Peltier temperature control and plate reader. The excitation wavelength was set at 495 nm, which corresponds to the SYBR Green absorption maximum in aqueous solution. The fluo- rescence spectra were recorded in the wavelength interval of 510–570 nm with excitation and emission slits of 10 nm and a scan rate of 240 nm/min. All measurements were carried out in triplicate and the average value of the fluorescence changes was used.

Enzyme Linked Oligonucleotide Assay (ELONA)

Reacti-BindTM Maleimide Activated Plates (8-well strips) were used as received. All washing steps were carried out with 0.1 M sodium phosphate, 0.15 M sodium chloride (pH 7.4). After washing the strips three times, CDPSH was immobilised via the addition of 150 μL of a 10-mg/mL solution in binding buffer (0.1 M sodium phosphate, 0.15 M sodium chloride, 10 mM EDTA; pH 7.4) to each well and incubated for 3 h at room temperature. Unreacted maleimide groups were blocked for 1 h with 200 μL of a 10-μg/mL aqueous solution of mercaptoethanol (prepared immediately before use). After washing with PBS, 150 μL of ADA-CMC- DNA or Fc-CMC-DNA polymers was added to the wells and incubated overnight at 4 °C, and

subsequent to another washing, 100 μL of 10 nM of HLA-DQA1*0201 target in PBS (pH 0 7.4 with 0.8 M NaCl) was added and incubated for different times (30, 60, 90, and 120 min) and temperatures (4 °C, 25 °C, and 37 °C) in order to elucidate optimum assay conditions. Detection was facilitated by addition of 100 μL of 10 nM of HLA-DQA1*0201 HRP-labelled probe in PBS (pH 7.4 with 0.8 M NaCl), again for 1 h and at room temperature. After a final washing step, 50 μL of TMB solution was added and 30 min later, the absorbance was recorded at 450 nm following addition of 50 μL of 1 M H_2SO_4. In the case of the surface modified with Fc units, the absorbance was referenced to a CDPSH/Fc-CMC-DNA surface to subtract the possible contribution of the Fc chromo- phore to the absorbance at this wavelength.

To prepare the calibration curve, the target was incubated at the optimum conditions (37 °C and 1 h) with a range of concentrations of the HLA-DQA1*0201 target (from 0 to 300 nM) in PBS (pH=7.4 with 0.8 M NaCl) and the detection was carried out as described above. For comparison purposes, a calibration curve was obtained using a thiolated probe instead of the supramolecular system. In this case, the plate was initially modified with 150 μL of a 10 nM solution of HLA-DQA1*0201 thiolated capture probe in binding buffer (0.1 M sodium phosphate, 0.15 M sodium chloride, 10 mM EDTA; pH 7.4), incubated for 3 h at room temperature and blocked with mercaptoethanol. All other steps (washes, target incubation, detection) were carried out under the same conditions as described above.

Determination of amount of DNA attached to the supramolecular surface by polymer desorption

In order to determine the amount of DNA probe immobilised using the supramolecular system, CDPSH/ADA-CMC-DNA was prepared on maleimide-activated plates as previously described, and then the plate was rinsed with PBS and subsequently incubated with 200 μL of 1 M solution of sodium adamantanecarboxylate for 1 h at 37 °C to dissociate the ADA-CMC-DNA polymer from the cyclodextrin surface. The released ADA-CMC-DNA polymer was incubated with 100 nM of target for 1 h, followed by a 15 min incubation with SYBR Green I (1:10,000 dilution) for 15 min.

In order to construct a calibration curve for quantification of the number of DNA probes on the released ADA-CMC- DNA polymer, HLA-DQA1*0201 capture probe (0 to 100 nM) in PBS,

pH 7.4 containing 0.8 M NaCl and 50 mM KCl, was incubated with a constant amount of target (100 nM) for 1 h followed by 15 min of incubation with SYBR Green (1:10,000 dilution). The fluorescence intensity at 525 nm was recorded and the amount of DNA probe present in the released ADA-CMC-DNA was calculated by interpolation in the calibration curve obtained.

Determination of intraplate probe distribution homogeneity and stability

A maleimide-activated black microtitre plate for fluorescence measurement was modified with the supramolecular surface as previously described. The wells were rinsed with PBS and incubated with target (100 nM) and SYBR Green (1:10,000) in the presence of KCl (50 mM) before reading the fluorescence at 525 nm using a plate reader coupled to the spectrofluorimeter.

The stability of the supramolecular surface chemistry was carried out during 4 weeks at 4 °C. Each week the amount of coating DNA was measured in 8 wells of the plate, as previously described.

Real sample analysis

A PCR product obtained by amplification of a real HLA typed sample was diluted 1:10 and added as target following the procedure described above for the detection of HLA-DQA1*0201 target on CDPSH/ADA-CMC-DNA and CDPSH/Fc-CMC-DNA-modified plates. The values were interpolated in the respective calibration curves and compared with the results obtained using a maleimide plate modified with thiolated DNA.

2.4 RESULTS AND DISCUSSION

Two supramolecular platforms were evaluated using a modification of the Enzyme Linked Oligonucleotide Assay (ELONA). The plate was initially incubated with βCDPSH at pH 7.4 in order to form the cyclodextrin support layer by addition of the thiol groups to the double bond of the maleimide group thus forming a stable thioether linkage. Unreacted maleimide groups were then blocked with mercaptoethanol followed by the incubation of the polymeric DNA carrier (ADA-CMC-DNA or Fc-CMC-DNA). In these polymers, the presence of adamantane

and ferrocene units has the function of docking the polymer within the cyclodextrin layer via host-guest interactions. After hybridisation with the target DNA, a secondary probe labelled with HRP was used as a reporter probe and the detection was carried out colorimetrically by addition of tetramethylbenzidine (TMB) as substrate for HRP (**Figure 2.1**).

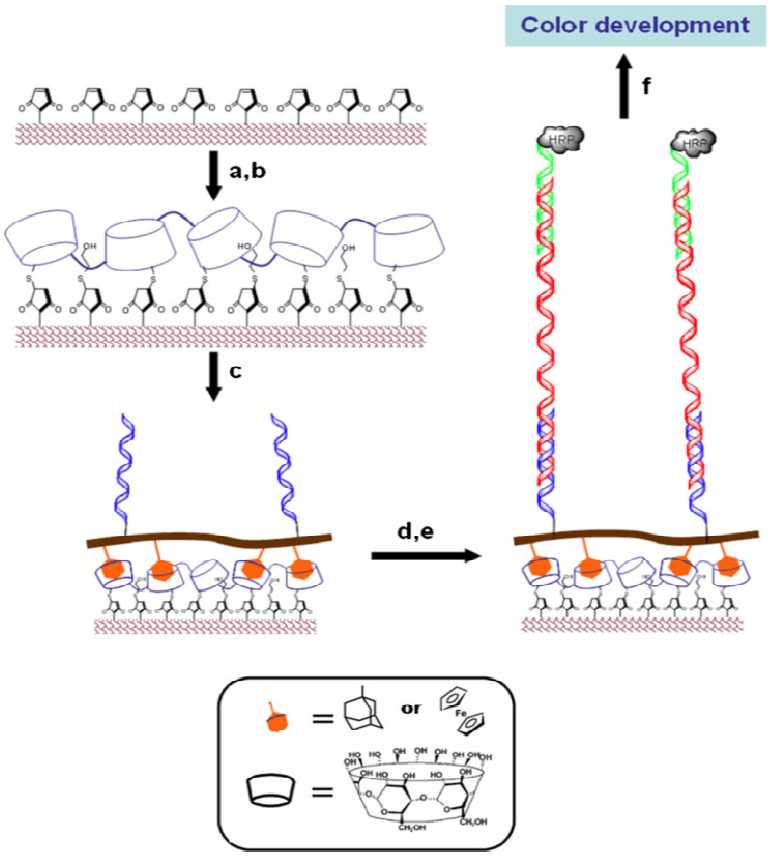

Figure 2.1. Principle of modified ELONA platform based on the self-assembly of CMC-polymers bearing DNA probes on cyclodextrin modified plates. a) CDPSH, b) mercaptoethanol, c) ADA-CMC-DNA or Fc-CMC-DNA, d) target DNA, e) HRP-labeled secondary DNA probe, f) colour development with TMB.

The supramolecular nature of the CDPSH/CMC interface was tested by comparing the response obtained using similar thiolated polymers derived from αCD and γCD, which have smaller and larger cavity diameters as compared to βCD. Both, αCDPSH and γCDPSH, were immobilised on the maleimide- activated surface in the same way as βCDPSH, and ADA or Fc-CMC-DNA polymers were allowed to with the host-modified surface. Since the amount of both hydrophobic moiety (0.86–0.90 mol/mol glucose) and DNA probe (0.012– 0.014 mol/mol of glucose) attached to both polymers is very similar, the differences in the optical response

can be attributed to the amount of DNA probe immobilised on the surface. As can be seen from **Figure 2.2a**, the response showed the trend βCDPSH > γCDPSH > αCDPSH with the βCDPSH/ADA- CMC-DNA system showing the highest absolute response. **Figure 2.2b** shows the dependence of the optical responses obtained in **Figure 2.2a** with the reported stability constants for cyclodextrin/ferrocene[19] and cyclodextrin/adamantanecar- boxylic acid[20] systems. As can be seen, there is a direct relationship between the stability of the inclusion complex and the optical response obtained, clearly demonstrating that the immobilisation of the polymeric carrier on the surface takes place through inclusion complexation. The strength of the inclusion complex thus modulates the amount of DNA probe immobilised on the surface, and consequently, assay sensitivity. The role of the inclusion complexation in the immobilisation of the CMC carrier is also demonstrated by the very low signal observed after the interaction of a CMC-DNA polymer (i.e. not carrying the hydrophobic moiety) with the βCDPSH- modified surface (see **Figure 2.2a**, inset).

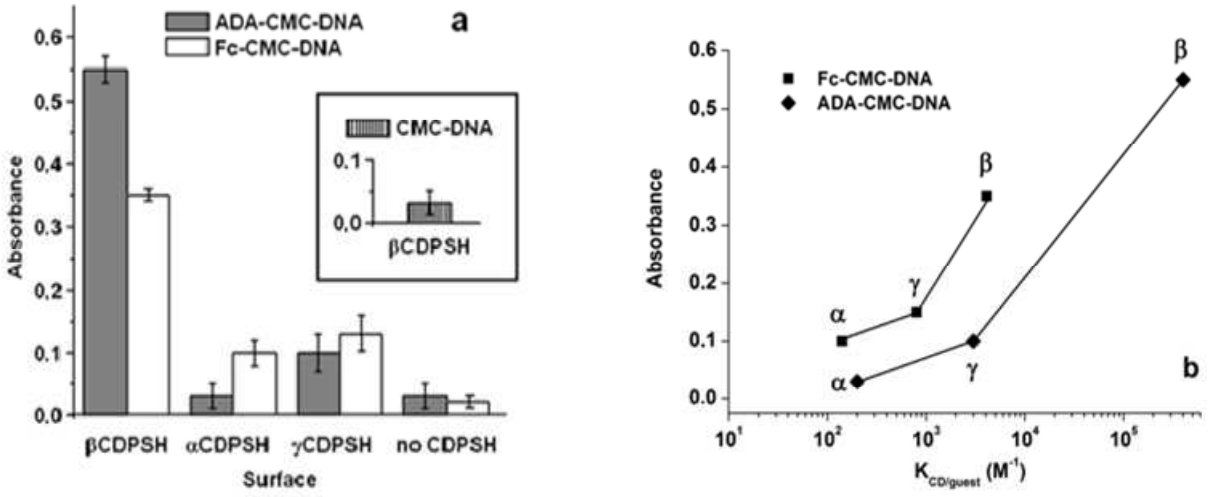

Figure 2.2. a) Optical response obtained in the detection of 10 nM HLA-DQA1*0201 target sequences on α, β, and γ-CDPSH modified surfaces using ADA-CMC-DNA and Fc-CMC-DNA polymers. Inset: response obtained using a CMC-DNA polymer (without hydrophobic moiety) on the βCDPSH surface. b) Dependence of the optical responses obtained in Figure 2a with the stability constants for the cyclodextrin/ferrocene and cyclodextrin/adamantanecarboxylic acid system.

To test the homogeneity of probe distribution in a plate (i.e. well–well reproducibility), the probes were incubated with the target sequence and the fluorescence of the intercalating agent SYBR Green was measured. As can be seen from **Figure 2.3a**, the resulting fluorescence readings were reproducible, with a standard deviation of 8 %, indicating a homogeneous

distribution of the polymer on the wells of the plate. The supramolecular architecture was observed to be completely stable over a period of 4 weeks a 4 °C (**Figure 2.3b**).

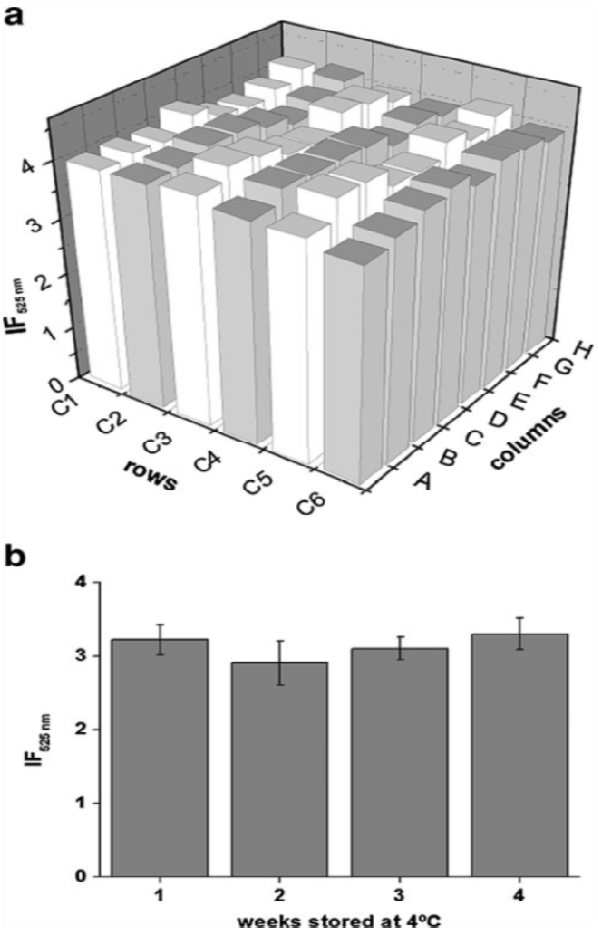

Figure 2.3. a) 3D plot showing the fluorescence values at 525 nm obtained on a 6×8 well section of a plate after incubation of the supramolecular surface with 100 nM of target and SYBR green (λ_{exc} = 495 nm). b) Stability of supramolecular surface coated plates with time at 4ºC.

Since the assay performance largely depends not only on the amount of capture probe attached to the CMC carrier but also on the amount of polymer immobilised on the surface, the ADA-CMC-DNA polymer was desorbed from the plate surface using a competitive displacement in the presence of a large excess of sodium adamantanecarboxylate in order to truly quantify the amount of probes at the surface. The detached DNA-carrying polymer was initially analyzed by UV–vis spectroscopy at 260 nm but the absorbance values were low and difficult to quantify. For this reason, the solution was incubated with a target sequence to form dsDNA,

which was then quantified by fluorescence using SYBR Green as intercalating agent (**Figure 2.4**). Normalisation of the measured concentration considering the well area gave a surface probe density of $(8.6\pm0.6)\times10^{-10}$ mol/cm^2, a value very close to the binding capacity of a thiolated peptide indicated by the manufacturer (1.5×10^{-10} mol/well, equivalent to ~5.8×10^{-10} mol/cm^2) and indicative of the formation of an almost complete monolayer at the surface.

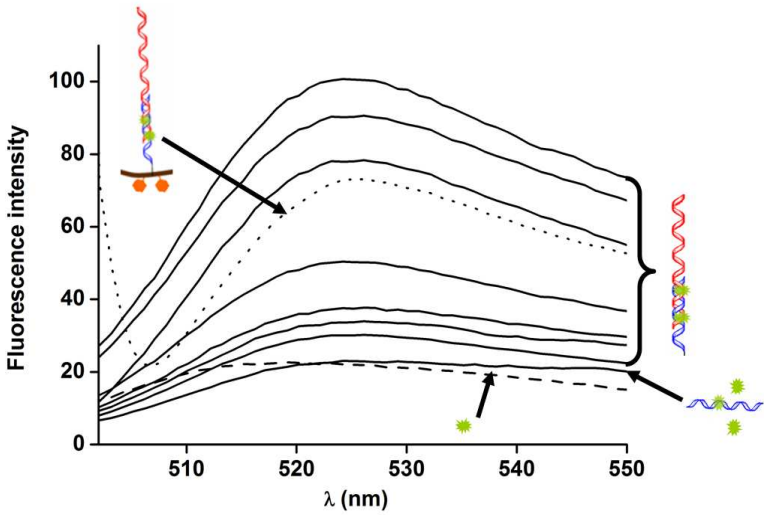

Figure 2.4. Fluorescence spectra of: SYBR Green intercalated in dsDNA formed by hybridisation of 100 nM target with different concentrations of HLA-DQA1*0201 probe in solution (———), ADA-CMC-DNA desorbed from supramolecular surface (……) and SYBR green in the absence of any DNA (-------). Excitation wavelength: 495 nm.

The optical response for the detection of 10 nM of the target (specific response) at different hybridisation times and temperatures in PBS (with 0.8 M NaCl) was studied in order to optimise assay conditions and a control measurement was carried out in the absence of target (non-specific response). As can be seen in **Figure 2.5**, the optimum hybridisation conditions are 60 min at 37 °C, where the highest $A_{specific}/A_{non\text{-}specific}$ ratio was observed representing a 77 % and 51 % signal increase as compared to the highest response obtained at 4 °C and 25 °C, respectively. The decrease of the signal at 37 °C after 60 min in the case of βCDPSH/Fc-CMC-DNA is due to the stability of the βCD/Fc inclusion complex, whilst in the case of CDPSH/ADA-CMC-DNA, this effect is less pronounced due to the higher stability of the βCD/ADA ($K_{\beta CD/ADA}\sim10^5$) inclusion complex, which is two orders of magnitude higher than the βCD/Fc system.

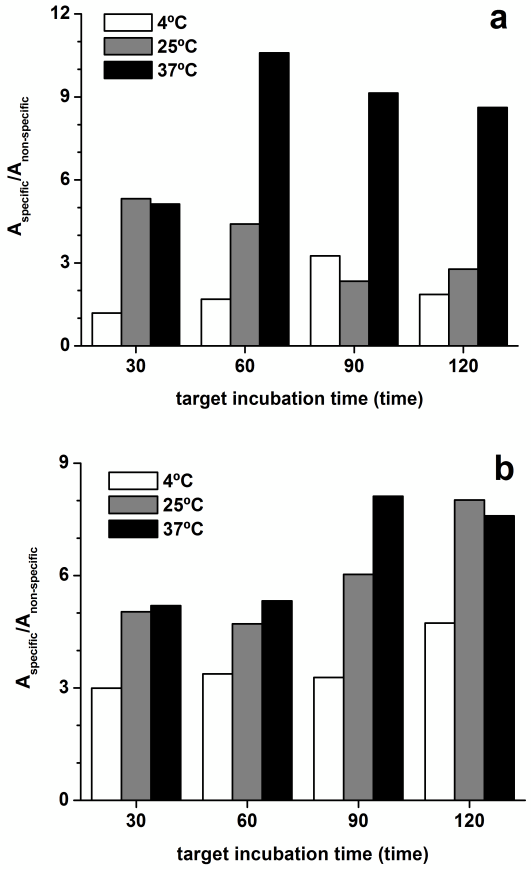

Figure 2.5. Dependence of the optical response for the detection of 10 nM HLA-DQA1*0201 target with target incubation times and temperatures for (a) βCDPSH/Fc-CMC-DNA system, (b) βCDPSH/ADA-CMC-DNA system. Conditions: Target concentration: 10 nM in PBS (with 1 M NaCl); Target incubation times: 30, 60, 90, 120 min; Incubation temperatures: 4, 25 and 37°C.

Using the optimum conditions to immobilise the target for both systems the corresponding calibration curves were obtained in the concentration range 0–300 nM (**Figure 2.6**). As can be seen, the optical response increased with target concentration and tends to saturation above 100 nM. At low concentrations (0–10 nM), the response showed a linear dependence with the concentration with a sensitivity (taken as the slope of the A vs c curve) of 0.034 and 0.056 AU/nM for the Fc and ADA systems, respectively and a limit of detection of 0.7 and 0.8 nM, respectively. These limits of detection are similar to the value obtained using a thiolated capture probe (0.5 nM), whilst the sensitivity of the supramolecular assay is 4 and 7 times higher compared with the thiolated probe (0.0086 AU/nM). This highlights the role of the CMC backbone in spatially orienting the capture probes, avoiding possible steric hindrance to target recognition. The use of an increased number of DNA probes attached to CMC or shorter CMC backbones that could be better accommodated on the underlying CDPSH layer may help

to extend the linear range and sensitivity if necessary by increasing the density of probes on the plate and this is currently being explored. This probe density is more difficult to control in the case of the direct reaction of a thiolated probe with the maleimide surface, often requiring lengthy optimisation steps of probe/backfiller ratios as well as incubation times and temperatures. In addition, the hydrophilic nature of the CMC backbone effectively suppresses non-specific interactions, as is evident from the very low response observed in the absence of target, indicating that the HRP-labelled probe has a negligible tendency to interact with the CDPSH/CMC-modified surface.

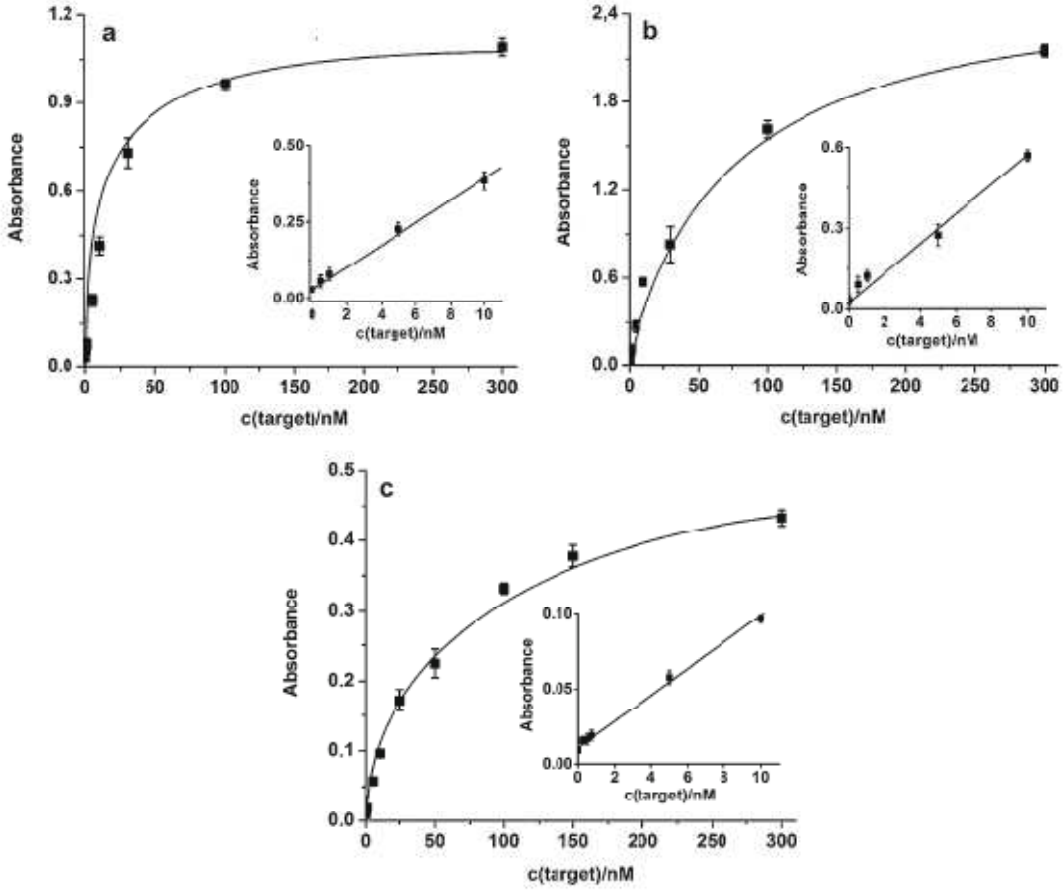

Figure 2.6. Calibration curves for the detection of HLA-DQA1*0201 target sequence using (a) βCDPSH/Fc-CMC-DNA system, (b) βCDPSH/ADA-CMC-DNA system, c) HLA-DQA1*0201 thiolated capture probe.

For DNA detection, selectivity is critical, and **Figure 2.7** shows the optical response obtained with the βCDPSH surface in the presence of two potential interfering alleles, which only differ by base pairs, and no cross-reactivity was observed, and the low signal obtained is attributed to a minor amount of non- specific binding of the reporter probe.

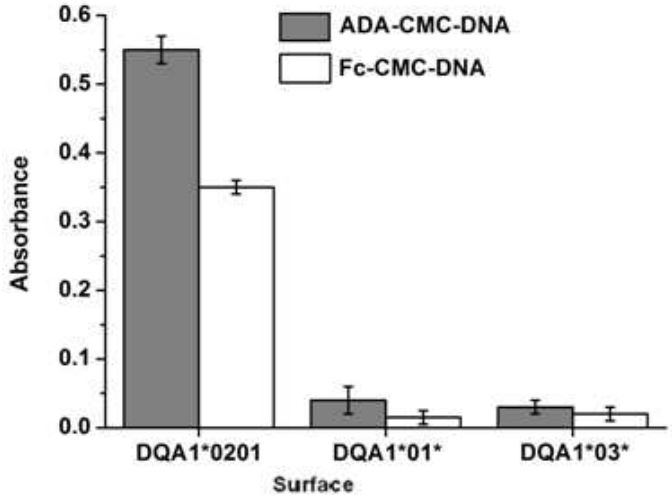

Figure 2.7. Optical responses obtained in the detection of 10 nM HLA-DQA1*0201 target and two HLA-related interferences.

2.5 CONCLUSIONS

In conclusion, we have demonstrated the applicability of supramolecular host–guest interactions in the development of colorimetric DNA tests based on the self-assembly of bifunctionalised CMC polymers on cyclodextrin-modified microtitre plates. Adamantane and ferrocene-appended polymers were demonstrated to have a preference to interact with βCD-modified surfaces over αCD and γCD, demonstrating the supramolecular nature of the immobilisation process. The CMC polymer facilitated a spatial orientation of the DNA probes on the surface giving better access to target DNA, References resulting in a markedly more sensitive colorimetric assay than a similar assay based on the immobilisation of thiolated probes, with subnanomolar limits of detection. In addition, the presence of the hydrophilic cyclodextrin and CMC polymers min- imise non-specific interactions, as demonstrated by the very low response obtained in the absence of target. A real PCR- amplified sample of a celiac patient, demonstrated to carry the HLA-DQA1*0201 allele using Luminex-based HLA typing, was tested using the supramolecularly coated plates and compared with the thiolated probe-coated plates. The results obtained using supramolecular plates were 0.78 ± 0.07 nM for ADA-CMC-DNA/CDPSH and 0.96±0.09 nM for Fc-CMC- DNA/CDPSH, showing an excellent correlation with thiolated DNA capture probe (0.86±0.05 nM), clearly demonstrating that the supramolecular chemistry is not affected by the sample matrix and does not need to be pre-

treated. The multiplexing ability of this platform in the detection of several HLA alleles is currently under investigation.

2.6 REFERENCES

1. N.A. Holtzman, P.D. Murphy, M.S. Watson and P.A. Barr, Science, **1997**, 278, 602.
2. W. Vercoutere and M. Akeson, Curr. Opin. Chem. Biol., **2002**, 6: 816.
3. A. M. Lazaro, M.A. Fernandez-Viña, Z. Liu and P. Stastny, Hum. Immunol.,**1993**, 36, 243.
4. D.W. Drolet, L. Moon-McDermott and T.S. Romig, Nature Biotechnol., **1996**, 14, 1021.
5. D.D. Kostyu, J. Pfohl, F.E. Ward, J. Lee and A. Murray, D. B. Amos, Hum. Immunol., **1993**, 38,148.
6. A. Landgraf, B. Reckmann and A. Pingoud, Anal. Biochem., **1991**,198, 86.
7. J..L. Acero, O.Y.F. Henry, T. Mairal, N. Laddach, A. Nygren, S. Hauch, J. Fetisch and C..K. O'Sullivan, Anal. Bioanal. Chem., **2010**, 397, 2325.
8. L. Välimaa and K. Laurikainen, J. Immunol. Meth., **2006**, 308, 203.
9. G.T. Hermanson, Bioconjugate Techniques, **2008**. 2nd edition, Academic Press, New York. Chapter 19.
10. R. Villalonga, R. Cao and A. Fragoso, Chem. Rev., **2007**, 107, 3088.
11. O. Crespo-Biel, B. J. Ravoo, D. N. Reinhoudt and J. Huskens, J. Mater. Chem. **2006**, 16, 3997.
12. J. Szejtli, Cyclodextrin Technology, **1988**, Kluwer Academic Publishers. Dordrecht.
13. J. W. Ludden, , X. Li, J. Greve, van A. Amerongen, M. Escalante, V. Subramaniam, D.N. Reinhoudt and J. Huskens, J. Am. Chem. Soc., **2008**, 130, 6964.
14. M. Ortiz, A. Fragoso and C.K. O'Sullivan, Anal. Chem., **2011**, 83, 2931.
15. M. Ortiz, M. Torréns, N. Alakulppi, L. Strömbom, A. Fragoso and C. K. O'Sullivan, Electrochem. Commun, **2011**, doi:10.1016/j.elecom.2011.03.014

16. A. Fasano and C. Catassi, Gastroenterology, **2001**, 120, 636

17. L. M. Sollid, Ann. Rev. Immunol., **2000**, 18, 53

18. A. Fragoso, B. Sanromà, M. Ortiz and C.K. O'Sullivan, Soft Matt., **2009**, 5, 400

19. A.U. Moozyckine, J.L. Bookham, M.E. Deary and M.D. Davies, J. Chem. Soc., Perkin Trans., **2001**, 2, 1858

20. W.C. Cromwell, K. Bystrom, and M. R. Eftink , J Phys Chem, **1998**, 589, 326.

CHAPTER 3

AMPEROMETRIC SUPRAMOLECULAR GENOSENSOR SELF-ASSEMBLED ON CYCLODEXTRIN-MODIFIED SURFACES

(Electrochem Comm, 2011, 13, 578-581)

CHAPTER 3

AMPEROMETRIC SUPRAMOLECULAR GENOSENSOR SELF-ASSEMBLED ON CYCLODEXTRIN-MODIFIED SURFACES

3.1 ABSTRACT

In this chapter a novel genosensor platform based on supramolecular interactions has been developed based on the self-assembly of bifunctionalised polymer bearing adamantane and DNA onto cyclodextrin surfaces. The surface chemistry can undergo a controlled regeneration, as revealed by SPR and impedance spectroscopy, has an excellent detection limit of 0.08 nM and demonstrated high selectivity, clearly differentiating between complementary and non-complementary DNA sequences. The performance of the developed genosensor was validated by applying it to the detection of DNA in a real patient sample that had been previously genotyped.

3.2 INTRODUCTION

Supramolecular architectures[1] are an attractive strategy for the construction of biosensor platforms as they facilitate the fabrication of highly organised molecular systems on surfaces and the design of novel functional materials and devices.[2] Recently, the host-guest interactions of cyclodextrins (CDs)[3] with size-compatible hydrophobic molecules have been used for the reversible immobilisation of different biomolecules based on the inclusion of adamantane (ADA) containing polymers, dendrimers or enzymes.[4] In this strategy, the CD/ADA host-guest complex docks the biological element to the surface of the transducer whilst also offering the possibility of a stepwise surface regeneration to re-use the supramolecular platform.[5] This method has been employed to immobilise proteins such as cytochrome c[6] and xanthine oxidase.[7] More recently, our group has reported the construction of a tri-dimensional catalytic biosensor surface based on the layer-by-layer technique,[8] in which successive layers of enzyme-adamantane conjugates are deposited on a CD-modified surface using CD-coated gold nanoparticles as the gluing element.

To the best of our knowledge, this type of supramolecular architecture has not been applied to the construction of DNA biosensors. Here we report a novel strategy for the construction of

genosensors exploiting the interfacial self-assembly of ADA-modified carboxymethylcellulose (CMC) polymers on CD-modified surfaces. We exemplify this approach in the construction of a genosensor, where the self-assembled polymer is modified with an oligonucleotide capture probe, which acts as the biorecognition element. The target DNA is detected by hybridisation in a sandwich format, between the capture probe and an enzyme labelled reporter probe (**Figure 3.1**).

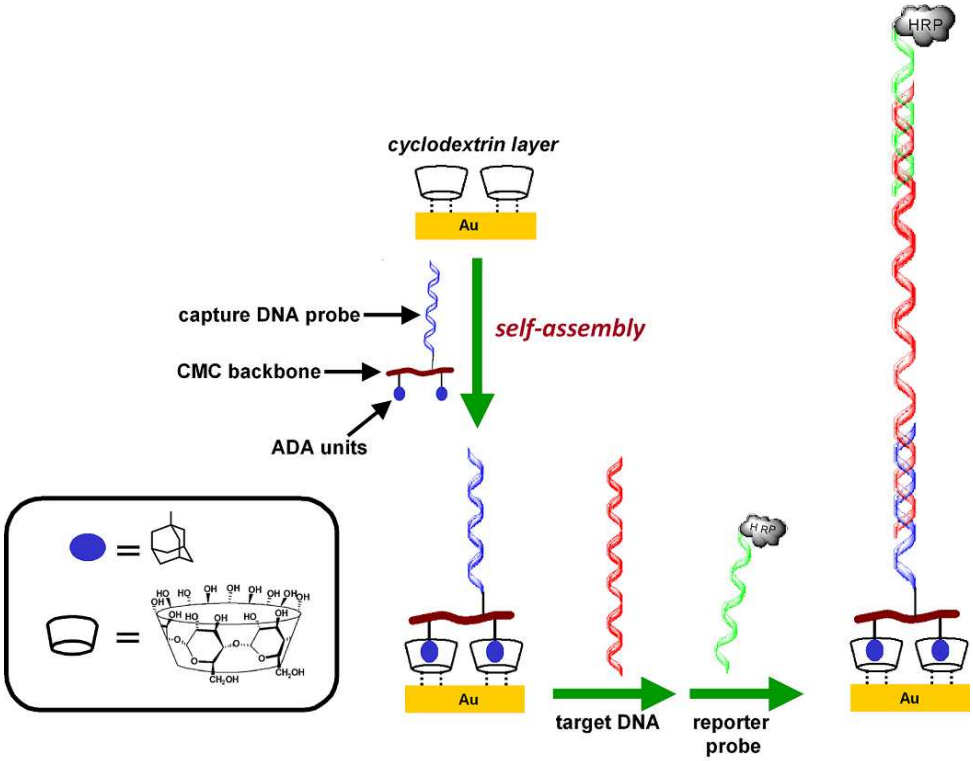

Figure 3.1. Strategy employed for the construction of the supramolecular genosensor.

The surface was characterised using surface plasmon resonance (SPR) and electrochemical impedance spectroscopy (EIS). The genosensor platform was applied to the detection of a human leukocyte antigen allele associated with celiac disease,[9] an autoimmune condition of known genetic predisposition.[10]

3.3 EXPERIMENTAL SECTION

Materials

Cyclodextrins were a gift from Wacker Chemie (Germany). Thiolated α, β and γ –cyclodextrin polymers (CDPSH)[8] and aminated CMC (CMC-NH_2)[11] were prepared as reported. Synthetic oligonucleotides were purchased from Biomers.net (Ulm, Germany) with the following sequences:

HLA-DQA1*0201 aminated capture probe: NH_2-$(CH_2)_6$-5'-CAA ATC TAA GTC TGT GGA-3'

HLA-DQA1*0201 target: 5'- GAG AGG AAG GAG ACT GTC TGG AAG TTGttg CCT CTG TTC CAC AGA CTT AGA TTT GAC CCG CAA TTT GCA CTG ACA AAC ATGatg GCT GTG CTA AAA CAT A-3'

HLA-DQA1*0201 HRP-labeled probe: 5'-GAC AGT CTC CTT CCT CTC-HRP-3'

Instrumentation and methods

Synthesis of modified CMC carrying adamantane and DNA (ADA-CMC-DNA)

0.5 g of adamantane carboxylate sodium salt dissolved in 0.1 M acetate buffer pH 5 were treated at 4°C with 0.5 g of EDC for 1 hour and added dropwise over a solution of CMC-NH_2 [11] (0.5 g) in 2 mL carbonate buffer pH 9 under stirring conditions overnight. The mixture was dialysed against water and concentrated to dryness to give ADA-CMC (Yield: 0.8 g). IR (ATR): 3310 (υ_{O-H}), 2931 (υ_{C-H}), 1106 (υ_{C-O}), 1579 ($\upsilon_{C=O}$). ^{1}H-NMR (300 MHz, D_2O, 300 K) δ (ppm): 0.5-1.2 (m, adamantane protons); 2.0-3.2 (m, $N(CH_2)_6N$); 3.2-4.6 (m, glucose skeletal protons). 4.9-5.3 (anomeric protons). Integration of the protons in the 0.5-1.2 ppm region with respect to the anomeric protons (δ = 4.9-5.3 ppm) indicate an average of 0.9 adamantane residues per glucose unit.

To attach the DNA probe, 0.5 g of ADA-CMC in 5 mL of 0.1 M acetate buffer pH 5 was activated with 0.5 g of EDC and the mixture stirred for 1 hour at 4ºC. The DNA probe was conjugated by adding 500 μL of 0.5 mM HLA-DQA1*0201 aminated capture probe and the solution stirred overnight. The ADA-CMC-DNA conjugate was purified using a Microcon® centrifugal filter device (MW cut-off 10 kDa) and absence of DNA in the residual water was

tested using UV spectroscopy. The obtained stock solution was stored at -20 ºC. The amount of DNA attached to ADA-CMC (0.012 mol of DNA per mol of glucose unit) was estimated using UV-Vis spectroscopy at 260 nm.

Surface plasmon resonance

SPR studies were carried out using a Biacore® 3000 instrument at 20°C. Clean gold chips were modified overnight with a 10 mg/mL solution of thiolated cyclodextrin polymers, mounted in the Biacore support and a 5 μL/min flow of running buffer (10 mM PBS pH 7.4) was established. After baseline stabilisation a layer of ADA-CMC-DNA polymer was created by injecting a 1 mg/mL solution in PBS. Target hybridisations (0.5 and 1 nM) were followed by a denaturation step in 10 mM NaOH. The CDPSH surface was regenerated with 0.1% v/v sodium dodecylsulfate (SDS).

Measurements

Electrochemical measurements were performed using a standard three-electrode configuration; working electrode: gold disk (ϕ = 1.6 mm), reference electrode: Ag/AgCl(sat), counter electrode: Pt wire. The gold electrodes were polished three times with alumina slurry (1, 0.5, 0.03 μm) followed by cleaning in hot *Piranha's* solution (30 % H_2O_2/H_2SO_4 (conc) = 3/1 (v/v)) for 5 minutes (*Warning: Piranha's solution is very corrosive)*.

To modify the electrodes, 100 μL of a 10 mg/mL βCDPSH solution were incubated on the electrodes overnight. After rinsing with water, 100 μL of ADA-CMC-DNA (0.1 mg/mL) were incubated overnight. The next incubation steps were carried out immediately prior to the amperometric measurements. For this purpose, 100 μL of HLA-DQA1*0201 target (previously heated at 70ºC to disrupt any self-folding) at different concentrations (0, 0.1, 0.2, 0.5, 0.75, 1, 1.5, 2, 5 nM) in PBS pH 7.4 containing NaCl 0.8 M were incubated with the surface modified genosensor for 1 hour at 37ºC. Following another rinse with water, a 100 nM solution of HLA-DQA1*0201 HRP-labelled probe was added and the genosensor was incubated for 1 hour at 25ºC. The amperometric measurements were carried out by first recording the background response at 0.2 V in PBS buffer pH 6 followed by injection of 1 mM TMB/H_2O_2 in 0.1 M PBS pH 6 + 0.15 M KCl.

3.4 RESULTS AND DISCUSSION

The formation of the interfacial supramolecular platform involves a two-step process: i) deposition of βCDPSH on bare gold electrodes, ii) supramolecular capture of ADA-CMC-DNA by ADA/CD host-guest interactions. The deposition of a SAM of βCDPSH was confirmed via observation of a cathodic desorption peak of the thiolated polymer at -1.02 V in alkaline solution (0.5 M KOH), the integration of which indicated a surface concentration of 2×10^{-12} mol/cm^2. This translates into 2.4×10^{-11} mol/cm^2 of cyclodextrin units taking into consideration that each βCDPSH molecule has ~12 mol of cyclodextrin per mol of polymer, which is in the same order of magnitude of the surface coverage of a monolayer of hepta-6-thio-6-deoxy-β- cyclodextrin.[12]

Electrical impedance spectroscopy (EIS) is a powerful tool to study bimolecular interactions at interfaces.[13] The formation of the interfacial supramolecular platform was confirmed using EIS by observing the variations of the charge transfer resistance (Rct) exerted by the deposition of the successive layers on an electroactive ferricyanide probe (**Figure 3.2**). Deposition of a SAM of βCDPSH caused a 175 kΩ increase in R_{ct} with respect to the bare electrode (R_{ct} = 2 kΩ). The Rct values further increased to 348 kΩ after interaction of the βCDPSH-modified surface with ADA-CMC-DNA and then to 530 kΩ after capture of the HLA-DQA1*0201 target sequence by the Au/ βCDPSH/ADA-CMC-DNA surface. In contrast, the interaction of ADA-CMC-DNA with a αCDPSH-modified surface provoked only a 6 % variation in R_{ct}, indicating that the immobilised αCD hosts cannot recognise the ADA polymer, in agreement with the SPR results (see below).

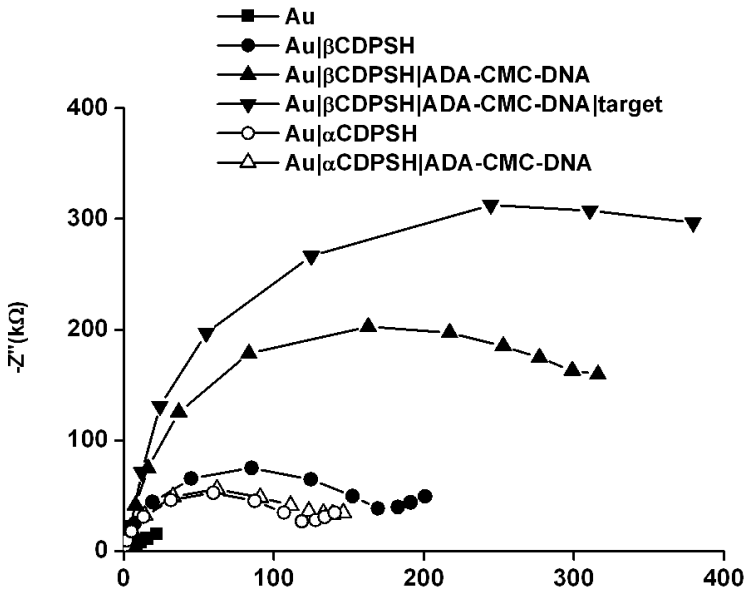

Figure 3.2. Complex impedance plots (in 1 mM $K_3Fe(CN)_6$ in 0.1 M KCl) obtained alter successive electrode modifications.

The interaction of ADA-CMC-DNA carrier with βCDPSH was also studied by surface plasmon resonance (SPR) (**Figure 3.3**).

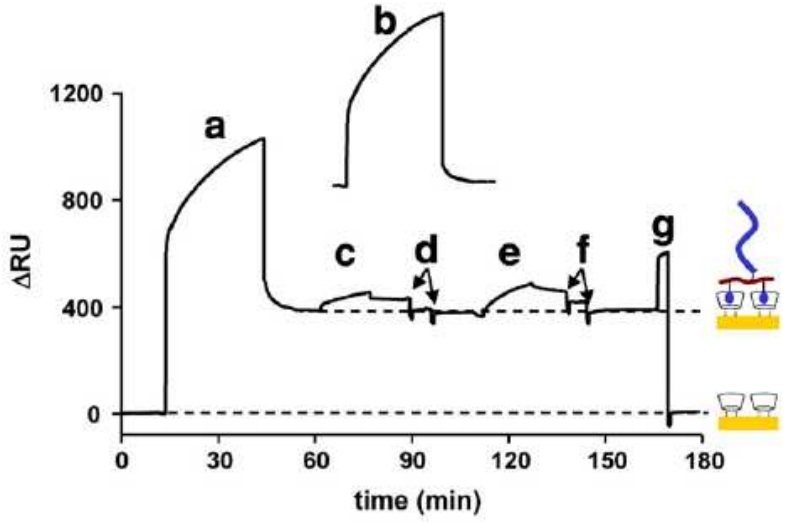

Figure 3.3. SPR sensorgram of injections of (a) 1 mg/mL βCDPSH, (b) 1 mg/mL βCDPSH, c) 0.5 nM HLA-DQA1*0201 target, (d) 10 mM NaOH pulses, (e) 1 nM HLA-DQA1*0201 target, (f) 10 mM NaOH pulses, (g) 0.1% SDS. Conditions: running buffer: 0.1 M PBS pH 7.4, flow rate 5 µL/min.

The individual channels of an SPR Au chip were modified with α, β and γCDPSH polymers. When ADA-CMC-DNA was injected to the βCDPSH- modified channel, a significant response of 400 RU was observed (**Figure 3.3a**). Assuming the equivalence 1 RU = 1 pg/mm^2,[14] this response affords a surface coverage of ~2×10^{-13} mol/cm^2 assuming a molecular weight for ADA-CMC-DNA of 205 kDa, corresponding to a CMC polymer of molecular weight 90 kDa and a degree of substitution of 0.9 adamantane and 0.012 oligonucleotide probes per glucose unit, respectively. This represents a probe density of ~ 1.2×10^{11} molecules/ cm^2, which is in the typical range of 10^{11}–10^{13} molecules/cm^2 considered to be the optimal to avoid inter-probe electrostatic repulsions on the surface.[15] The SPR response obtained with βCDPSH markedly differs from those observed with αCDPSH (19 RU, **Figure 3.3b**) and γCDPSH (25 RU) modified surfaces. These differences are explained by the lower association constants (about two orders of magnitude) observed for ADA derivatives with αCD (smaller cavity) and γCD (larger cavity) compared with βCD (K_{ass} = 4×10^5 M^{-1}), due to an optimum geometric matching of cavity size and ligand size in the ADA/βCD system.[16] In addition, when a CMC-DNA polymer (i.e. not carrying ADA units) was injected on the βCDPSH-modified surface, a very small response was obtained (11 RU). Finally, no interaction with the βCDPSH modified surface was observed by SPR using a CMC polymer prepared in a similar manner to ADA-CMC but modified with a bulkier residue (3,5,7-trimethyladamantane-1-carboxylic acid). The selectivity observed in the interaction of the ADA-CMC-DNA polymer with the different surfaces and the lack of response in the absence of ADA units or presence of bulkier residues clearly indicate that the ADA-CMC-DNA polymer is immobilised on the βCDPSH surface via specific ADA-βCD host–guest interactions.

Injection of 0.5 nM of target to a channel modified with the Au/ βCDPSH/ADA-CMC-DNA supramolecular platform gave a response of 44 RU (**Figure 3.3c**). The biosensor surface could be regenerated by applying two pulses of 10 mM NaOH to denature the formed DNA duplex. This restored the SPR signal at ~ 400 RU corresponding to the Au/βCDPSH/ADA-CMC-DNA surface, which indicates that the ADA- βCD assembly is essentially unaltered (**Figure 3.3d**). Subsequently 1 nM of target was injected, obtaining 90 RU, a value that is in good correspondence with the value obtained with 0.5 nM target (**Figure 3.3e**). Finally, the DNA probe surface was again regenerated in alkaline conditions (**Figure 3.3f**), demonstrating the reusability of the biosensor surface. Whilst it is not envisaged that the genosensor would be re-used when applied to clinical diagnostics, re-usability of the sensor surface is very useful during developmental work. Injection of a 0.1 % v/v solution of SDS caused desorption of

ADA-CMC-DNA from the cyclodextrin support, rendering it available to capture a new probe layer (**Figure 3.3g**).

The developed βCDPSH/ADA-CMC-DNA surface was then applied to the amperometric detection of the HLA-DQA1*0201 target sequence using a peroxidase-labelled secondary probe as reporter.

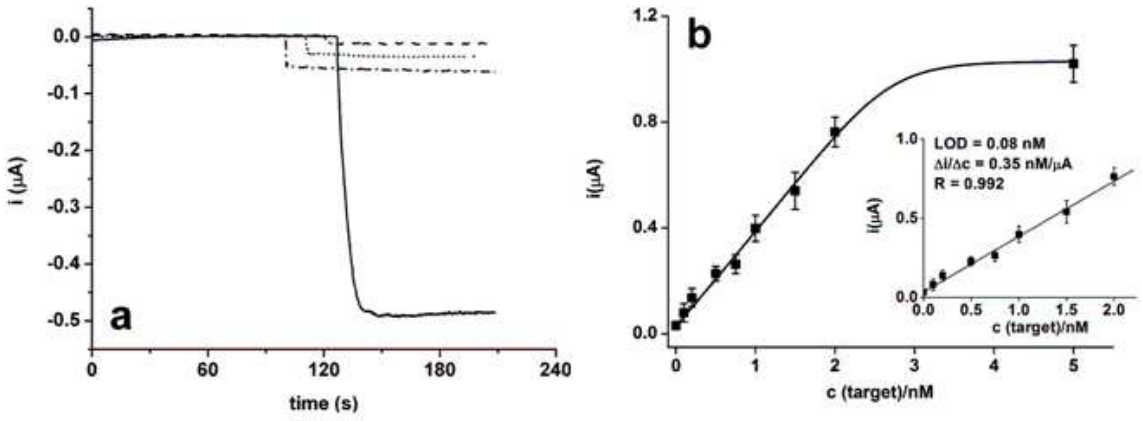

Figure 3.4. a) Amperometric responses for the detection of HLA-DQA1*0201 sequence in the presence (——) and absence of target (-------), absence of cyclodextrin support (·-·-·-·-·-·) and in the presence of a non-complementary target (·····). b) Calibration curve for the amperometric detection of HLA-DQA1*0201 target sequence.

Figure 3.4a shows a comparison of the specific (presence of target) and non-specific (absence of target) signals obtained. The non-specific signal represented only 4 % of the specific signal obtained at 1 nM concentration, indicating a very low tendency of the reporter probe to interact with the surface in the absence of target. In addition, when the βCDPSH support layer was not present, a signal about 10 % was observed demonstrating the importance of the cyclodextrin layer in assisting the immobilisation of the probe. Three possible interference sequences were added in place of the target and only ~5 % of the signal was observed, demonstrating the high selectivity of this biosensor.

Figure 3.4b shows the calibration curve obtained with the βCDPSH/ADA- CMC-DNA modified surface, which was linear in the range 0–2 nM with a sensitivity of 0.35 nM/μA and a limit of detection of 80 pM. A preliminary study was carried out using a real PCR-amplified sample of a coeliac patient, who had been previously genotyped and shown to carry the HLA-

DQA1*0201 allele using Luminex based HLA typing. Single stranded DNA was generated via exonuclease digestion and directly applied to the electrode surface and the quantitative result obtained compared to enzyme linked oligonucleotide assay, showing a high degree of correlation with values of 0.75 ± 0.09 nM) and 0.86 ± 0.05 nM, obtained respectively, demonstrating the genosensor to have detection limits that easily allow it to be applied to the direct analysis of real PCR products. Negligible performance changes (<5 %) were observed for the supramolecular biosensor in the detection of 1 nM of target sequence after one week of storage at 4 °C in a commercial stabilising buffer (StabilCoat® Plus Microarray Stabilizer), indicating an excellent stability of the self-assembled structure.

3.5 CONCLUSIONS

A novel biosensor platform based on supramolecular interactions has been developed for genosensor construction based on the self-assembly of bi-functionalised polymer bearing adamantane and DNA onto cyclodextrin surface. The developed amperometric genosensor has an excellent LOD of 0.08 nM as well as high selectivity and was applied to the detection of DNA in a real patient's sample. The combination of a hydrophilic support layer (βCDPSH) with the controlled attachment of the capture probe to a polymeric backbone minimises non-specific interactions and provides an optimal probe separation to avoid electrostatic repulsions, which is essential in the development of DNA biosensors. The CMC backbone allows an optimal spacing of the DNA probes to avoid steric hindrance for target binding due to an excessively dense layer of probe DNA, with the negative charge of the CMC vertically orienting the probe, and the combination of the CD and the CMC facilitate maximal binding of the target DNA. The work reported here highlights the feasibility of using cyclodextrin based supramolecular surface chemistries for the detection of DNA and the work is being extended to the multiplexed, microsystem packaged, genosensor array with a focus on reducing hybridisation time and the number of PCR cycles required.

3.6 REFERENCES

1. J.M. Lehn, Supramolecular Chemistry. Concepts and Perspectives, **1995**, Wiley-VCH,.
2. L. C. Palmer, Y. S. Velichko, M. O. Cruz, and S. I. Stupp, Phil. Trans. Royal Soc. A., **2007**, 365, 1417.
3. J. Szejtli, Chem. Rev., **1998**, 98, 1743.
4. R. Villalonga, R. Cao, and A. Fragoso, Chem. Rev., **2007**, 107, 3088.
5. O. Crespo-Biel, B. J.Ravoo, D. N. Reinhoudt, and J. Huskens, J. Mater. Chem., **2006**, 16, 3997.
6. Fragoso, J. Caballero, E. Almirall, R.Villalonga, and R. Cao, Langmuir, **2002**,18, 5051.
7. R. Villalonga, M. Matos, and R. Cao, Electrochem. Comm., **2007**, 9, 454.
8. A. Fragoso, B. Sanromà, M. Ortiz, and C. K. O'Sullivan, Soft Matt., **2009**, 5, 400.
9. A. Fasano, and C. Catassi, Gastroenterology, **2001**,120, 636.
10. L. M. Sollid, Ann. Rev. Immunol., **2000**, 18, 53.
11. H. L. Ramirez, R. Cao, A. Fragoso, J. J. Torres-Labandeira, A. Dominguez, E. H. Schacht, M. Baños, and R. Villalonga, Macromol. Biosci., **2006**, 6, 555.
12. M. T. Rojas, R. Koniger, J. F. Stoddart, and A. E. Kaifer, J. Am. Chem. Soc., **1995**, 117, 336.
13. E. Katz, and I. Willner, Electroanalysis, **2003**, 15, 913.
14. E. Stenberg, B. Persson, H. Roos, and C. Urbaniczky, J. Colloid. Interface Sci., **1991**, 143, 513.
15. J. J. Gooding, Electroanalysis, **2002**, 14, 1149.
16. W. C. Cromwell, K. Byström, and M. R. Eftink, J. Phys. Chem., **1985**, 89, 326.

CHAPTER 4

SUPRAMOLECULAR CONFINEMENT OF POLYMERIC ELECTRON TRANSFER MEDIATOR ON GOLD SURFACE FOR PICOMOLAR DETECTION OF DNA

(Soft Matter, 2011, 7, 10925-10932)

CHAPTER 4

SUPRAMOLECULAR CONFINEMENT OF POLYMERIC ELECTRON TRANSFER MEDIATOR ON GOLD SURFACE FOR PICOMOLAR DETECTION OF DNA

4.1 ABSTRACT

In this chapter a novel route for the immobilisation of an electron transfer mediator on electrode surfaces based on the interfacial complexation of a bifunctionalised carboxymethylcellulose (CMC) polymer backbone bearing ferrocene units and a DNA probe on a cyclodextrin-functionalised surface is described. The interfacial self-assembly has been studied using surface plasmon resonance and electrochemical techniques and the applicability of the modified surface for the construction of an amperometric genosensor was explored for the detection of a celiac disease associated allele. The supramolecular strategy simplifies the operation of the biosensor, only requiring the addition of enzyme substrate and the proximity of the mediator to the electrode surface greatly improves the detection limits attained (10 pM) with respect to a similar supramolecular system based on electrochemically inactive adamantane/CD inclusion complexes (80 pM) and requiring addition of the mediator in solution. In addition, the use of the hydrophilic CMC backbone contributes to the elimination of non-specific interactions and to an optimal spacing of the immobilised DNA probes.

4.2 INTRODUCTION

Supramolecular strategies based on self-assembly and host-guest interactions[1] have recently attracted great interest as surface modification tools to achieve pre-organization and improved functional properties in a vast array of molecular assemblies.[2] An interesting approach to construct organized structures on surfaces exploits the formation of host-guest pairs using molecular receptors (cyclodextrins, calixarenes, cyclotriveratrylenes, etc.), allowing the self-assembly of two-dimensional[3-8] and three-dimensional nanoarchitectures.[9-12] These systems have been used for the immobilisation of different molecules, rendering functional structures with high specificity and affinity. In the case of cyclodextrins (CD),[13] supramolecular immobilisation is in most cases achieved by the interaction of adamantane-appended

bifunctional linkers or biomolecule conjugates with a surface modified with a monolayer of thiolated CD.[14] This method has been employed to immobilise proteins such as cytochrome c[15] and streptavidin[10] or for the construction of catalytic biosensors.[16,18] Recently, we reported a supramolecular genosensor for the detection of a human leukocyte antigen allele associated with celiac disease based on the self-assembly over a cyclodextrin surface of a bifunctionalised polymer bearing adamantane units and a DNA probe.[19] Using amperometric detection, a very low limit of detection (LOD) of 80 pM was obtained and the genosensor was validated using a previously genotyped patient sample.

Ferrocene (Fc) is a redox active metallocene commonly used as an electron transfer mediator in oxidase-based biosensors as it undergoes reversible one-electron oxidation at a low potential to give a ferrocenium cation. Fc moieties have been incorporated on electrode surfaces for the construction of reagentless biosensors via anion-exchange of ferrocenecarboxylate on polypyrrole films,[20] layer-by-layer deposition of Fc-terminated dendrimers,[21] casting of Fc-polysaccharide derivatives,[22] sol-gel,[23] and carbon nanotube[24] composites, among others. The supramolecular deposition of linear Fc-functionalized polymers derived from chitosan and poly(allylamine)[25] and Fc-appended biotin terminated linkers[26] on gold surfaces modified with b-cyclodextrin has recently been reported, where a quartz crystal microbalance coupled with cyclic voltammetry was used to monitor the deposition of the Fc-polymers and their subsequent desorption, triggered by the in situ oxidation of the Fc moieties that destabilize the inclusion complex. In another report, layer-by-layer polymer films based on host-guest interactions were formed by the stepwise adsorption of poly(allylamine) and poly(*N*-hydroxypropylmethacrylamide) derivatives bearing ferrocene or β-cyclodextrin moieties.[27]

Here we report the interfacial complexation of a Fc-containing polymer backbone on a cyclodextrin surface and explore its applicability in the construction of an amperometric genosensor for the detection of DNA (**Figure 4.1**). A bifunctionalised carboxymethylcellulose (CMC) polymer tethers ferrocene units on one side and a short linear DNA probe on the other. The target DNA sequence is then detected via hybridization to the immobilised probe using a reporter probe labelled with horseradish peroxidase (HRP) in a sandwich type format. Thus, the Fc residues present in the structure of the self-assembled platform not only serve to dock the polymer structure on the CD-surface by via inclusion complexation but also act as an electron transfer mediator for the peroxidise label and the

interfacial association constants are measured by surface plasmon resonance (SPR). As a model detection system, we selected a target oligonucleotide sequence belonging to the human leukocyte antigen HLA-DQA1 allele family, which is associated to celiac disease,[28] an autoimmune condition showing almost 100% genetic predisposition.[29,30] As a consequence of the proximity and confinement of the Fc mediator at the electrode surface, a significant signal enhancement and a markedly lower detection limit are observed as compared to the use of a solution-based mediator.

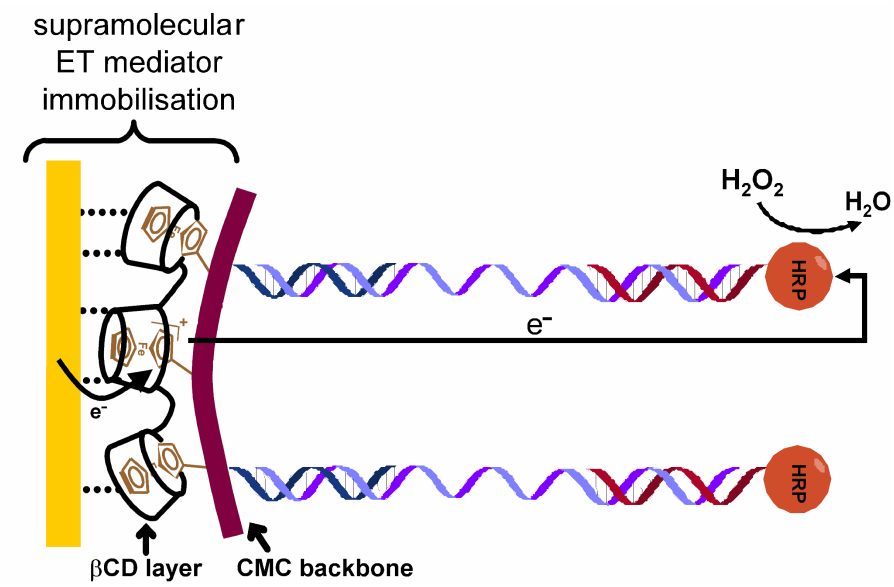

Figure 4.1 Strategy employed for the supramolecular immobilisation of electron transfer mediator.

4.3 EXPERIMENTAL SECTION

Materials

All reagents used were commercially available and used as received. Carboxymethylcellulose (CMC, MW 90 kDa), N-Ethyl-N′-(3-dimethylaminopropyl)carbodiimide hydrochloride (EDC), Phosphate Buffered Saline (PBS) dry powder and ferrocenecarboxaldehyde were purchased from Sigma-Aldrich. All solutions were prepared with Milli-Q water (Millipore Inc., Ω = 18 MΩ·cm). Thiolated α, β and γ cyclodextrin polymers were prepared as previously reported.[17] The synthesis of Fc-appended CMC conjugate bearing DNA probes is depicted in **Scheme 4.1.**

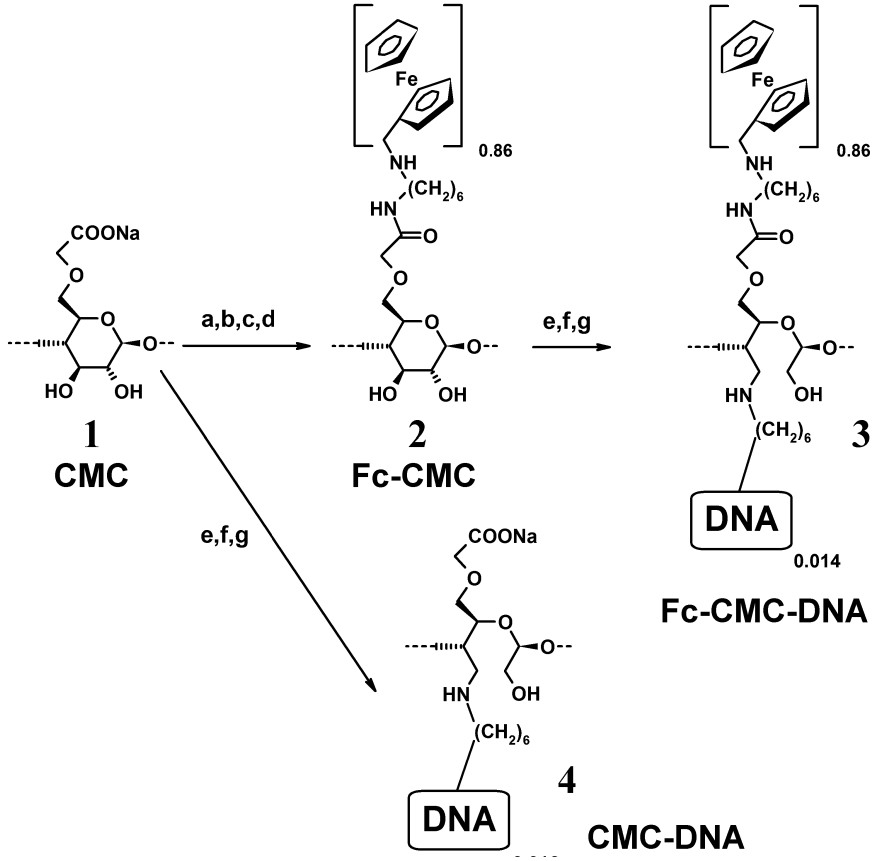

Scheme 4.1. Synthesis of Fc-modified polymers: a) EDC, b) 1,6-diaminohexane, c) Fc-CHO, d) $NaBH_4$, e) $NaIO_4$, f) aminated DNA, g) $NaCNBH_3$.

Synthetic oligonucleotides were purchased from Biomers.net (Ulm, Germany) and their sequences are shown below:

HLA-DQA1*0201 aminated capture probe: NH_2 C_6-5'-CAA ATC TAA GTC TGT GGA-3'.

HLA-DQA1*0201 target: 5'- GAG AGG AAG GAG ACT GTC TGG AAG TTG CCT CTG TTC CAC AGA CTT AGA TTT GAC CCG CAA TTT GCA CTG ACA AAC ATG GCT GTG CTA AAA CAT A-3'.

HLA-DQA1*0201 HRP-labeled probe: 5'- GAC AGT CTC CTT CCT CTC-HRP-3'.

Interference 1: 5'-GAG AGG AAG GAG ACT G**C**C TGG **CG**G T**G**G CCT **GA**G TTC

AGC A**A**A **T**TT GGA GGT TTT GAC CCG CAG GGT GCA CTG AGA AAC ATG GCT GTG GCA AAA CAC A-3'.

Interference 2: 5'-GAG AGG AAG GAG ACT GTC TGG CAG TTG CCT CTG TTC CGC AGA TTT AGA AGA TTT GAC CCG CAA TTT GCA CTG ACA AAC ATC GCT GTG CTA AAA CAT A-3'.

Interference 3: GGG AGG AAG GAG ACT GTC TGG TGT TTG CCT GTT CTC AGACAA TTT AGA TTT GAC CGG CAA TTT GCA CTG ACA AAC ATC GCT GTC CTA AAA CAC A-3'.

Instrumentation and methods

Synthesis of Fc-CMC (2)

0.5 g of aminated CMC[31] (1.5 mmol of aminohexane groups) were dissolved in 25 mL of Milli-Q water. A solution of 0.32 g (1.5 mmol) of ferrocenecarboxaldehyde in 2 mL of DMSO was added dropwise with continuous magnetic stirring. After 3 hours an excess (60 mg, 15 mmol) of sodium borohydride was added and the solution was stirred overnight at room temperature. The mixture was concentrated to about half the initial volume by roto-evaporation and dialysed for 24 hours to remove impurities and was then dried *in vacuum* to give Fc-CMC (Yield: 0.31 g). ^{1}H-NMR (300 MHz, D_2O, 300 K) δ (ppm): 1.9-3.2 (m, Fc-C*H*$_2$-N, N(C*H*$_2$)$_6$N); 3.2-4.6 (m, overlapped Fc and glucose skeletal protons). 4.9-5.3 (m, anomeric protons). ^{13}C-NMR (75 MHz, D_2O, 300 K); 169 (bs, N*C*=O), 181 (bs, O*C*=O). UV-Vis: λ_{max} 430 nm (e = 1700 cm·M^{-1}, Fc M→L charge transfer). The amount of Fc units in **2** (0.86 mol Fc/mol glucose) was estimated by UV-Vis spectroscopy at 400 nm by interpolation of absorbance values of a polymer solution in a calibration curve prepared using aminoferrocene.

Synthesis of Fc-CMC-DNA conjugate (3)

Sodium meta-periodate (20 mg) was added to **2** (20 mg) in water (5 mL) and stirred for 3 hours at room temperature, followed by overnight dialysis to remove non-reacted material. The dialysed solution (containing aldehyde-activated Fc-CMC) was used in the next step. The presence of aldehyde groups was qualitatively confirmed using 2,4-dinitrophenylhydrazine. The dialyzed solution was treated with 2.5 μmol of HLA-DQA1*0201 aminated capture probe under stirring for 3 hours, after which 10 mg of sodium cyanoborohydride were added and the

solution was stirred overnight. The Fc-CMC-DNA conjugate was purified using a Microcon® centrifugal filter device (Mw cut-off 10 kDa) for 3 minutes at 10000 rpm and washed twice with water. The absence of DNA in the filtrate was confirmed using UV spectroscopy at 260 nm and the obtained stock solution was stored at -20 ºC. The amount of DNA in Fc-CMC-DNA (0.014 mol of DNA per mol of glucose unit) was estimated using UV-Vis spectroscopy at 260 nm by interpolation of Fc-corrected absorbance values of a solution of Fc-CMC-DNA in a calibration curve prepared using HLA-DQA1*0201 aminated capture probe and considering that the molecular weight of the probe is 5700 Da. To correct the absorbance at 260 nm from the contribution of Fc, solutions of Fc-CMC-DNA and Fc-CMC having identical absorbance at 430 nm (where only Fc absorbs) were prepared and the absorbance at 260 nm of the Fc-CMC solution was subtracted from Fc-CMC-DNA to calculate the contribution of DNA to the overall absorbance at this wavelength.

Synthesis of CMC-DNA conjugate (4)

CMC (10 mg) dissolved in 5 mL of water were treated with 20 mg of sodium meta-periodate with stirring at room temperature. DNA probe was attached in a similar way as described for the synthesis of **3**. The CMC-DNA conjugate contained 0.012 mol of DNA per mol of glucose unit and was purified as described above.

Surface plasmon resonance (SPR) studies.

SPR studies were carried out using a Biacore® 3000 instrument operating at 25°C. Gold chips from a Biacore SIA kit were cleaned with Piranha's solution (*Warning: Piranha's solution is very corrosive)* for 3 minutes, washing with water, followed by thorough washing with water and finally treated with ozone using a PSD-UVT cleaning instrument (from Novascan, USA) for 9 min, rinsed with ethanol and dried under a filtered Ar stream. The chip was modified with thiolated cyclodextrin polymer (CDPSH) by overnight immersion in a 10 mg/mL solution followed by extensive rinsing with water, after which the chip was mounted in the Biacore support and a 5 μL/min flow of running buffer (10 mM PBS pH 7.4) was established. After baseline stabilisation (~ 3 hours) a layer of Fc-CMC-DNA polymer was created by injecting 50 μL of a 1 mg/mL solution in PBS followed by HLA-DQA1*0201 target injection (1 nM in PBS pH 7.4 containing NaCl 0.8 M). Surface regeneration was carried out using 10 mM NaOH to dehybridise the target-probe complex or 1 mM adamantanecarboxylate to remove the Fc-containing polymer from the surface.

Electrochemical Instrumentation

Electrochemical measurements were performed on a PC controlled PGSTAT12 Autolab potentiostat (EcoChemie, The Netherlands) with a built-in frequency response analyzer FRA2 module using a standard three-electrode configuration (working electrode: gold disk, reference electrode: Ag/AgCl(sat), counter electrode: Pt wire).

The gold disk electrodes (f = 1.6 mm, from Bioanalytical Systems) were first polished three times with alumina slurry (1, 0.5, 0.03 μm) until a mirror finish was obtained. After sonication in water for one minute, the electrodes were cleaning in hot *Piranha* solution (30% H_2O_2/H_2SO_4(conc) = 3/1 (v/v)) for 5 minutes (*Warning: Piranha solution is very corrosive)*. The electrodes were then electrocleaned by applying a series of 40 potential cycles in 1 M H_2SO_4 in the range 0-1.7 V vs Ag/AgCl at 0.2 V/s. The quality of the cleaning step was checked using cyclic voltammetry in 1 mM $K_3[Fe(CN)_6]$ in 0.1 M KCl.

Modification of gold electrodes and DNA detection

In a first step, 100 μL of a 10 mg/mL CDPSH solution was incubated on the electrodes overnight to form a self assembled monolayer (SAM) containing cyclodextrin hosts. After rinsing with water, 100 μL of Fc-CMC-DNA (1 μg/mL) was added and incubated overnight. The next incubation steps were carried out immediately prior to the amperometric measurements. One hundred microlitres of HLA-DQA1*0201 target at different concentrations (0 - 5 nM) in PBS pH 7.4 containing NaCl 0.8 M were incubated for 1 hour at 37 ºC. Before each incubation, the target solution was briefly heated to 70 ºC (above the melting temperature measured spectrophotometrically) in order to disrupt any self-folding. After rinsing with PBS, 100 μL of a 100 nM solution of HLA-DQA1*0201 HRP-labeled probe was further incubated for 1 hour at 25 ^oC.

The amperometric measurements were carried out by first recording the background response at 0.2 V in PBS buffer pH 6 followed by injection of 1 mM H_2O_2 in 0.1 M PBS pH 6 in a 2 cm^3 cell.

4.4 RESULTS AND DISCUSSION

Preparation of ferrocene-appended polymeric DNA carrier

The synthesis of the Fc-CMC-DNA conjugate is shown in **Scheme 4.1**. CMC was chosen as a carrier polymer as it provides two individually addressable modification points for the attachment of the DNA probe and Fc residues: the COOH group in the C6 position and the vicinal diol group formed between C2 and C3. The COOH groups of the polysaccharide were activated with EDC followed by amidation with 1,6-diaminohexane, which acts as a spacer. The amino-terminated precursor was reacted with ferrocenecarboxaldehyde under reductive alkylation conditions resulting in the Fc-modified CMC polymer. This polymer was activated with sodium periodate to oxidise the diol groups yielding a reactive aldehyde intermediate that was further reacted with an amino-terminated DNA probe followed by reduction of the formed imino-bond with sodium cyanoborohydride to give the desired Fc-CMC-DNA conjugate. The amounts of Fc and DNA were estimated using UV-Vis spectroscopy, indicating 0.86 mol of Fc and 0.014 mol of DNA per mol of glucose unit. For comparison purposes, a CMC-DNA conjugate was prepared from CMC by oxidation with $NaIO_4$ followed by coupling with amino-terminated DNA in the same reductive alkylation conditions as used for the preparation of the Fc-CMC-DNA.

Electrochemical characterisation of Fc-CMC-DNA deposition

The cyclic voltammogram of the CDPSH/Fc-CMC-DNA platform in PBS buffer pH 7.4 showed a reversible signal at $E_{1/2}$ = 0.19 V with a peak-to-peak separation ΔE_{ac} of 24 mV (**Figure 4.2**). ΔE_{ac} is essentially scan rate independent up to 0.3 V/s and the peak currents depend linearly on scan rate, indicative of the presence of a surface confined species. The ΔE_{ac} value is slightly higher than the ideal value of 0 mV for a surface-confined reversible redox couple, which may be by considering the polydispersion of the Fc-CMC-DNA polymer that causes the existence of multiple formal potentials for the Fc/Fc^+ couple in the monolayer film. Integration of the cathodic peak (to calculate the charge associated with the process and thus the number of moles of Fc from the Faraday's Law) and normalisation to the electrode surface indicated a surface coverage for the Fc units of 4×10^{-15} mol/cm^2.

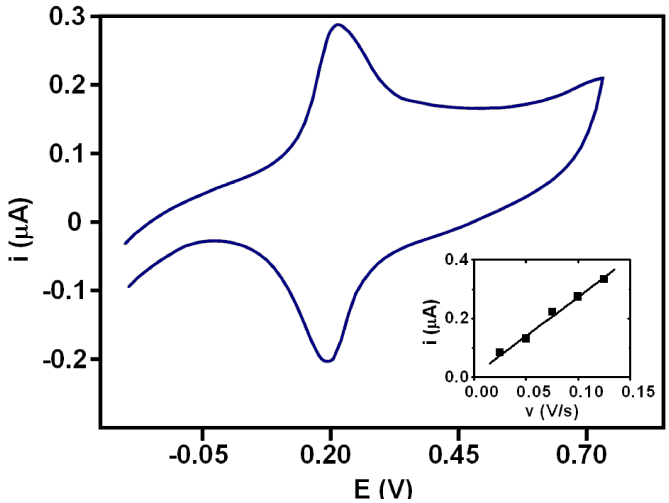

Figure. 4.2. Cyclic voltammogram (in 0.1 M PBS buffer pH 7.4, scan rate: 100 mV/s) obtained after the deposition of Fc-CMC-DNA on CDPSH-modified gold electrode. Inset: Dependence of peak currents with scan rate.

Surface plasmon resonance characterisation and measurement of interfacial association constants

The construction of the CDPSH/Fc-CMC-DNA platform was studied using surface plasmon resonance (**Figure 4.3**). Fc-CMC-DNA was injected into the chip previously modified with βCDPSH giving a SPR response of 433 RU (**Figure 4.3a**). This response affords a surface coverage of ~2×10^{-15} mol/cm^2 assuming a molecular weight for Fc-CMC-DNA of 213 kDa, which corresponds to a CMC polymer with 80% of COOH groups and a degree of substitution of 0.86 Fc and 0.014 DNA residues per glucose unit, respectively.

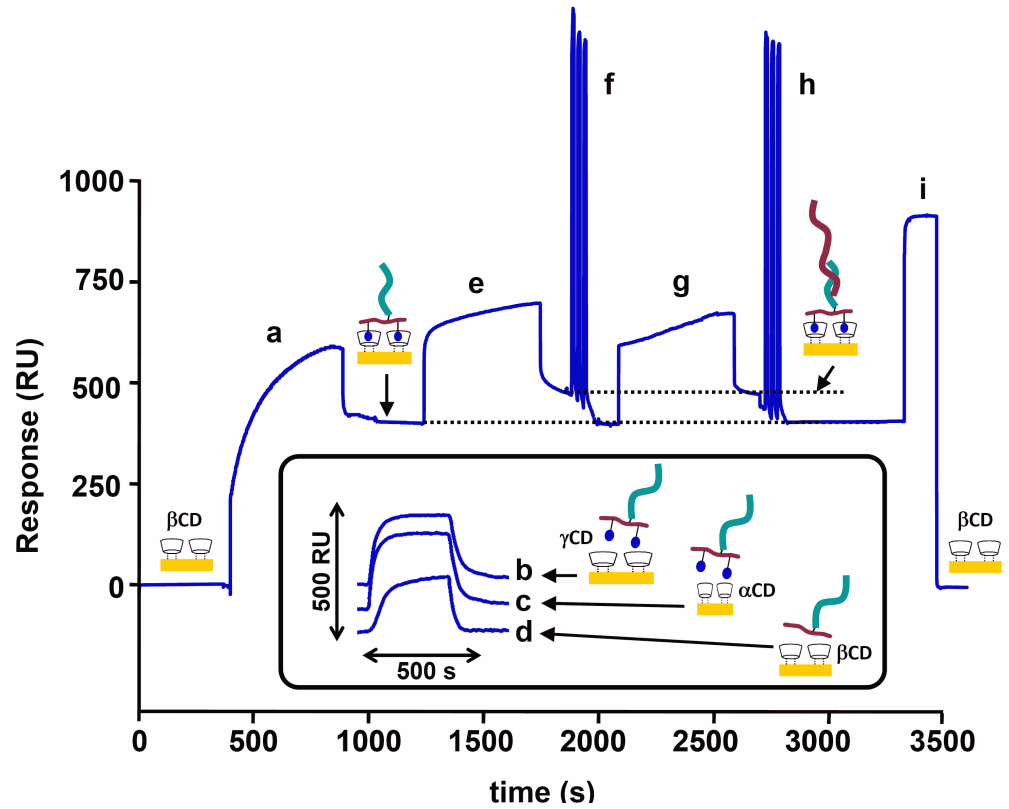

Figure. 4.3. SPR sensorgram for the immobilisation of Fc-CMC-DNA on bCDPSH surface (a), interaction of Fc-CMC-DNA with γCDPSH (b), and αCDPSH (c) modified surfaces, interaction of CMC-DNA with βCDPSH surface (d), injection of 1 nM HLA-DQA1*0201 target (e), regeneration of βCDPSH/Fc-CMC-DNA surface with three pulses of 10 mM NaOH (f), second 1 nM target injection (g), second NaOH regeneration (h) regeneration of βCDPSH surface with 1 mM adamantanecarboxylate (i). Conditions: running buffer: 0.1 M PBS pH 7.4, flow rate 5 mL/min.

The role of specific Fc/βCD interactions in the immobilisation of the Fc-CMC-DNA was confirmed by the low SPR signals observed due to its interaction with γCD (51 RU) or αCD (37 RU) modified surfaces (**Figure 4.3 b, c**). γCD and αCD have, respectively, larger and smaller cavity sizes as compared with βCD and, therefore, form weaker inclusion complexes.[32] This explains the marked difference in SPR response observed in the interaction of Fc-CMC-DNA with the three CD-modified surfaces and indicates a major contribution of specific Fc/βCD interactions in the immobilisation process. Due to the relative structural complexity of the DNA-modified polymer it can be expected that other types of interactions might occur between the Fc-CMC-DNA and the βCD-modified surface, such as hydrogen bonding to the amine, amide, and hydroxyl groups as well as non-specific hydrophobic interactions that do not involve inclusion of the Fc groups into

the βCD cavities. To assess the contribution of these interactions, a polymer that carries the DNA probe but lacks the Fc units (CMC-DNA), was prepared and allowed to interact with the βCD-surface. In this case, the SPR response was 23 RU (**Figure 4.3d**), which represents about 6 % of the signal obtained with the ferrocene functionalised polymer, indicative of a minor contribution of these interactions to the immobilisation process.

The target sequence (1 nM) was hybridised to the βCDPSH/Fc-CMC-DNA surface (**Figure 4.3e**), and surface regeneration via rupture of the DNA target-probe interaction was studied using a range of NaOH concentrations (1-50 mM) and number of pulses (1-3). Regeneration was successfully achieved by applying three pulses of 20 μL of 10 mM NaOH (**Figure 4.3f**). This restored the SPR signal at ~430 RU corresponding to the Au/βCDPSH/Fc-CMC-DNA surface, which indicates that the Fc/βCD assembly is essentially unaltered. DNA target at the same concentration was injected for a second time (**Figure 4.3g**) obtaining a response of 63 RU, which was very similar to the first hybridization value of 67 RU. The βCDPSH/Fc-CMC-DNA surface was easily regenerated again with NaOH following the second target injection (**Figure 4.3h**), demonstrating the reusability of the supramolecular platform for the detection of DNA. Injection of a large excess of adamantanecarboxylate (1 mM) displaced Fc-CMC-DNA from the βCDPSH support indicating the reversibility of the interfacial Fc/βCD complexation and further confirming the host-guest nature of the immobilisation process (**Figure 4.3i**).

The interfacial association constants for the complexation of Fc-CMC-DNA with the three different CD surfaces was determined by SPR using the Langmuir equation: $c/\Gamma = c/\Gamma_{max} + 1/K\Gamma_{max}$, where c and Γ are the bulk concentration and surface coverage of the polymers, K is the interfacial association constant and Γ_{max} is the maximum surface coverage of the polymers (**Figure 4.4**). Linear regression analysis of the data afforded $K_{\beta CD} = 4.4 \times 10^{10}$ M^{-1}, $K_{\gamma CD} = 2.4 \times 10^{7}$ M^{-1} and $K_{\alpha CD} = 7.2 \times 10^{6}$ M^{-1}. These values are several orders of magnitude higher than those observed for individual Fc/CD complexes in solution[32,33] as expected for a multivalent interaction and indicate a higher affinity of the Fc units for the βCD hosts although Fc-CMC-DNA is also able to form interfacial complexes with αCD and γCD modified surfaces. Interestingly, the obtained $K_{\beta CD}$ is very similar to the value recently obtained in our group for the complexation of an adamantane-appended CMC polymer.[34]

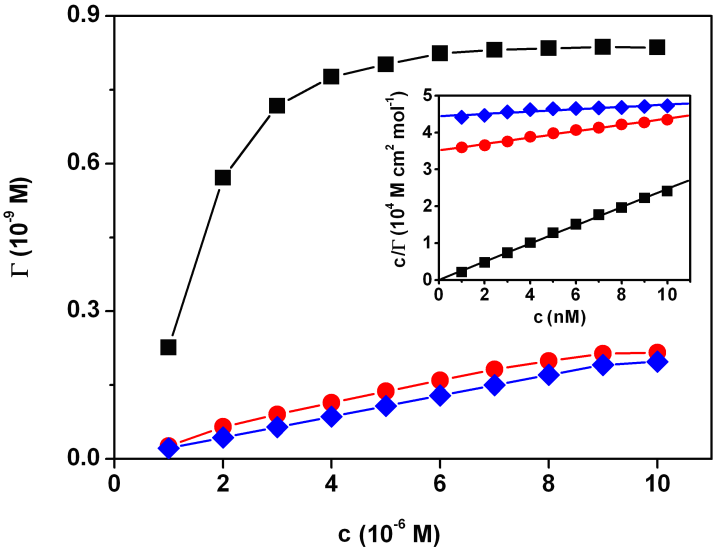

Figure 4.4. Variations of the surface coverage (Γ) with bulk concentration (c) for the interfacial complexation of Fc-CMC-DNA with αCD(♦), βCD(■) and γCD(●) modified surfaces. Inset: Langmuir plots.

Electrochemical detection

The possibility to develop an electrochemical genosensor based on the self-assembled CDPSH/Fc-CMC-DNA platform was evaluated using amperometry, where the presence of the ferrocene units in the platform serves, not only as a docking molecule of the probe to the CDPSH-modified surface, but also acts as an electron transfer mediator by shuttling electrons between the enzyme and the electrode. **Figure 4.5a-c** shows a comparison of the specific (trace a) and non-specific (trace b) amperometric signals obtained for the CDPSH/Fc-CMC-DNA system and the non-specific signal corresponding to the absence of target represented ~5 % of the specific signal in these conditions, highlighting the multifunctionality of the CMC polymer to not only hold the Fc docking molecules and DNA probes but also prevents non-specific interactions due to its hydrophilic nature. The role of the βCD support in assisting the immobilisation of the Fc-modified polymer is also evident by comparing the response obtained in the presence (trace a) and in the absence of the βCDPSH support (trace c). In the latter case, only 12 % or the original signal is observed, which can be attributed to some physical adsorption of the polymer on the gold surface.

Figure 4.5d shows the variation of the amperometric signal with target concentration in the range 0-5 nM. The excellent analytical performance observed, with a limit of detection of 10 pM, can be attributed to the presence of the mediator in the same structure of the

recognition layer, which avoids a possible slow diffusion of the mediator toward the surface. This explains the 8-fold improvement in the LOD found in this case with respect to a similar supramolecular platform but using adamantane as docking molecule and thus requiring the addition of the mediator in solution.[19] Furthermore, the supramolecular incorporation of ferrocene as mediator into the platform simplifies its operation as it only requires the addition of hydrogen peroxide. Finally, sequence selectivity was studied in the presence of three possible interfering sequences also associated to the HLA DQ system. These sequences gave less than 5 % amperometric signal with respect to the HLA-DQA1*0201 target sequence, indicating an excellent selectivity of the system.

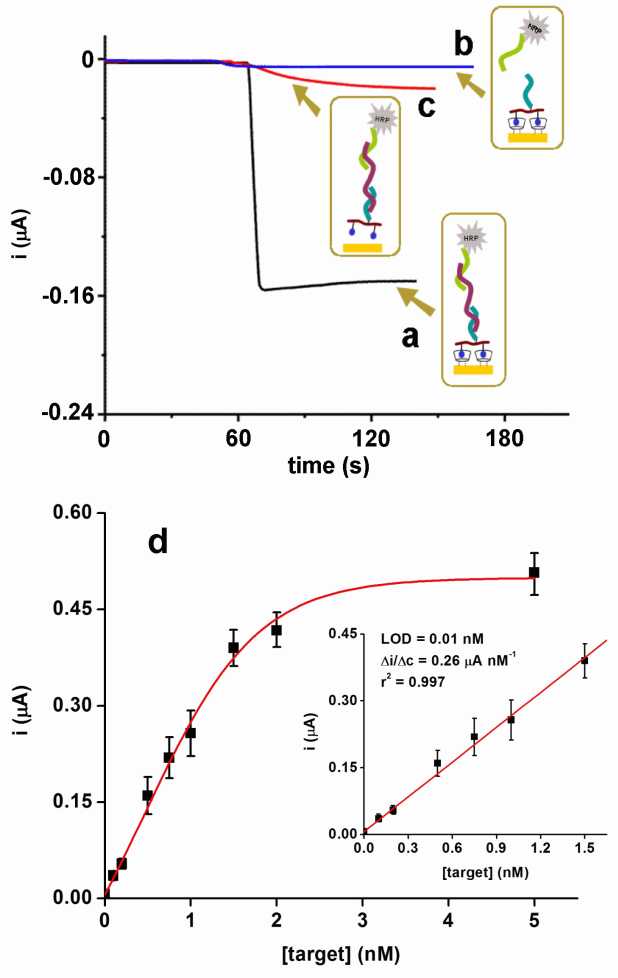

Figure. 4.5. Top: Amperometric responses obtained for different systems: a) full detection system, b) absence of target DNA, c) absence of CD layer. Conditions: E = 0.2 V, supporting electrolyte: 1 mM H_2O_2 in 0.1 M PBS + 0.15 M KCl (pH 6), Bottom: Amperometric calibration curve for the detection of HLA-DQA1*0201 target sequence (d).

4.5 CONCLUSIONS

In this work we describe a novel route for the immobilisation of electron transfer mediators on electrode surfaces based on the interfacial complexation of a polymer backbone bearing ferrocene units on a cyclodextrin surface and explore the applicability of the modified surface in the construction of an amperometric genosensor using a sandwich detection system involving a peroxidase labeled secondary probe. This strategy simplifies the operation of the biosensor, only requiring the addition of enzyme substrate and could be an attractive alternative to the development of packaged genosensors as it avoids the need to use and store unstable redox mediators such as TMB or hydroquinone. The proximity of the mediator to the electrode surface greatly improves the detection limits attained with respect to a similar supramolecular system based on electrochemically inactive adamantane/CD inclusion complexes and requiring addition of the mediator in solution. In addition, the use of the hydrophilic CMC backbone contributes to the elimination non-specific interactions and to an optimal spacing of the immobilised DNA probes. Therefore, the excellent performance of this type of self-assembled structure opens new perspectives in the development of highly sensitive biosensors. Studies in this direction are currently underway.

4.6 REFERENCES

1. D.A. Uhlenheuer, K. Petkau and L. Brunsveld, Chem. Soc. Rev., **2010**, 39, 2817.

2. O. Crespo-Biel, B. J. Ravoo, D. N. Reinhoudt and J. Huskens, J. Mater. Chem., **2006**, 16, 3997.

3. C. A. Nijhuis, J. Huskens and D. N. Reinhoudt, J. Am. Chem. Soc., **2004**, 126, 12266.

4. I. A. Banerjee, L. T. Yu and H. Matsui, J. Am. Chem. Soc., **2003**, 125, 9542.

5. F. Corbellini, A. Mulder, A. Sartori, M. J. W. Ludden, A. Casnati, R. Ungaro, J. Huskens, M. Crego-Calama and D. N. Reinhoudt, J. Am. Chem. Soc., **2004**, 126, 17050.

6. O. Crespo-Biel, B. Dordi, D. N. Reinhoudt and J. Huskens, J. Am. Chem. Soc., **2005**, 127, 7594.

7. J. Huskens, M. A. Deij and D. N. Reinhoudt, Angew. Chem., Int. Ed., **2002**, 41, 4467.

8. S. Zhang, A. Palkar, A. Fragoso, P. Prados, J. de Mendoza and L. Echegoyen, Chem. Mater., **2005**, 17, 2063.

9. O. Crespo-Biel, C. Lim, B. J. Ravoo, D. N. Reinhoudt and J. Huskens, J. Am. Chem. Soc., **2006**, 128, 17024.

10. M. J. W. Ludden, M. Péter, D. N. Reinhoudt and J. Huskens, Small, **2006**, 2, 1192.

11. M. J. W. Ludden, A. Mulder, R. Tampé, D. N. Reinhoudt and J. Huskens, Angew. Chem., Int. Ed., **2007**, 41, 4467.

12. M. J. W. Ludden, X. Li, J. Greve, A. van Amerongen, M. Escalante, V. Subramaniam, D. N. Reinhoudt and J. Huskens, J. Am. Chem. Soc., **2008**, 130, 6964.

13. J. Szejtli, Chem. Rev., **1998**, 98, 1743.

14. R. Villalonga, R. Cao and A. Fragoso, Chem. Rev,. **2007**, 107, 3088.

15. A. Fragoso, J. Caballero. E. Almirall, R. Villalonga and R. Cao, Langmuir, **2002**, 18, 5051.

16. R. Villalonga, C. Camacho, R. Cao, J. Hernández and J. C. Matías, Chem. Commun., **2007**, 942.

17. A. Fragoso, B. Sanromà, M. Ortiz and C. K. O'Sullivan, Soft Matt., **2009**, 5, 400.

18. A. Fragoso, B. Sanromà, M. Ortiz and C. K. O'Sullivan, J. Incl. Phenom. Macrocyclic Chem., **2011**, 69, 355.

19. M. Ortiz, M. Torréns, N. Alakulppi, L. Strömbom, A. Fragoso and C. K. O'Sullivan, Electrochem. Comm., **2011**, 13, 578.

20. N. C. Foulds and C. R. Lowe, Anal. Chem., **1988**, 60, 2473.

21. H. C. Yoon, M. Y. Hong and H. Kim, Anal. Chem., **2000**, 72, 4420.

22. W. Yang, H. Zhou and C. Sun, Macromol. Rapid Comm., **2007**, **28**, 265.

23. M. P. G. Armada, J. Losada, I. Cuadrado, B. Alonso, B. González, C. M. Casado and J. B. Zhang, Sens. Actuators B, **2004**, 101, 143.

24. V. Tripathi, V. Kandimalla and H. Ju, Biosens. Bioelectron., **2006**, 21, 1529.

25. G. V. Dubacheva, A. van der Heyden, P. Dumy, O. Kaftan, R. Auzély-Velty, L. Coche-Guerente and P. Labbé, Langmuir, **2010**, 26, 13976.

26. G. V. Dubacheva, M. Galibert, L. Coche-Guerente, P. Dumy, D. Boturyn and P. Labbé, Chem. Commun., **2011**, 47, 3565.

27. G. V. Dubacheva, P. Dumy, R. Auzély, P. Schaaf, F. Boulmedais, L. Jierry, L. Coche-Guerente and P. Labbé, Soft Matt., **2010**, 6, 3747.

28. C. A. Tennyson, S. K. Lewis and P. H. Green, Therap. Adv. Gastroenterol. **2009**, 2, 303.

29. A. S. Louka and L. M. Sollid, Tissue Antigens, **2003**, 61, 105.

30. M. Bourgey, G. Calcagno, N. Tinto, D. Gennarelli and P. Margaritte-Jeannin, Gut, **2007**, 56, 1054.

31. H. L. Ramirez, R. Cao, A. Fragoso, J. J. Torres-Labandeira, A. Dominguez, E. H. Schacht, M. Baños and R. Villalonga, Macromol. Biosci., **2006**, 6, 555.

32. A. U. Moozyckine J. L. Bookham M. E. Deary and M. D. Davies, J Chem Soc, Perkin Trans 2, **2001**, 1858.

33. M. V. Rekharsky and Y. Inoue, Chem. Rev., **1998**, 98, 1875.

34. M. Ortiz, A. Fragoso and C. K. O'Sullivan, Org. Biomol. Chem., **2011**, 9, 4770.

4.7 SUPPLEMENTARY INFORMATION

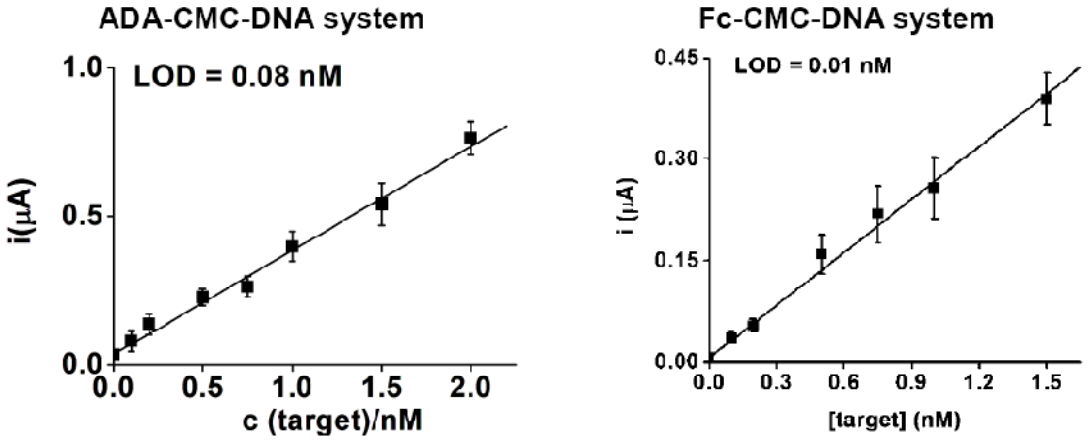

Figure. SI 4.1. Comparison of calibration plots obtained for ADA-CMC-DNA and Fc-DNA-DNA systems.

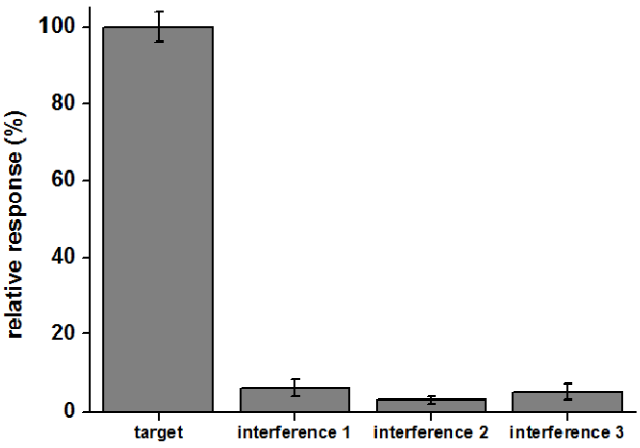

Figure. SI 4.2. Sequence selectivity. Comparison of amperometric responses obtained with the HLA DQA102 target sequence and with interfering probes 1-3 (see Experimental section for oligonucleotide sequences)

CHAPTER 5

CONTROLLED Zn-MEDIATED GRAFTING OF THIN LAYERS OF BIPODAL DIAZONIUM SALT ON GOLD AND CARBON SUBSTRATES.

(Chem. Eur. J. , 2014. DOI: 10.1002/chem.201405121)

CHAPTER 5

CONTROLLED Zn-MEDIATED GRAFTING OF THIN LAYERS OF BIPODAL DIAZONIUM SALT ON GOLD AND CARBON SUBSTRATES

5.1 ABSTRACT

A controlled, rapid and potentiostat-free method has been developed for grafting the diazonium salt (3,5-bis(4-diazophenoxy)benzoic acid tetrafluoroborate (DCOOH)) on gold and carbon substrates, based on a Zn-mediated chemical dediazonation. The highly stable thin layer organic platforms obtained were characterized by cyclic voltammetry, AFM, impedance, XP and Raman spectroscopies. A dediazonation mechanism based on radical formation is proposed. Finally, DCOOH was proved as a linker to an aminated electroactive probe.

5.2 INTRODUCTION

The dediazonation reaction, in which a diazonium loses a diazo group, forming aryl radicals or cations, has been widely reported for a plethora of chemical reactions.[1, 2] In 1992, Pinson *et al.* exploited these radicals for the electrochemical grafting of diazonium salts on carbon surfaces.[3] Initially, the majority of reports focused on the grafting of diazonium salts on carbon,[4–7] but since then this mechanism has been expanded to different metal substrates including, copper,[8] nickel,[8, 9] zinc, [8, 9] iron, [8-11] gold,[12] indium oxide,[13] and semiconductors.[14] These diazonium-grafted surfaces have found widespread application in diverse areas such as sensors,[15, 16] catalysis,[17] nanotubes,[18] and anti-corrosive agents.[10,11]

The stability of electrografted diazonium layers is well known and can be attributed to the C-C and metal–C covalent bond between the aryl groups and carbon or metal surfaces, respectively.[19] Highlighting this stability, depending on the nature of the carbon used, the grafted diazonium film can only be removed by exposure to extreme temperatures or by mechanical abrasion.[4] Furthermore, grafted layers have been exposed to ultrasound in different organic solvents with no effect on the formed film.[4, 9] Their stability upon exposure

to elevated temperatures[20] or positive[21,22] and negative[13,16] electric potentials has also been demonstrated, as well as their long-term stability under atmospheric conditions.[4]

The modification of substrates with diazonium salts has been carried out in acidic aqueous solution[6,23] or organic[23,24] media and by electrochemical[6,7,20] or spontaneous grafting by immersing the substrate in diazonium salt solution[8,9,11] or by microcontact printing.[25] The reduction of the diazo group has also been achieved by ultrasonication,[26,27] heating microwave assistance,[28] photochemistry,[29] or through the use of a chemical reducing agent such as iron.[30]

The most widely reported of these approaches is that of electrochemical grafting; however, this method results in uncontrolled multilayer film structures, which can be ascribed to radical attack on surface-grafted aryl groups.[31] The thickness of the resulting layers prepared by electrochemical grafting has been demonstrated to be dependent on the number of potential cycles[32] as well as the concentration.[4] Thin layers have been obtained taking advantage of steric hindrance provided by a bulky silyl protecting group to avoid the post-grafted reaction[33] or in the presence of a radical scavenger.[34] Another alternative to obtain an organised platform by electrochemical grafting is based on the co-immobilisation of two diazonium salts with opposite charges.[35]

The spontaneous grafting of the diazonium salt can be accomplished by *in situ* production of the diazonium salt from the corresponding amine in presence of the surface[36] or by immersing the substrate in a solution of the already synthesised diazonium salt.[8,37] Sodium nitrite acts as nitrosating agent and the acidic medium required for the reaction can be provided by a mineral acid or taking advantage of the acidic effect of organic acid substituents, like carboxylic or sulfonic acid moieties.[36] The average time needed for spontaneous grafting ranges from just a few minutes to 24 h,[38] requiring deaerated solutions, and is mainly carried out in organic solvents.[8,36,38] The concentration[8,39] and nature of the functional group[36] present in the precursor amine determines the thickness of the final organic layer, which ranges from a few nanometers to 40 nm.[39] Although the covalent nature of the aryl–surface bond has been established by X-ray photoelectron spectroscopy (XPS)[8,38] the type of formation mechanism (homolytic[8,38] or heterolytic[37]) and the nature of the final bond (Ar-N-metal or Ar-C-metal) is still controversial and the overall mechanism probably has both radical and cationic contributions. Some spontaneously grafted layers have been demonstrated to be stable at negative potential[39] and under sonication at relatively high temperatures,[39,40] although there are contrasting reports that outline that during immobilisation of the diazonium salt, both covalent

bond formation and physical adsorption are present,[23] contributing to an instability of the final organic layer.

Furthermore, the term "spontaneous" is used to describe grafting that is not assisted by additional factors such as applied potential, but it is generally accepted that the surface has a marked influence on the efficiency of grafting and on the stability of the resulting layer. This phenomenon is enhanced on metallic surfaces, in which the higher the reduction potential of the surfaces, the higher the number of molecules that will be immobilised, indicating that the surface contributes as a reducing agent facilitating dediazonation.[9,8] In the case of carbon, spontaneous grafting of the diazonium salt has been reported using a core-shell composite of carbon-coated $LiFePO_4$, but the metals in the core of the composite contribute to the grafting process.[38]

In the work reported here, we combine the principal advantage of potentiostat-free spontaneous grafting with the rapidness of electrografting. In our method, by exploiting zinc as a reducing agent for the formation of aryl radicals, we accomplished the grafting in few minutes with no instrumentation required. A carboxylate containing-bipodal diazonium salt (3,5-bis(4-diazophenoxy)benzoic acid tetrafluoroborate) was used to demonstrate the feasibility of this methodology and its potential applicability as surface modification strategy for the immobilisation of aminated molecules through the COOH group. The chemically modified surface was compared with both electrografted and spontaneously prepared surfaces in terms of thickness of the layers, the viability for linking an aminated electroactive probe and stability at extremes of temperature, and electric potential, as well as storage stability.

5.3 EXPERIMENTAL SECTION

Materials

All reagents were of analytical grade and used as received.N-ethyl-N`-(3-dimethylaminopropyl) carbodiimide hydrochloride (EDC), $NaH_2PO_4.H_2O$, Na_2HPO_4, strontium nitrate, tetrafluoroboric acid solution, zinc dust, sodium nitrite 99.5%, potassium ferricyanide (III) and potassium ferrocyanide (II), (2,2-diphenyl-1-picrylhydrazyl (DPPH)) were purchased from Sigma-Aldrich (Barcelona, Spain). The sulfuric acid, sodium chloride and hydrogen peroxide were purchased from Scharlau (Barcelona, Spain), potassium hydroxide

was obtained from J.T. Baker, 3,5-bis(4-aminophenoxy) benzoic acid was received from TCI and dimethyl sulfoxide from Abcam plc. All solutions were prepared with Milli-Q water (Millipore Inc.). SERS substrates for Raman were purchased from Renishaw.

Instrumentation and methods

Electrochemical instrumentation and electrode cleaning

Electrochemical measurements were performed on a PC controlled PGSTAT12 Autolabpotentiostat (EcoChemie, The Netherlands) with a built-in frequency response analyzer NOVA module using two electrode configurations: 1) Screen printed carbon (DRP-110) and gold (DRP-250BT) electrodes configuration; working electrode: carbon or (gold) disk (φ=4 mm), pseudo-reference electrode: silver (silver), counter electrode: carbon (Pt), and 2) a three-electrode configuration of Ag as a reference (CH Instruments., model CHI111), Pt wire as a counter (BAS model MW-1032), and conventional glassy carbon or Au (BAS model MF-2014, 1.6 mm diameter) as the working electrode.

Electrode preparation

Screen-printed electrodes: Gold electrodes were cleaned by cycling three times in 0.5 M H_2SO_4 from -0.4 V to 1.0 V versus Ag at 100 mVs^{-1} and the carbon electrodes were activated by cycling three times from 0 to -1.2 V versus Ag in 0.5 M KOH at 50 mVs^{-1} scan rate.

Conventional electrodes: Gold electrodes were polished with alumina powder of 0.3 μm and sonicated in ethanol and Milli-Q water twice for 5 min each. The electrodes were then immersed in room temperature Piranha's solution (1:3 v/v H_2O_2 to H_2SO_4) for 5 min and once again sonicated twice in ethanol and Milli-Q water for 5 min each (Caution! Piranha's solution is highly corrosive and violently reactive with organic materials; this solution is potentially explosive and must be used with extreme caution). The electrodes were dried using nitrogen and electrochemically cleaned in 0.5 M H_2SO_4 solution by cycling 40 times from -0.4 to 1.7 V versus Ag at 100 mVs^{-1}, and then washed with Milli-Q water and dried with nitrogen. Glassy carbon electrodes were sequentially polished with alumina powder (0.3, 0.1, and 0.05 μm) and sonicated in ethanol and Milli-Q water twice for 5 min each and cycled 25 times from 0 to -1.2 V versus Ag in 0.5 M KOH at 50 mVs^{-1} scan rate, washed with Milli-Q water and dried under nitrogen.

The quality of the cleaning and subsequent steps was checked by using cyclic voltammetry and Electrochemical Impedance Spectroscopy (EIS) in 1 mM $K_4[Fe(CN)_6]/K_3[Fe(CN)_6]$ in 50mM of $[Sr(NO_3)_2]$. The CV was recorded from -0.4 to 0.6 V at 100 mVs^{-1}. EIS was recorded in the frequency range from 100 kHz to 0.05 Hz at 0.2 V and amplitude of 5 mV. The Nyquist plots obtained were fitted to an equivalent circuit (**Figure 5.4**) to extract the value of charge-transfer resistance.

Synthesis of 3,5-bis(4-diazophenoxy)benzoic acid tetrafluoroborate (DCOOH)

The synthesis was carried out according as previously reported[32] with minor modifications. 3,5-bis(4-diazophenoxy)benzoic acid tetrafluoroborate was synthesized by dissolving 0.5 g of 3,5-bis(4-aminophenoxy) benzoic acid in tetrafluoroboric acid (3 equivalent of tetrafluoroboric acid per amine group). Following dissolution of the amine, a cold solution of sodium nitrite was added (1.5 equivalent per amine group). The mixture was stirred for 30 min at 48 ºC. A white precipitate was separated from solution by filtration and the product was washed with cold water three times and dried under vacuum during 24 h, protected from light. Finally, the product (DCOOH) was stored at -20 ºC in the dark.

Modification of gold and carbon electrodes via Zn-mediated grafting, spontaneous grafting and electrochemical grafting

Zn-mediated grafting: To modify the electrodes through Zn-mediated grafting, a mixture of 20 µL of a 1, 5, or 10 mM 3,5-bis(4-diazophenoxy) benzoic acid tetrafluoroborate in 0.5 M sulfuric acid containing an excess of Zn powder was stirred for 5 seconds, added to the electrode surface and incubated for 2 or 5 min. To elucidate the grafting mechanism, the following experiments were carried out: a) (to study the function of Zn as reducer) the Zn was substituted by $ZnCl_2$ and the same procedure was followed b) (to study the radical contribution to the overall mechanism) 1 µL of acetonitrile solution of DPPH was added to a sulfuric acid solution containing 5 mM of 3,5-bis(4-diazophenoxy)benzoic acid tetrafluoroborate and Zn powder. The mixture was then stirred during 5 seconds and added to the surface of gold and carbon electrodes and left to react for 5 min.

Spontaneous grafting: A similar procedure was followed for spontaneous grafting, To modify the electrodes via chemical grafting, 20 µL of a 1, 5 or 10 mM 3,5-bis(4-diazophenoxy)benzoic acid tetrafluoroborate in 0.5 M sulfuric acid (not containing any Zn) were added to the electrode surface and incubated for 5 minutes.

Electrochemical grafting: The electrochemical grafting was performed using a solution of 5 mM of 3,5-bis(4-diazophenoxy)benzoic acid tetrafluoroborate in 0.5 M sulfuric acid. The potential was cycled from 0.1 V to -0.6 V for two cycles at 50 mV/s. (In the case of the screen-printed electrodes a drop of 70 µL of solution was added to the electrode surface, and for the conventional electrodes a volume of 1 mL of solution was required for the three electrode system).

Finally, the modified electrodes were rinsed with isopropanol under continuous stirring for 5 minutes, then with water for 30 minutes and dried with nitrogen. Grafting of the 3,5-bis(4-diazophenoxy)benzoic acid tetrafluoroborate using the different techniques was monitored using CV and EIS using the same methodology as described above for the evaluation of the cleanliness of the electrodes**.**

FTIR Spectroscopy

FTIR spectra were recorded on a Jasco FT/IR-600 PlusATRSpecac Golden Gate spectrometer. 128 scans at 2 cm^{-1} resolution were recorded.

Raman Spectroscopy

Raman spectra were recorded using a Renishaw 2003 spectrometer operating at wavelength of 514 nm, of HeNe laser, for carbon and of 633 nm for gold.A CCD camera was used as detector. The spectra were analyzed using Wire 3.3 version software (Renishaw plc, New Mills, Wotton-underEdge, and Gloucestershire, GL12 8JR, United Kingdom).

Surface enhanced Raman scattering (SERS) surface

Gold coated nanostructured silicon Klarite® SERS substrates were used for Raman characterization and the 3,5-bis(4-diazophenoxy)benzoic acid tetrafluoroborate was immobilised as previously described for the screen-printed electrodes but without a previous cleaning procedure.

X-ray Photoelectron spectroscopy (XPS)

All measurements were recorded in a PHI ESCA-5500 spectrometer with an Aluminum X-ray source. The surfaces were analysed in an ultra-high vacuum (UHV) chamber with pressure

between 5×10^{-9} and 2×10^{-8}torr. The samples used for XPS analysis were prepared using a concentration of diazonium salt of 5 mM and immobilisation time of 5 minutes.

Atomic Force Microscopy

The images were recorded in a 5420 Atomic Force Microscope (AFM) from Agilent Technologies (USA) and processed using WSxM 5.0 Develop 3.2[47] and Pico View 1.8. HOPG (from SPI supplier) software. Flat gold prepared by sputtering on mica was used as substrate for AFM studies.

A thin layer of HOPG was freshly cleaved with adhesive tape prior to each experiment and fixed in a magnetic support. Using a 300 KHz frequency tip the surface was scanned in tapping mode to select a flat section and the surface was then scratched in lithographic mode. Different conditions were tested, and finally the optima were: force set point voltage: 1 V and speed 0.050 micron/s. In this mode, the organic material is removed from the substrate in a well-defined way. Finally the surface was scanned again in tapping mode to obtain the image. Where the material was removed, a hole appeared and the thickness of the organic layer in the vertical section was determined with the WSxM 5.0 Develop 3.2 program.[47]

5.4 RESULTS AND DISCUSSION

The 3,5-bis(4-diazophenoxy)benzoic acid tetrafluoroborate (DCOOH) was selected as a model diazonium salt for the demonstration of the reported methodology. DCOOH has a singular structure with double linking aryl groups and the sp_3 oxygen bridge prevents the formation of a densely packed layer, which could lead to insulation of the electrode surface. In addition, the carboxylate can be used for further functionalization and immobilisation of aminated molecules (**Figure 5.1**).

The electrophilic character of the diazo group leads to the grafting of diazonium salts on surfaces through a dediazonation step, which produces reactive radicals that can attack the surface.[19] In our potentiostat-free methodology, Zn powder is used as a reducing agent

favoring the production of aryl radicals, whereas Zn^0 is oxidized to Zn^{II} (**Figure 5.1**). It accelerated the rate of grafting, reducing the time from hours[8, 38, 39] to a few minutes, without the necessity of using a potentiostat.

Grafting was carried out in dilute sulfuric acid to achieve a pH lower than 3, which avoids decomposition of diazonium salt and favors the formation of a thinner layer in comparison with those produced in organic solvents such as acetonitrile.[6]

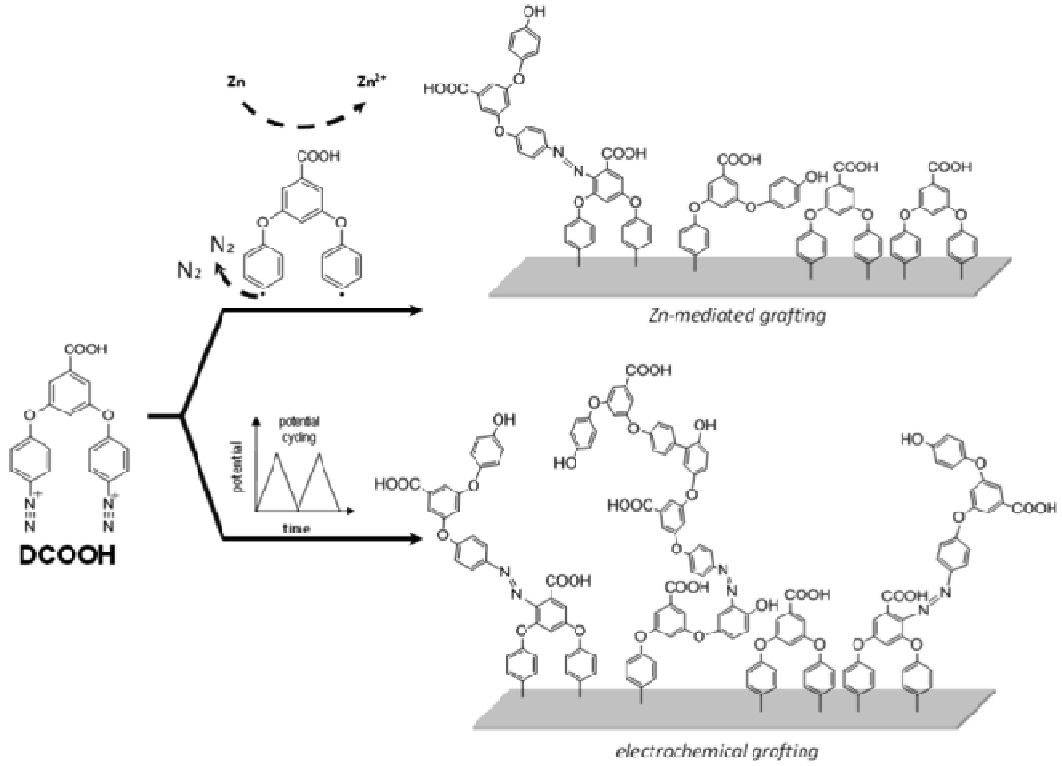

Figure 5.1 Schematic of the Zn-mediated (top) and electrochemical (bottom) graftings on gold and carbon substrates.

In a first attempt, DCOOH was produced *in situ* from 3,5- bis(4-aminophenoxy) benzoic acid by reaction with $NaNO_2$ in acidic media at 48 ºC in the presence of the surface for grafting but this procedure was rapidly discarded due to the formation of a dark gummy product that completely insulated the electrode. DCOOH was thus prepared ex-situ, precipitated, dried, and used for the present study (**Figure SI5.1**).

In our methodology, the presence of metallic Zn leads the production of radicals for their subsequent grafting. It was probed by preparing two diluted sulfuric solution of 3,5-bis(4-diazophenoxy)benzoic acid tetrafluoroborate, one containing Zn powder and the other, $ZnCl_2$ (instead of Zn).They were both added to the gold and carbon surfaces and left to react for 5 min (**Figure SI5.2**).

The grafting was evaluated by cyclic voltammetry using $[Fe(CN)_6]^{3-}/[Fe(CN)_6]^{4-}$ as electroactive probe (**Figure 5.2 a** and **b**), following the criteria that the decrease in current is related to a blocking of electron transfer due to the surface insulation due to the grafting of the diazonium salt. For surfaces modified in the presence of Zn, a blocking of electron transfer was observed, whereas a negligible decrease in current was noticed for surfaces modified in the presence of $ZnCl_2$, which can be attributed to some spontaneous immobilization.

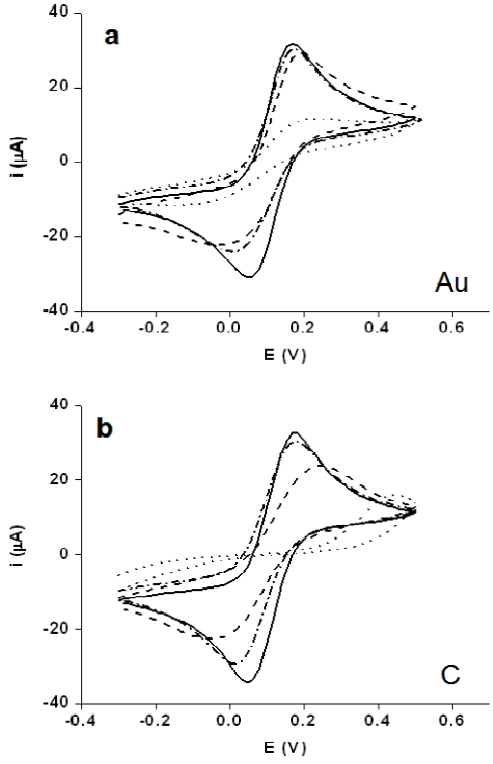

Figure 5.2. Cyclic voltammograms recorded in 1 mM $[Fe(CN)_6]^{3-}/[Fe(CN)_6]^{4-}$ on gold (a) and carbon (b) at bare electrode (—), after Zn-mediated grafting (·····), using $ZnCl_2$ in instead of Zn (·-·-·-·) and after Zn-mediated grafting in presence of DPPH (----). Supporting electrolyte: 0.1 M $Sr(NO_3)_2$. Scan rate: 0.1 V/s

To understand the grafting mechanism, the reaction was carried out in the presence and absence of a radical scavenger (2,2-diphenyl-1-picrylhydrazyl (DPPH)), which has been

already demonstrated to successfully capture radicals originating from the diazonium salt produced in situ in acetonitrile.[34] A solution of DPPH in acetonitrile was added to a sulfuric acid solution containing DCOOH and Zn powder and the mixture was added to the surface of gold and carbon electrodes and left to react for 5 min. **Figure 5.2 c** and d show the cyclic voltammograms obtained before and after grafting, in the presence and absence of DPPH. A higher current intensity was observed when DPPH was used indicating a lower degree of grafting. This is because the aryl radicals produced from diazonium salts are sequestered by DPPH and are not able to graft to the surface. This result confirms the hypothesis of a significant contribution of homolytic dediazonation to the overall mechanism.[34] Nevertheless, some potential heterolytic contributions should not be disregarded. In addition, a side reaction between DPPH and protons from the acidic media, even if the mixture was left to react just a few minutes, cannot be ruled out.

The product from the reaction of DPPH and DCOOH was isolated and characterized by FTIR and Raman and mass spectroscopies (**Figures SI 5.3–SI 5.5**). In both FTIR and Raman spectra, the band corresponding to the diazo group is absent. The most conclusive criteria that the reaction took place is elucidated from the obtained m/z ratio (1003), which corresponds to a compound with a molar ratio DCOOH/ DPPH of 2:1. The proposed structure is based on a suggested mechanism[34] in which the aryl radicals from diazonium salt react with one of the diphenyl amino moieties of DPPH, and at the same time react with another aryl radical.

The Zn-mediated grafting was also characterized by X-ray photoelectron spectroscopy (XPS). **Figure 5.3** shows the XP spectra of both gold and carbon surfaces modified with 3,5-bis(4-diazophenoxy)benzoic acid using Zn as reducing agent. The Zn-mediated modified gold surface clearly shows immobilisation of DCOOH with the presence of C–O–C and C–H energy bands. The typical peaks of diazonium groups (N1s) at 403.8 and 405.1 eV are not present, indicating that there is no physical adsorption of diazonium salt,[11] although a weak N1s peak appears at 398.84 eV on gold and 400.6 eV for carbon. The presence of a peak in this position has been extensively discussed in the literature and, in our case, could indicate some contribution of a heterolytic mechanism with the formation of Ar–N–Au bonds[8] or, alternatively, a small amount of multilayer formation bridged by azo groups[7] (–N=N–) on the electrodes.

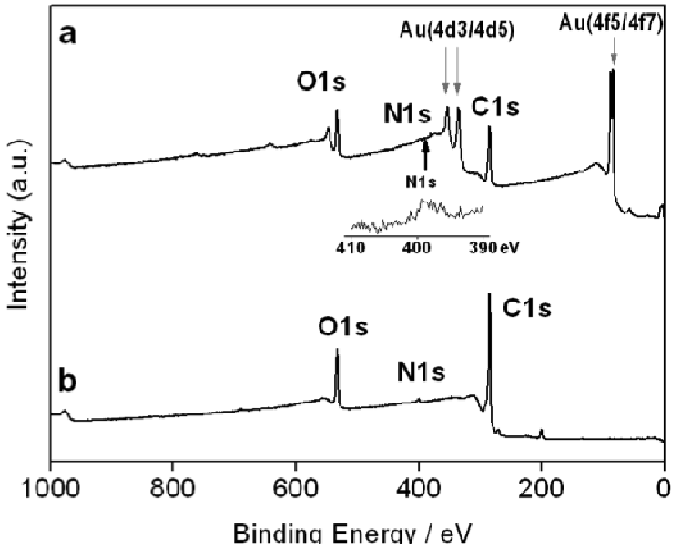

Figure 5.3. XPS spectra of Zn-mediated grafted DCOOH on gold (a) and carbon (b). The N1s region for gold surface (taken from the high resolution spectrum) is shown in the inset.

From the CV and XPS data it is not possible to establish whether the two radicals obtained from the two diazonium groups of DCOOH actually bind to the surface, because if one of the radicals does not react with the surface it will be transformed into a phenol that is not easy to detect by FTIR or Raman spectroscopy in a very thin film. Besides, this phenol group is difficult to derivatise due to the steric hindrance of the surface. A similar problem has been observed in the electrografting of a calix[4]-tetraarenediazonium salt[41] but should not markedly affect the reactivity of the COOH group and hence the applicability of the modified surface for the attachment of other molecules.

Electrochemical characterisation of modified surfaces

The variation of the electron-transfer resistance of both carbon and gold electrodes after grafting with DCOOH respect to unmodified surfaces was followed by impedance spectroscopy (EIS) and cyclic voltammetry. As can be seen in **Figure 5.4** and Table 1, for both the gold and carbon surfaces, a reduction in the current peaks and increase in peak-to-peak separation was observed for the cyclic voltammograms of modified surfaces respect to the clean electrodes. The developed methodology was then compared with surfaces obtained from electrochemical and spontaneous grafting. Electrochemical grafting resulted in an increased blockingof the signal, indicative of a higher level of immobilization or the formation of multilayers. For the interpretation of the EIS data and to determine the electron-transfer resistance the Randles equivalent circuit was used (**Figure 5.4**). This circuit was composed by

the electrolyte solution resistance (RS) in series with the parallel combination of the constant phase element (Q) and the charge-transfer resistance (Rct) and Warburg impedance (W). The values of charge-transfer resistance for Zn-mediated method were found 30 and 45 % lower for carbon and gold, respectively, with respect to those obtained after electrochemical grafting. In addition, these values were 3.2- and 2.6-fold higher in comparison to spontaneous modification. Thus, the higher electron-transfer resistance in ESI spectra and higher peak-to-peak separation and lower current in the voltammograms indicate the presence of more organic material linked to the substrate in the following order of modification approach: Electrografting > Zn-mediated grafting > spontaneous grafting.

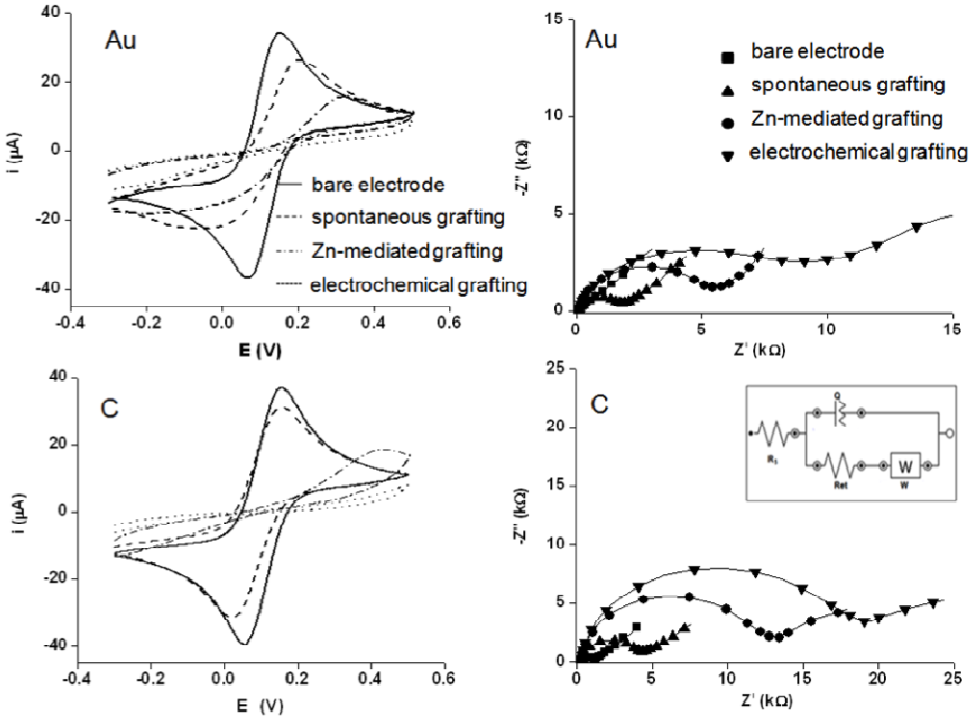

Figure 5.4. Cyclic voltammograms (left) and faradic complex impedance plots (right) in 1 mM $[Fe(CN)_6]^{3-}$ /$[Fe(CN)_6]^{4-}$ for the different immobilisation routes on gold and carbon electrodes. Supporting electrolyte: 0.1 M $Sr(NO_3)_2$. Scan rate (in CV): 0.1 V/s. Impedance measurement conditions, frequency range 100 kHz to 0.05 Hz, amplitude of 5 mV. (inset) Randles equivalent circuit of faradaic EIS measurement: Rs: electrolyte solution resistance; Ret: electron transfer resistance; W: Warburg impedance; Q: Constant phase element.

In the case of the spontaneous grafting, it can be seen that some organic material was deposited on the surface. However, or a 5 min deposition time, it is evident that the presence of Zn is essential to accelerate the grafting process. The short deposition time achievable using the

developed Zn-mediated grafting is very important when working with sensitive molecules such as diazonium salts, because they can be easily damaged, with a pronounced effect on the final organic layer.

Table 1. Electrochemical and Raman properties of non-modified and modified surfaces.

Surface modification	ΔE(mV)*	R_{ct} (kΩ)	Raman D/G ratio
Gold Surface			
Bare electrode	75	0.2	-
Zn-mediated grafting	308	5.6	-
Electrochemical grafting	547	10.1	-
Spontaneous grafting	211	2.1	-
Carbon Surface			
Bare electrode	80	0.9	0.74
Zn-mediated grafting	364	13.8	1.36
Electrochemical grafting	589	19.7	1.51
Spontaneous grafting	156	4.3	1.23

*$\Delta E = E_{ox}-E_{red}$

The Zn-mediated grafting of the diazonium salt was also studied by using Raman spectroscopy. Due to the difficulty in observing a thin molecular layer deposited on a gold substrate, a gold-coated nanostructured silicon substrate, specifically designed for surface enhanced Raman scattering (SERS), was used to study the binding process of DCOOH on gold. A drop of DCOOH at micromolar concentration was left for 5 min on the SERS substrate and then dried slowly under vacuum to create a thin layer. The recorded spectrum corresponds to the compound in its powder form (**Figure 5.5**). The sample was then re-hydrated in acid media containing Zn powder and left to react for 5 min, and then dried again under vacuum. The most

notable difference between the Raman spectrum of the modified surfaces and the corresponding of starting DCOOH was the absence of the (C–N–N) band at 2260 cm^{-1}. In addition, a slight shift in the position of the bands corresponding to the aromatic region was observed, which can be attributed to binding to the gold substrate and probably some contribution from van der Waals interactions of neighboring molecules, thus clearly demonstrating the successful grafting of the diazonium salt.

Analysis of the D and G Raman bands is very useful for characterising the modification of carbon surfaces. The G Raman band appears at 1575 cm^{-1} and is related with the C–C bond vibration and is evidently present in all carbon surfaces. The origin of the D band (at 1353 cm^{-1}) is related with structural disorders[42] produced by mechanical treatments including polishing[43] or chemical reactions due to changes on the hybridisation of carbon from sp_2 to sp_3. The intensity of the D band can range from close to zero in highly organised non-modified surfaces, to values comparable with those of the G band in damaged or modified substrates. The important parameter is the D/G band intensity ratio, which increases with the modification and, in our case, provided useful structural information regarding the different routes for diazonium grafting (**Figure 5.5**, top, and Table 1). As expected, a low D/G Raman band ratio was observed for the unmodified carbon electrode following reductive desorption at basic pH, to remove any surface localized impurities. When DCOOH is surface bound, an increase of D/G band ratio was observed for spontaneous, electrochemical, and the Zn-mediated grafting. Although, for the binding of aryl rings to the carbon surface a high sp_2 contribution is expected, steric hindrance provokes distortion from the planar sp_2 surface, as demonstrated by the higher intensity of the D bands. This behaviour correlates with the ΔE (Table 1) trend reported above. Again, the D/G ratio is markedly higher in the case of electrochemical grafting, possibly due to the formation of multilayers.

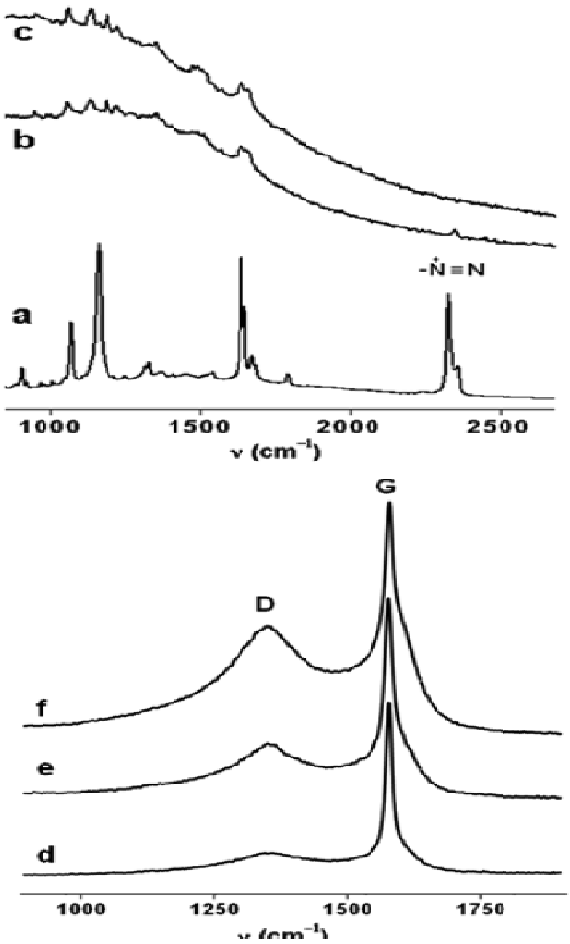

Figure 5.5. *Top:*Raman spectra of: (a) solid DCOOH, (b) DCOOH from aqueous solution dried on gold SERS substrate and (c) DCOOH deposited on gold SERS substrate by Zn-mediated method. *Bottom:* Raman D and G bands of: (d) bare carbon, (e) after Zn-mediated grafting of DCOOH and (f) after electrochemical grafting of DCOOH.

Atomic force microscopy characterisation of modified surfaces

AFM facilitates not only the possibility to acquire topographic images of surfaces in two-dimensions, but can also be used for the estimation of the number of molecular layers deposited on a substrate using the so-called "AFM scratching" method, which allows the controlled removal of the deposited organic material using the AFM tip, after which, the thickness of the removed layer is determined by scanning the surface.[5]

For this purpose, flat gold, prepared on mica by sputtering technique and freshly cleaved highly oriented pyrolitic graphite (HOPG) were used for this experiment; both substrates were fixed on a magnetic support. Zn-mediated chemical grafting was carried out using 5 mM DCOOH

and 5 min grafting time. After grafting, both surfaces were thoroughly washed to eliminate any residual salt. Following scanning of the surfaces using tapping mode AFM, a geometric figure was created by scratching the organic layer using the lithographic mode. Following scratching, the surface was scanned again in tapping mode to obtain the image, with the organic material removed during scratching creating a hole that is equivalent in height to the deposited organic layer.

In the case of gold substrate modified by Zn-mediated grafting, it was difficult to determine the thickness of the organic layer because the dimension of the molecule is close to the roughness of the clean substrate. The force needed for scratching was tested to ensure that the substrate is not damaged and that only the organic layer is removed (**Figure SI5.6**). Finally the thickness of the aryl layer on gold was found to be between 1 and 2 nm, which is close to the dimension of one molecule (0.8 nm), whereas a layer with a higher thickness was observed on carbon (≈3 nm; **Figure 5.6**). In the case of the electrochemically grafted carbon, surface thicknesses from 4 to 10 nm (corresponding to 5 to 8 molecules) were obtained, whereas a 5 nm thickness (around 6 molecules) was observed for the electrochemically grafted gold surface, in agreement with previous reports.[5, 32] Scratching the spontaneously grafted surfaces, resulted in removal of negligible amounts of material. These results agree with the differences in percent of oxygen and nitrogen found by XPS present in both substrates.

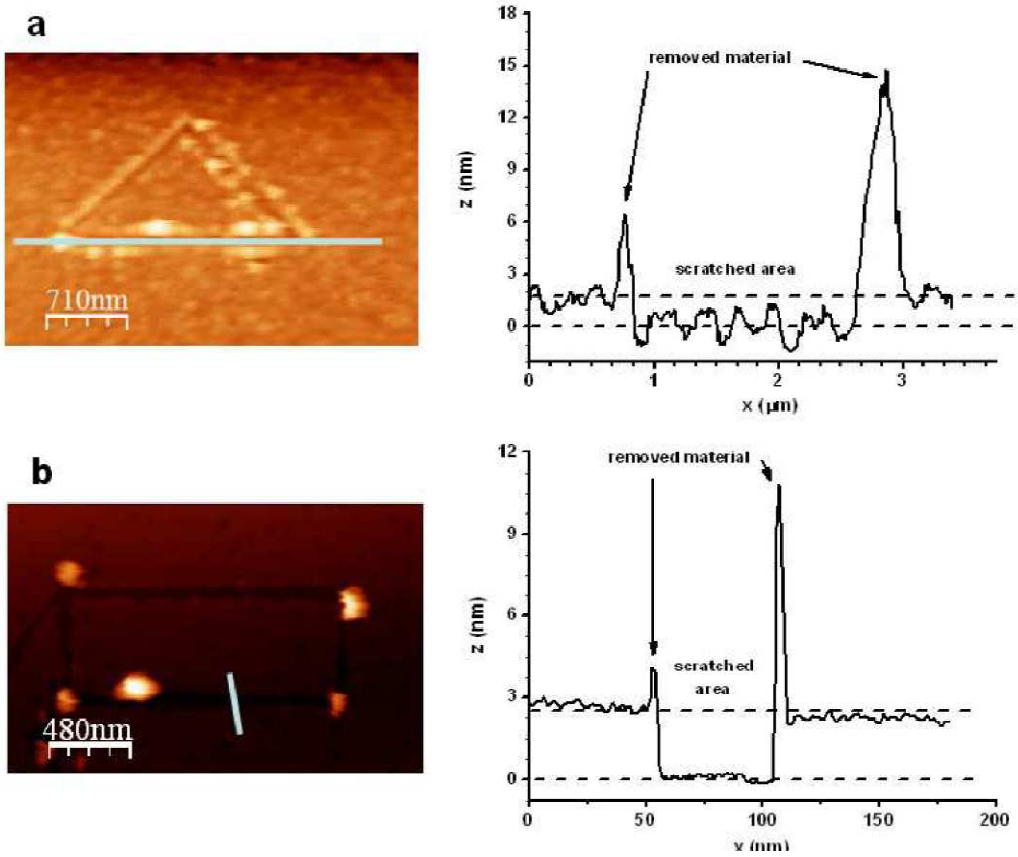

Figure 5.6. AFM scratched surfaces (left) and the corresponding profiles (right) of Zn-mediated grafted diazonium salt in gold a), and in carbon b).

X-ray photoelectron spectroscopy (XPS) monitoring of different steps of immobilisation

The XPS analyses of both carbon and gold substrates modified by both electrochemical and Zn-mediated immobilisation methods made it possible to follow the different modification steps by analysing the percentage of atomic concentration of oxygen (%O) and nitrogen (%N) (**Figure 5.7**). The higher %O for carbon than for gold is in agreement with the voltammetric, impedance and AFM results.

To facilitate the understanding of the layer formation, an additional diazonium salt (3,5-bis(4-diazophenyl tetrafluoroborate (DH)) with a similar structure to DCOOH but without the ⁻COOH moiety was prepared and immobilised by the same procedure as DCOOH to corroborate the effect of the negatively charged carboxylate group on the multilayer formation. Amino-ferrocene was then linked to the carboxylate group of DCOOH, which transformed the ⁻COOH group into ⁻CONH⁻. **Figure 5.7a** shows an increment in the oxygen percentage for both substrates and immobilization methods in the order: Bare electrode > DH > DCOOH

followed by a decrease in %O associated with an amide bond in which the oxygen content is lower.

For the gold substrate, the %O is duplicated from DH to DCOOH, which correlates with the 2DCOOH/DH oxygen atomic ratio. In the case of carbon substrate the %O is increased in about 10 % for DCOOH respect to DH. This could be related with the higher roughness of carbon, which translates into higher surface area for the immobilisation of molecules. This effect is more significant in the case of DCOOH, in which the negative carboxylate moiety of the first layer of immobilised aryl molecules interacts with the positive diazonium salt, accelerating the modification of the substrate.

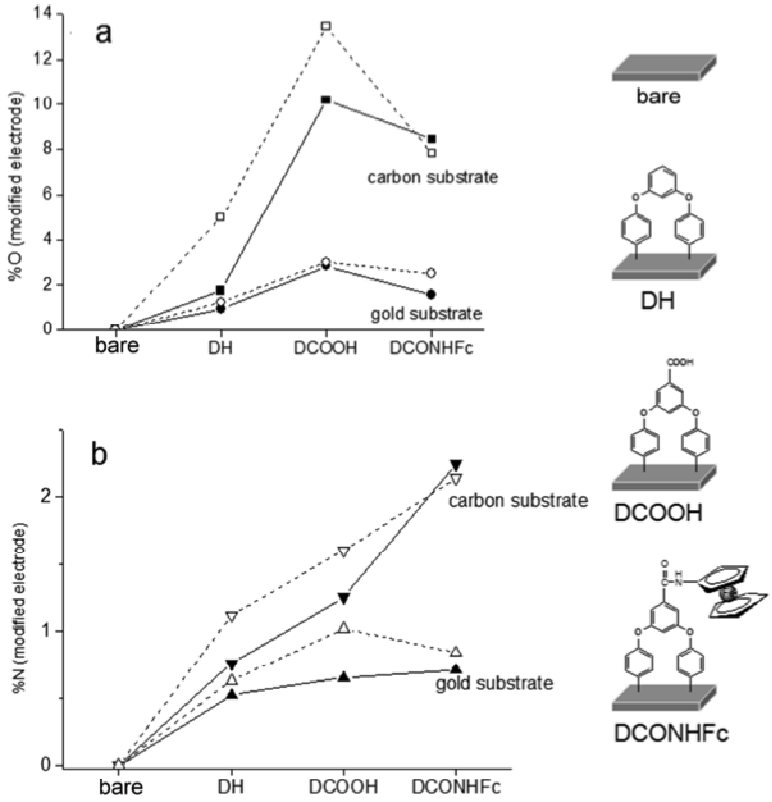

Figure 5.7. Elemental percent of atomic concentration for different surfaces as measured by XPS. The percent of the element in unmodified substrates was subtracted. a) % of oxygen —■— Zn-mediated on C, ---□ --- electrografting on C, —●— Zn-mediated on Au, ---○ --- electrografting on Au, b) % of nitrogen —▼— Zn-mediated on C, ---▽--- electrografting on C, —▲— Zn-mediated on Au, ---△--- electrografting on Au.

The formation of more than one layer is evidenced by the increased %N from DH to DCOOH due to the formation of ⁻N=N⁻ bridges with a band at 398 eV for gold and 400.6 eV for carbon. The amide formation, due to the reaction of DCCOH on the surface with amine-ferrocene, increases the final %N.

In all cases the %N is lower for gold than that of carbon, which is in agreement with the thinner layers formed on gold, as observed in AFM. In addition, the band corresponding to the stretching vibration mode of ⁻N=N⁻ bridge is not present in the Raman spectra even when a SERS surface was used due to the nanometric thickness of the DCOOH layer evidenced by AFM, being higher for electrochemical grafted in comparison with Zn-mediated modified surfaces.

X-ray photoelectron spectroscopy (XPS) of modified surfaces for testing the viability of linking a probe molecule

To evaluate the viability of COOH moieties to bind an aminated molecule, the DCOOH layers immobilized on gold and carbon substrate by Zn-mediated, electrochemical, and spontaneous grafting were linked to amino-ferrocene through carbodiimide chemical cross-linking, and the modified surfaces were analysed by XPS. **Figure 5.8** (top) shows the successful linking of amino-ferrocene to the Zn-mediated and electrochemically grafted surfaces, as evidenced by the presence of $Fe2p_{3/2}$ and $Fe2p_{1/2}$ [44] signals at 720.9 and 708.9 eV, respectively. The Fe content can be used as a criterion of the presence of ferrocene immobilized on the surface. Similar values were obtained for the same type of substrate prepared by Zn-mediated grafting when compared with traditional electrochemical method. On gold, the obtained percentages were 1.31 and 1.26 for Zn-mediated and electrochemically grafted DCOOH, respectively, whereas for carbon the values were 1.51 and 1.45 %.

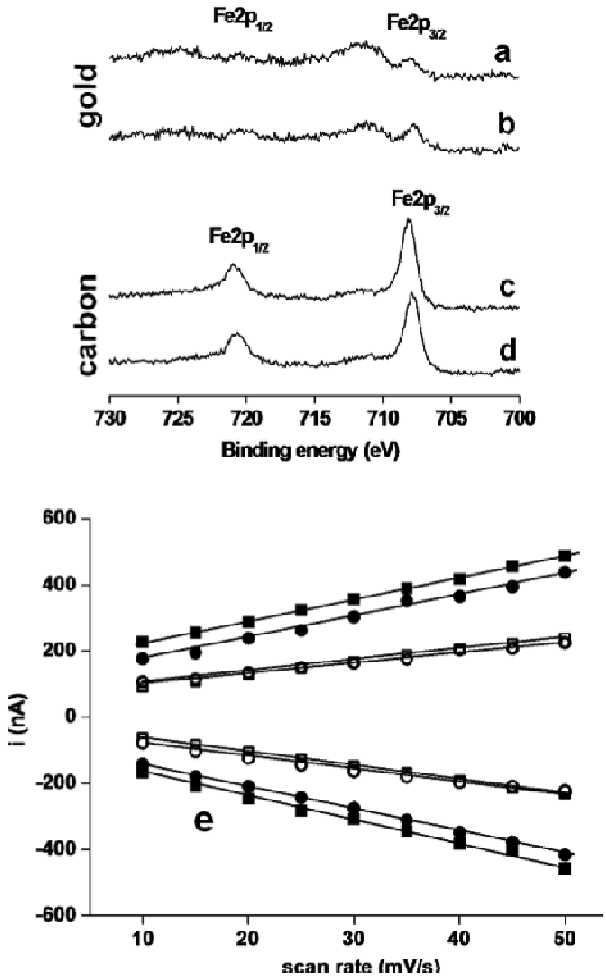

Figure 5.8. Top: High resolution XPS spectra of Fe region of Zn-mediated (a, c) and electrochemical (b, d) grafted gold and carbon. Bottom: Dependence of peak current with scan rate of immobilised amino ferrocene for Zn-mediated grafting on carbon (•), chemical grafting on gold (○), electrochemical grafting on carbon (■), and electrochemical grafting on gold (□).

The surface confinement of the ferrocene group was also confirmed using cyclic voltammetry by observing a low peak-to-peak separation and obtaining a linear behaviour of cathodic and anodic peak currents versus scan rate (**Figure 5.8**, bottom). A negligible XPS signal as well as oxidation/reduction peaks were observed for 5-minute spontaneously grafted surfaces.

Evaluation of stability of Zn-mediated grafted layers of diazonium salts

As one of the more notable properties of grafted diazonium layers is their remarkable stability, an evaluation of the stability of the Zn-mediated grafted layers on gold and carbon at elevated temperatures and upon exposure to high applied potentials, as well as a storage stability of the grafted layers at different temperatures over a four-week period was carried out. The Zn-

mediated modified surfaces were stable up to 95 ºC, in which less than 10 % of organic layer was removed following exposure of the substrates at this temperature. The surfaces were also stable after applying +1 V and after storage at 37 ºC for four weeks, demonstrating the high stability of these surfaces in different conditions (**Figure SI 5.7** and **SI 5.8**). Considerably higher stability was observed for Zn-mediated surfaces in comparison with the spontaneously deposited layers during 5 min. This indicates that in the absence of Zn, mainly physical adsorption occurs, which can be easily removed by heating or applying a positive potential. This also highlights the role of Zn in our potentiostat-free method.

5.5 CONCLUSIONS

Zn-mediated grafting of diazonium salts on gold and carbon surfaces was achieved by using zinc as a reducing agent. The decrease of the immobilisation of DCOOH on gold and carbon in the presence of a radical scavenger demonstrated that there was an important radical contribution to the overall mechanism of dediazonation by using the Zn-mediated approach. Grafting was extremely rapid (achieved in just five minutes) and was highly controllable, resulting in very thin layers.

Zn-mediated, electrochemically, and spontaneously grafted layers of a bipodal diazonium salt model system, on both gold and carbon surfaces were compared. Thinner layers were obtained using chemical approach in comparison with electrochemical grafting, in which the formation of multilayers is less controllable. In addition, the surface coverage using Zn-mediated grafting was markedly higher than spontaneous grafting at 5 min, demonstrating the importance of the Zn as reducer.

In all cases, a notably higher efficiency was achieved on carbon as compared with gold. Stability at high-applied potentials, elevated temperatures and upon storage was evaluated and the grafted surfaces were shown to be extremely stable.

In summary, an extremely rapid, potentiostat-free methodology for the grafting, with high spatial resolution, of highly stable thin layers of diazonium salts on gold and carbon surfaces, exploiting zinc as a reducing agent, has been demonstrated, and the underlying grafting mechanism elucidated. Work is ongoing to apply the grafted surfaces to molecular sensing.

5.6 REFERENCES

1. C. Galli, Chem. Rev., **1988**, 88, 765.
2. D. Bélanger, J. Pinson, Chem. Soc. Rev., **2011**, 40, 3995.
3. M. Delamar, R. Hitmi, J. Pinson, J. M. Savant, J. Am. Chem. Soc., **1992**, 114, 5883.
4. P. Allongue, M. Delamar, B. Desbat, O. Fagebaume, R. Hitmi, J. Pinson, J. M. Savéant, J. Am. Chem. Soc., **1997**, 119, 201.
5. F. Anariba, S. H. DuVall, R. L. McCreery, Anal. Chem., **2003**, 75, 3837.
6. S. Baranton, D. Bélanger, J. Phys. Chem. B., **2005**, 109, 24401.
7. C. Saby, B. Ortiz, G. Y. Champagne, D. Bélanger, Langmuir, **1997**, 13, 6805,.
8. A. Adenier, E. Cabet-Deliry, A. Chaussé, S. Griveau, F. Mercier, J. Pinson, C. Vautrin-Ul, Chem. Mater., **2005**, 17, 491.
9. Adnier, N. Barré, E. Cabet-Deliry, A. Griveau, S. F. Mercier, J. Pinson, C. Vautrin-Ul, Surf. Sci., **2006**, 600, 4801.
10. M. Chussé, M. Chehimi, N. Karsi, J. Pinson, F. I. Podvorica, C. Vautrin-Ul, Chem. Mater., **2002**, 14, 392.
11. Combellas, M. Delamar, F. Kanoufi, J. Pinson, F. I. Podvorica, Chem. Mater., **2005**, 17, 3968.
12. CA. Ricci, C. Bonazzola, E.Calvo, J. Phys. Chem. Chem. Phys., **2006**, 8, 4297.
13. X. Chen, M. Chockalingam, G. Liu, E. Luais, A. L. Gui, J. J. Gooding, Electroanalysis, **2011**, 23, 2633.
14. J. Pinson, F. Podvorica, Chem. Soc. Rev., **2005**, 34, 429.
15. H. M. Nassef, L. Civit, A. Fragoso, C. K. O'Sullivan, Analyst, **2008**, 133, 1736.
16. M. Revenga-Parra, C. Gómez-Anquela, T. García-Mendiola, E. Gonzalez, F. Parientea, E. Lorenzo, Anal. Chim. Acta, **2012**, 747, 84.

17. Bourdillon, M. Delamar, C. Demaille, R. Hitmi, J. Moiroux, and J. Pinson , J. Electroanal. Chem., **1992**, 336, 113.

18. S. Lee, S. E. Baker, M. S. Marcus, W. Yang, M. A. Eriksson, R. J. Hamers, Nano Lett . **2004**, 4, 1713.

19. J. Pinson, In Aryl diazonium Salts: New Coupling agents in polymer and Surface Science. Chehimia, M. M. Ed., Wiley-VCH Verlag, **2012**, Chapter 1.

20. L. Civit, A. Fragoso, C. K. O'Sullivan, Electrochem. Comm.**2010**, 12, 1045.

21. J. E. Piper, G. J. Barbante, N. Brack, P. J. Pigram, C. F. Hogan, Langmuir, **2011**, 27, 474.

22. A-M. J. Haque, K. Kim, Chem. Commun., **2011**, 47, 6855.

23. B. Cui, J. Y. Gu, T. Chen, H. J. Yan, D. Wang, L. J. Wan, Langmuir, **2013**, 29, 2955.

24. S. Baranton, D. Bélanger, Electrochim. Acta, **2008**, 53, 6961.

25. J. Lehr, D. J. Garrett, M. G. Paulik, B. S. Flavel, P. A. Brooksby, B. E. Williamson, A. J. Downard, Anal. Chem., **2010**, 82, 7027.

26. C. Mangeney, Z. Qin, S. A. Dahoumane, A. Adenier, F. Herbst, J. P. Boudou, J. Pinson, M. M. Chehimi, Diamond Relat. Mater., **2008**, 17, 1881.

27. F. Mirkhalaf, T. J. Mason, D. J. Morgan, V. Saez, Langmuir, **2011**, 27, 1853.

28. N. Rubio, M. A. Herrero, M. Meneghetti, A. Díaz-Ortiz, M. Schiavon, M. Prato, E. Vázquez, J. Mater. Chem., **2009**, 19, 4407.

29. Z. Wei, T. Bin, Z. Jun-Ge, P. Yue-Xiu, S. Jin-Bo, S. Jian-Bing, D. Yu-Ping, Acta Phys. Chim. Sin., **2010**, 26, 822.

30. V. Mévellec, S. Roussel, L. Tessier, J. Chancolon, M. Mayne-L'Hermite, G. Deniau, P. Viel, S. Palacin, Chem. Mater., **2007**, 19, 6323.

31. J. K. Kariuki, M. T. McDermott, Langmuir, **1999**, 15, 6534.

32. L. Civit, O. El-Zubir, A. Fragoso, C. K. O'Sullivan, Biosens. Bioelectron., **2013**, 41, 840 .

33. C. Combellas, F. Kanoufi, J. Pinson, F. I. Podvorica, J. Am. Chem. Soc., **2008**, 130, 8576.

34. T. Menanteau, E. Levillain, T. Breton, Chem. Mater., **2013**, 2, 2905.

35. A. L. Gui, H. M. Yau, D. S. Thomas, M. Chockalingam, J. B. Harper, J. J. Gooding, Langmuir, **2013**, 29, 4772.

36. E. Lebègue, T. Brousse, J. Gaubicher, Ch. Cougnon, Electrochim. Acta, **2013**, 88, 680.

37. A. Mesnage, X. Lefèvre, P. Jégou, G. Deniau, S. Palacin, Langmuir, **2012**, 28, 11767.

38. L. Madec, D. Robert, P. Moreau, P. Bayle-Guillemaud, D. Guyomard, J. Gaubicher, J. Am. Chem. Soc., **2013**, 135, 11614.

39. K. Guo, X. Chen, S. Freguia, B. C. Donose, Biosens. Bioelectron., **2013**, 43, 184.

40. C. Combellas, F. Kanoufi, J. Pinson, F. I. Podvorica, Langmuir, **2005**, 21, 280.

41. A. Mattiuzzi, I. Jabin, C. Mangeney, C. Roux, O. Reinaud, L. Santos, J-F. Bergamini, P. Hapiot, C. Lagrost Nat. Commun., **2012**, 3:1130, DOI: 10.1038/nc0mms2121.

42. T.-C. Kuo, L. R. McCreery, Anal. Chem., **1999**, 71, 1553.

43. B. Li,L. Zhou, D. Wu, H. Peng, H. Yan, Y. Zhou, Z. Liu, ACS Nano, **2011** 5, 5957.

44. T. Kitagawa, H. Matsubara, K. Komatsu, K. Hirai, T. Okazaki, T. Hase, Langmuir, **2013**, 29, 4275.

45. The images were processed using Nanotec Electronica WSxM freeware: I. Horcas, R. Fernández, J. M. Gómez-Rodríguez, J. Colchero, J. Gómez-Herrero, A. M. Baro, Rev. Sci. Instrum., **2007**, 78, 013705.

5.7 SUPPORTING INFORMATION

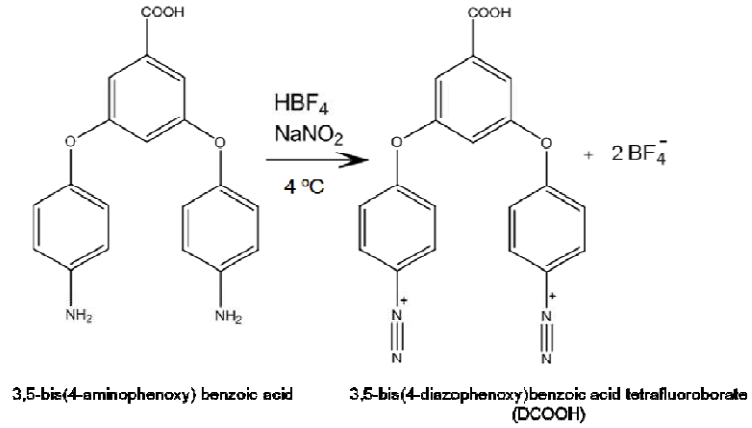

Scheme SI 5.1. Schematic representation of the structure of the starting amine and diazonium salt (DCOOH), and synthetic route.

Diazonium salt was synthesised material is formed. This dark material should be discarded and for this reason DCOOH was isolated as a tetrafluoroborate salt and characterised using FTIR, Raman and NMR (**Figure SI 5.1, and SI 5.3 (a)**). In the FTIR spectrum, the band corresponding to the diazonium salts, with a concomitant appearance of band indicative of the (C group at 2260 cm^{-1}, which is also observed in Raman spectrum. In addition the increase in electroaceptor properties of diazo group respect to the starting evidenced in a significant shift of carboxylic FTIR band from 1677 cm^{-1} to 1744 cm^{-1} in DCOOH. It is also evidenced in the carbon adjacent to diazo group (102.5 ppm) respect to their initial chemical shift in the precursor amine (140.4 ppm).

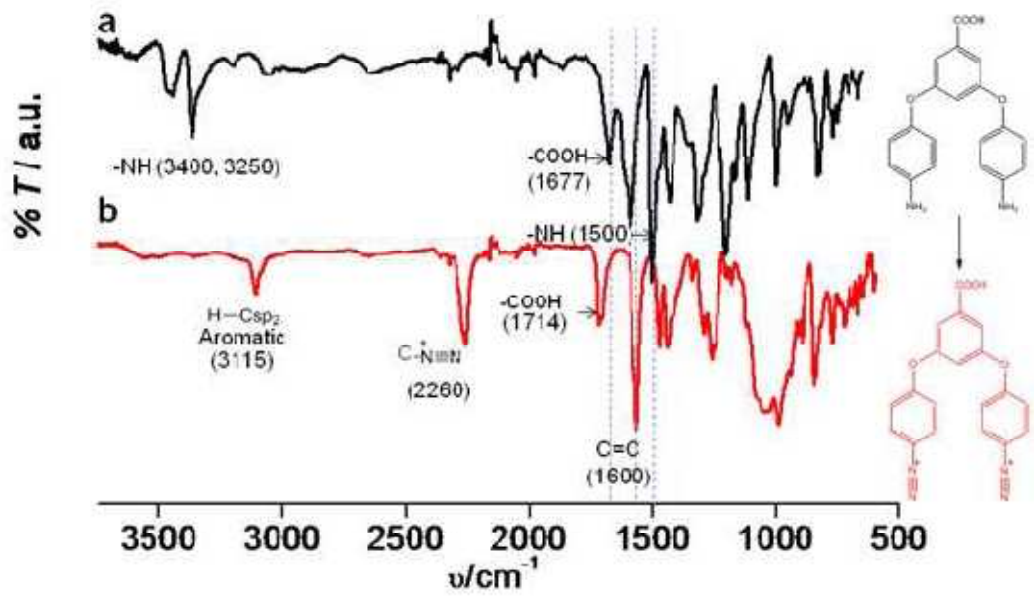

Figure SI 5.1a. ATR-FTIR spectra of (a) 3,5-bis(4-aminophenoxy) benzoic acid and (b) 3,5-bis(4-diazophenoxy)benzoic acid tetrafluoroborate.

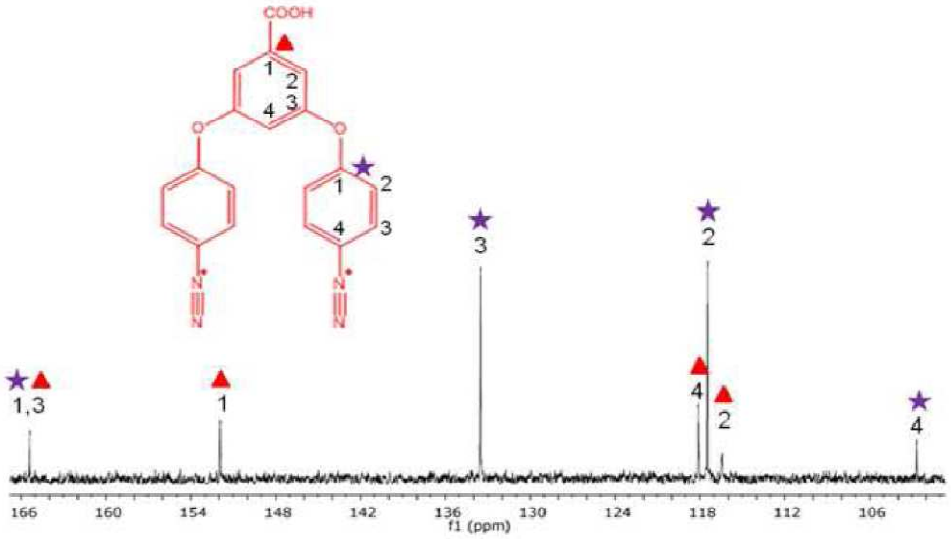

Figure S 5.1b. 100 MHz ^{13}C-NMR spectrum of aromatic region of 3,5-bis(4-diazophenoxy)benzoic acid tetrafluoroborate

Optimisation of Zn-mediated grafting on gold and carbon substrates

Several driving forces, including applied potential/potential range, nature of the diazonium salt and the diazonium salt concentration have been shown to control electrochemical grafting. In order to evaluate them in the proposed Zn-mediated method a study was carried out to optimize the duration of the chemical grafting step and the concentration of the diazonium salt. 3,5-bis(4-diazophenoxy)benzoic acid tetrafluoroborate at 1, 5 and 10 mM concentrations was dissolved in deoxygenated acid media in the presence of Zn as a reducing agent and drop casted on carbon or gold substrates and left to react for 2 or 5 minutes. After washing and drying, cyclic voltammetric measurements were carried out, in triplicate, in a $[Fe(CN)_6]^{3-}$ /$[Fe(CN)_6]^{4-}$solution. The percentage decrease in current of the reduction and oxidation peaks of Fe(II) /Fe(III), with respect to the clean electrode, was indicative of the formation ofthe organic layer on the electrode.

As can be seen in **Figure SI 5.2**, using both gold and carbon the highest degree of grafting is accomplished at 5 minutes with 5 mM concentration of DCOOH. These conditions were thus used for all further experiments.

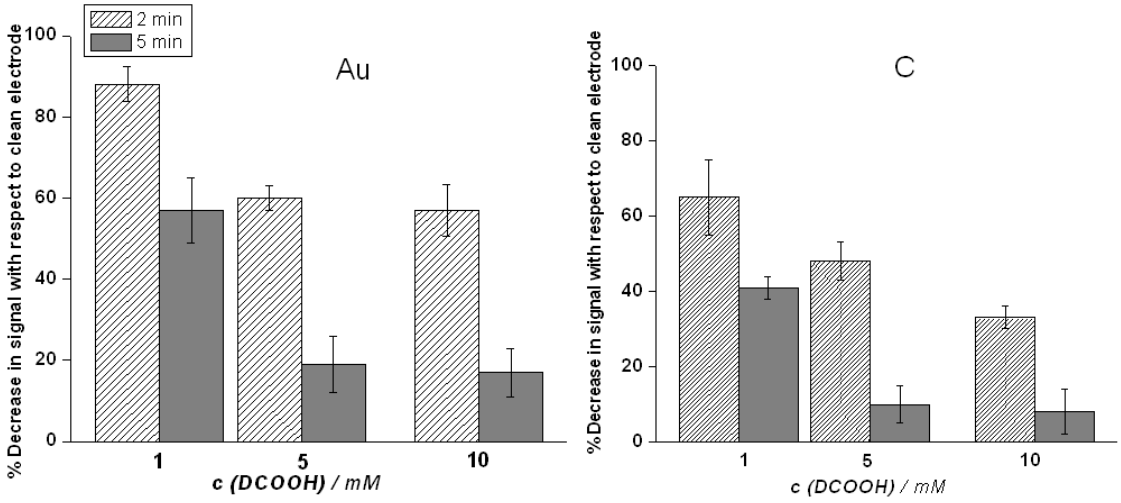

Figure SI 5.2. Effect of different incubation times and concentration of DCOOH on the modification of gold (left) and carbon (right) surfaces by measuring the intensity of current of the oxidation peak of $[Fe(CN)_6]^{3-}$ /$[Fe(CN)_6]^{4-}$ at same potential of the clean electrode. Error bars represent the relative standard deviation of three measurements.

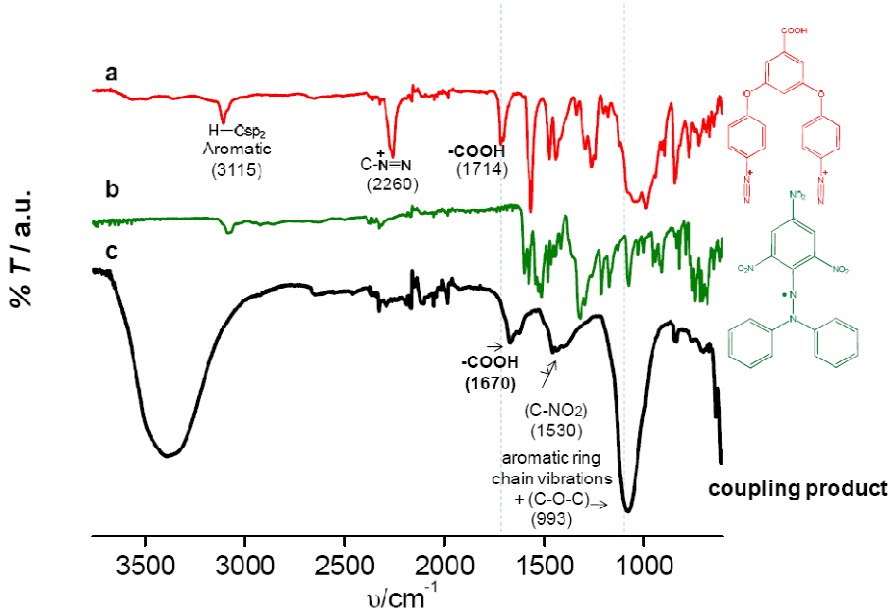

Figure SI 5.3. ATR-FTIR spectra of (a) 3,5-bis(4-diazophenoxy)benzoic acid tetrafluoroborate, b) (2,2-diphenyl-1-picrylhydrazyl (DPPH)) and c) the coupling product after isolation.

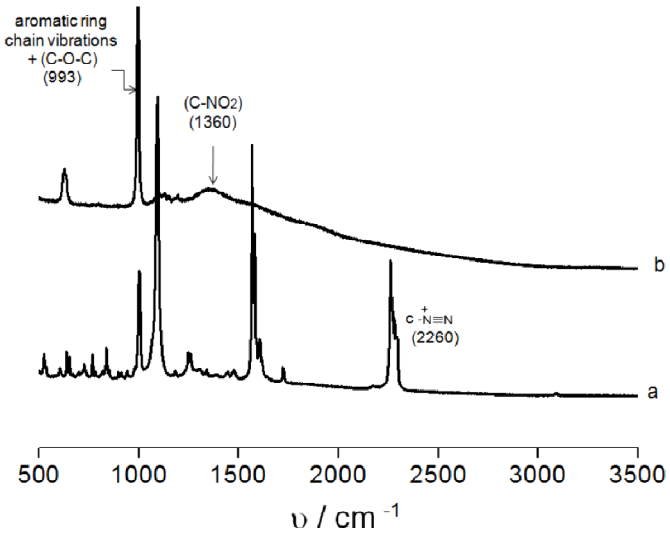

Figure SI 5.4. Raman spectra of (a) 3,5-bis(4-diazophenoxy)benzoic acid tetrafluoroborate and b) the coupling product after isolation.

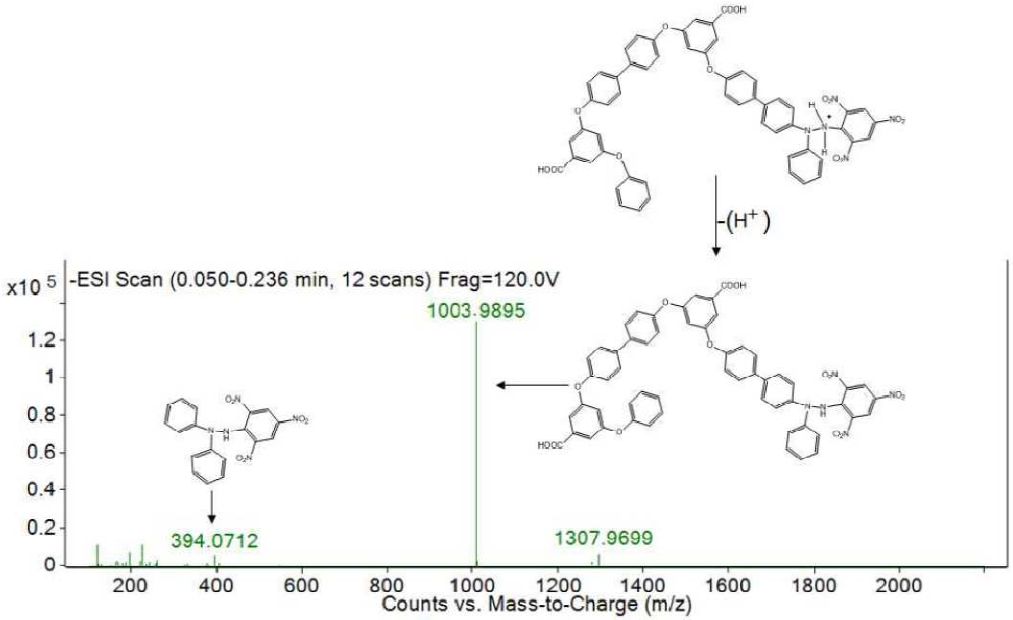

Figure SI 5.5. ESI-TOF spectrum of the coupling product between DCOOH and DPPH, obtained with negative detector. The spectrum was obtained by direct injection of the sample in an Agilent G3250AA LC-MSTOF spectrometer.

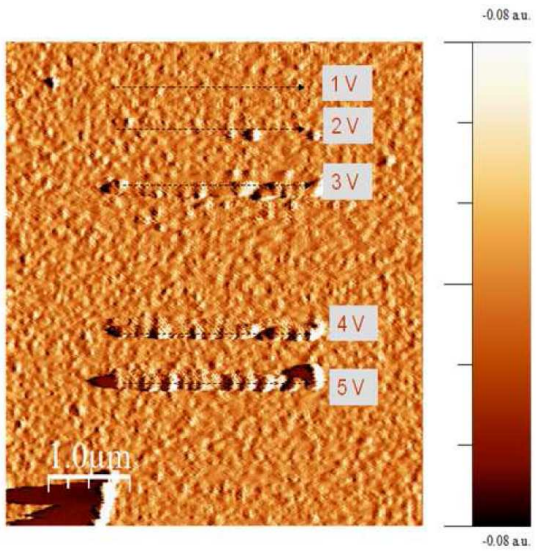

Figure SI 5.6. AFM scratched surfaces (left) and the corresponding profiles (right) of chemical grafted diazonium salt in gold a), and in carbon b).

Stability studies

Temperature stability

Modified electrodes were exposed to different temperatures (from 25 to 95 ºC at 10 ºC intervals) during 5 min in a thermomixer (Eppendorf Iberica, Spain) and then gently washed in Milli-Q water and dried under nitrogen. The changes in kinetic properties with temperature were evaluated using cyclic voltammetry using a 1 mM $K_4[Fe(CN)_6]$ /$K_3[Fe(CN)_6]$ solution in 50 mM of $Sr(NO_3)_2$. The CVs were recorded from -0.4 to 0.6 V at 0.1 V/s

Stability to applied potentials

Modified electrodes were exposed to different potentials using amperometry during 5 sec in buffer phosphate, pH = 7.4. They were then gently washed in Milli-Q water and dried under nitrogen. The changes in kinetic properties with temperature were evaluated by cyclic voltammetry as described above.

Storage stability

The electrodes were modified, dried and stored at different temperatures (4, 25 and 37 ºC) during several weeks and following a gentle wash in Milli-Q water and drying under nitrogen, the grafted surfaces were evaluated using cyclic voltammetry of 1 mM $K_4[Fe(CN)_6]$ /$K_3[Fe(CN)_6]$ in 50 mM of $Sr(NO_3)_2$. The CV was recorded from -0.4 to 0.6 V at 0.1 V/s.

Thermal and electrochemical stability of grafted diazonium surface

In order to p**r**obe the thermal stability of the grafted layers, the electrodes were immersed in phosphate buffer at pH 7.4 and heated to the desired temperature in a thermostatted bath, and subsequently were washed and a cyclic voltammogram was recorded in a $[Fe(CN)_6]^{3-}$ /$[Fe(CN)_6]^{4-}$ solution.

For the study of stability at high applied potentials, electrodes grafted with DCOOH spontaneously, electrochemically and Zn-mediated, were immersed in phosphate buffer at pH 7.4 and different potentials were applied, followed by cyclic voltammetric analysis (**Figure SI 5.7**).

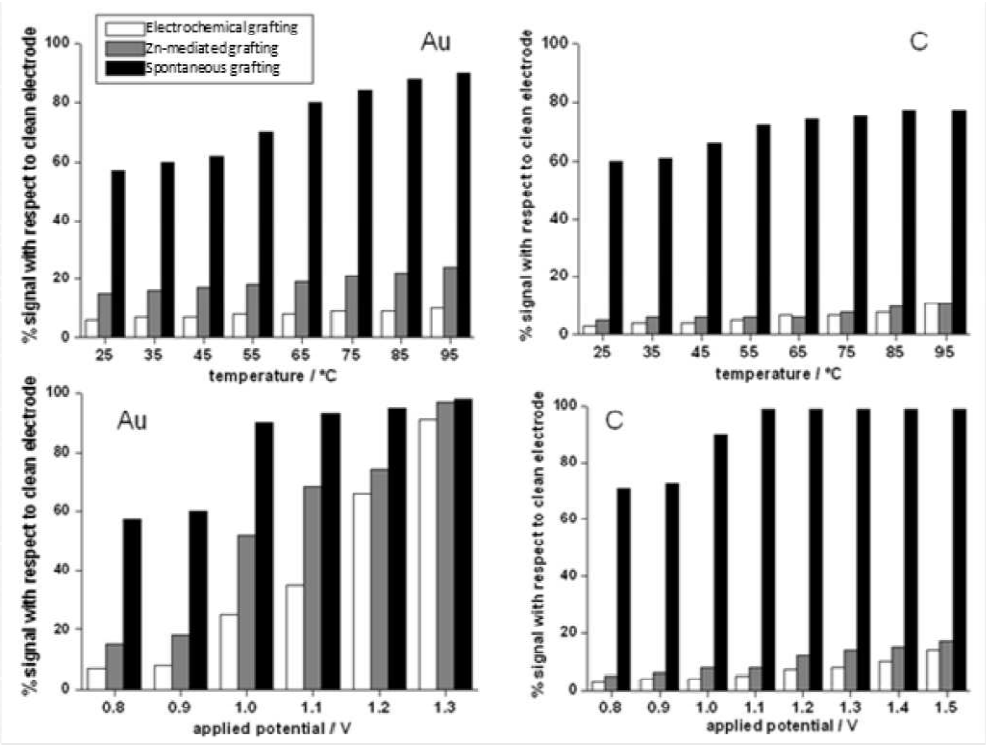

Figure SI 5.7. Stability study with temperatures (from 25 to 95 ºC, during 5 min) and upon exposure to applied potentials (from 0.8 to 1.5 V, during 5 s) for gold (left) and carbon (right) by measuring the intensity of current of the oxidation peak of $[Fe(CN)_6]^{3-}$ /$[Fe(CN)_6]^{4-}$ at same potential range of the clean electrode.

A higher degree of immobilisation as well as stability at high temperatures and applied potentials was observed for the Zn-mediated grafted surfaces in comparison to the spontaneously grafted surfaces, clearly demonstrating the importance of the Zn as a reducing agent. Indeed, the Zn-mediated grafted surfaces demonstrated a similar behavior to the electrochemically grafted surfaces. In the case of carbon modified by Zn-mediated and electrochemical grafting, less than 10 % of organic layer was removed following exposure of the substrates to 95 ºC, while in the spontaneously grafted surface almost all the aryl molecules desorbed.

When looking at the effect of applied electric potential, a more evident difference was observed between carbon and gold surfaces, as well as Zn-mediated/ electrochemically vs spontaneously grafted surfaces. As expected, a higher stability was observed using carbon substrates due to the higher covalent contribution in DCOOH binding to the carbon rather than the gold

substrate. At applied potentials higher than 1 V vs Ag, the organic layer on gold was affected and this was observed to be more significant in the case of the spontaneously grafted surface. In contrast, on the carbon substrate the signal remains very stable even when potentials as high as 1.4 V vs Ag are applied, for both chemically and electrochemically grafted surfaces, while the surface prepared by spontaneous grafting was drastically affected. The Zn-mediated grafted carbon substrates can thus find application in areas where a high applied potential is required, such as electrochemiluminescence of immobilised moieties.[21]

Storage stability of chemical grafted diazonium surface

The Zn-mediated grafted surfaces were stored at different temperatures (4 ºC, 25 ºC and 37 ºC) over a 4 weeks period, and the stability of the grafted layers was studied using cyclic voltammetry, where an increasing signal reflects loss of molecules from the surface. As can be seen in **Figure SI 5.8**, as expected a higher grafting efficiency was achieved using the carbon surface, but for both surfaces excellent storage stabilities were observed at all evaluated temperatures.

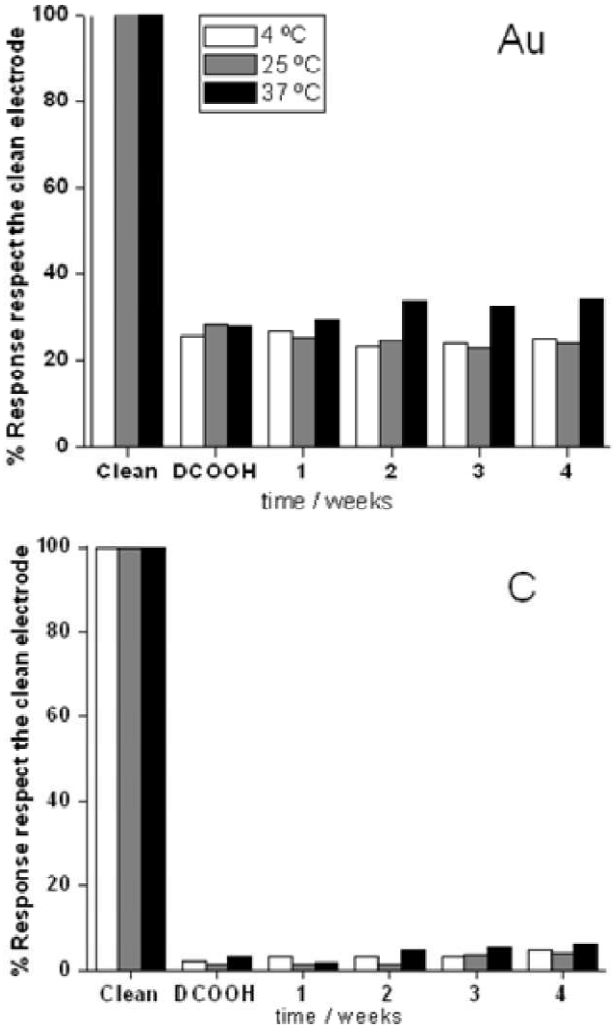

Figure SI 5.8. Stability study at different times (4 weeks) and temperature (4, 25 and 37 ºC) of storage of Zn-mediated grafted DCOOH on gold (top) and on carbon by measuring the intensity of current of the oxidation peak of $[Fe(CN)_6]^{3-}$ /$[Fe(CN)_6]^{4-}$ at same potential of the clean electrode, (Scan rate, 0.1 V/s).

CHAPTER 6

AMPEROMETRIC DETECTION OF FRANCISELLA TULARENSIS GENOMIC SEQUENCE ON DIAZONIUM MODIFIED SUBSTRATES

(Submitted, 2014)

CHAPTER 6

AMPEROMETRIC DETECTION OF FRANCISELLA TULARENSIS GENOMIC SEQUENCE ON Zn-MEDIATED DIAZONIUM MODIFIED SUBSTRATES

6.1. ABSTRACT

A new simple and rapid potentiostat-free method for preparing diazonium salt based platforms is applied for biosensor purposes, promoting better analytical performances when comparing with traditional electrografting.

6.2 INTRODUCTION

Biosensors are promising analytical tools for the detection of proteins[1] and DNA.[2] The success of these devices is highly dependent of the transducer surface engineering in which the recognition element should be properly confined.[3] Self-assembled monolayers (SAM) of thiolated molecules on gold have been widely used because its simplicity and possibility of functionalisation of, for example, bi-functionalised molecules with an end-thiol moiety and a reactive functional group (usually, amine, carboxylate or maleimide) able to covalently bind proteins or DNA[4-6]. In general, these SAM-based platforms provide an appropriate analytical performance for biosensor development in mild conditions. But, the quasi-covalent Au-S bond (E_{bond}(Au-S) = 167 kJ/mol can be affected when exposing to the ambient UV irradiation [7], high temperatures[7,8] or extreme potentials.[9] Significant stability improvement can be achieved when grafting thiolated molecules on carbon substrates by increasing the covalent nature of the binding (E_{bond}(C-S) = 272 kJ/mol). In these approaches the carbon surfaces should be chemically or electrochemically pre-treated for activation.[10-12]

The higher reactivity of diazonium salts versus thiols have made them attractive alternatives for surface modification due to an easier grafting without the need of special treatment on surfaces.[13-16] In addition, the strong binding of diazonium salts to gold and carbon (E_{bond} (Au-C) = 290 kJ/mol,[17] E_{bond}(C-C) = 451.9 kJ/mol[18]) makes possible its derivatisation in similar manner to the reactions in solution and use them as biomolecule linkers to the surfaces.[7]

In both of the most common grafting approaches, namely "spontaneous"[19] and electrochemical,[13-16] multilayer formation is difficult to avoid due to the reactive nature of the diazonium radical formed. For biosensing applications, a monolayer is highly desirable as it permits the availability of the functional group for the subsequent binding of the biomolecules without a total blocking of the surface.[20] As a combination of the advantages from both approaches, we recently developed a controlled Zn-mediated method for grafting thin layers of a bipodal diazonium salt on gold and carbon substrates. The grafted molecule demonstrated to be able of linking ferrocene groups to the gold and carbon surfaces.[21] In the present work the viability of using these platforms as linkers for DNA probes on gold and carbon electrodes was studied using surface platform resonance (SPR) and chronocoulometry (CC). The developed surfaces were applied in the amperometric detection of a DNA sequence associated to *Francisella tularensis* (a potential warfare agent).

6.3. EXPERIMENTAL SECTION

Materials

All reagents used were used as received. N-ethyl-N-(3-dimethylaminopropyl) carbodiimide hydrochloride (EDC), *N*-hydroxysuccinimide (NHS), phosphate buffered saline (PBS), strontium nitrate ($Sr(NO_3)_2$), potassium chloride (KCl), sodium acetate, tetrafluoroboric acid solution, zinc dust (Zn), sodium nitrite, hydroquinone, potassium hexacyanoferrate(III) ($K_3Fe(CN)_6$, 99 + %), and ethanolamine hydrochloride were purchased from Sigma-Aldrich. The sulfuric acid (H_2SO_4), sodium chloride (NaCl) and hydrogen peroxide (H_2O_2) were invested on Sharlau. The potassium hydroxide (KOH) were bought from J. T. Baker and 3,5-bis(4-aminophenoxy) benzoic acid from TCI. All solutions were prepared with Milli-Q water (Millipore Inc., U 1⁄4 18 MU cm). The 5-bis(4-diazophenoxy)benzoic acid tetrafluoborate (DCOOH) was prepared as reported.[21]

Synthetic HPLC-grade oligonucleotides were purchased from Biomers.net (Ulm, Germany):

Capture probe: NH_2-TEG-5'-CTT AGT AA TTG GGA AGC TTG TAT CAT GGC ACT TAG AA-3'

Complementary Target: 5-'ATT ACA ATG GCA GGC TCC AGA AGG TTC TAA GTG CCA TGA TAC AAG CT TCC CAA TTA CTA AGT ATG CTG AGA AGA ACG ATA AAA CT TGG GCA-3'

HRP-labeled secondary probe: 5'-TCT GGA GCC TGC CAT TGT AAT-HRP-3'

Non-complementary target: :5'-GAG AGG AAG GAG ACT GTC TGG AAG TTG CCT CTG TTC CAC AGA CTT AGA TTT GAC CCG CAA TTT GCA CTG ACA AAC ATG GCT GTG CTA AAA CAT A-3'

Instrumentation and Methods

Surface functionalisation

DNA sequences were immobilised or detected as following: The carboxylate of DCOOH was activated with EDC:NHS 4:1 molar ratio in acetate buffer at pH 5.6 during 30 minutes. After rinsing with water, 1 µM aminated-DNA capture probe (in 10 mM PBS buffer pH 7.4) was added was allowed to interact for 1 hour. The unreacted carboxylate groups were deactivated by reacting with ethanolamine (pH 8) during 30 min. After washing with PBS, the electrode will be ready for using.

Electrochemical measurements

Electrochemical measurements were performed on a PC controlled PGSTAT12 Autolab potentiostat (EcoChemie, The Netherlands) using screen printed carbon (DRP-110) and gold (DRP-250BT). The electrode configuration was: working electrode: carbon or (gold) disk (φ = 4 mm), reference electrode: silver (silver), counter electrode: carbon or (platinum). All electrochemical experiments were performed a minimum of three times. The electrodes were modified and checked as previously described.[21]

Cyclic voltammetry (CV) and chronocoulometry (CC**)** were performed in a Autolab model PGSTAT12 potentiostat/galvanostat controlled with the General Purpose Electrochemical System (GPES) software (Eco Chemie B.v. The Netherlands). The parameters employed were: CV, sweep rate) 100 mV/s; CC, pulse period: 500 ms, pulse width: 500 mV. 150 µM of $[Ru(NH_3)_6]Cl_3$ was used as electroactive species. The surface excess of redox marker $[Ru(NH_3)_6]^{3+}$ (Γ_{Ru} in mol/cm^2), and the surface coverage of ssDNA (probe on the surface: Γ_{ssDNA} in molecule/cm^2) and dsDNA (probe+target captured on the surface: Γ_{sdDNA} in

molecule/cm^2), where calculated from integrated Cottrell expression, extrapolating at time = 0 and substituting in the equation 1 (Eq1):[22-24]

Eq1. $$\Gamma DNA = \Gamma Ru\left(\frac{z}{m}\right) NA$$ where z = 1 (number of electrons involved in the reduction of Ru(III) to Ru(II)) m is the number of bases of ssDNA (37) or dsDNA (ssDNA + complementary target) (128) and dsDNA (131) (ssDNA + noncomplementary target)

The areas of electrodes needed for calculations were determined by carrying CV of 2 mM $K_3Fe(CN)_6$ + 0.2 M KCl at different scan rates and using the simplified Randles-Sevcik equation at 25 ºC,[20] being 0.127 ± 0.05 cm^2 for gold and 0.140 ± 0.02 cm^2 for carbon (geometric surface area 0.125 cm^2, r = 0.2 cm).

Amperometric detection of Francisella tularensis DNA target.

The target at different concentrations (0 to 10 nM) and the secondary horse radish peroxidise labelled DNA (DNA-HRP) (10 nM) in 10 mM PBS pH 7.4 + 0.8 M NaCl were added consecutively and incubated for 1 hour each in electrodes (gold and carbon) tethered ssDNA, at 25 ºC. The Step and Swep (SAS) amperometric detection at -0.2 V. was achieved firstly by recording the background in PBS buffer at pH 6, followed by the addition of the mediator hydroquinone (1 mM) and the substrate of the enzyme, H_2O_2 (1 mM) and measuring again. Final values were obtaining by subtracting the background from total signal. A noncomplementary target was used at 10 nM concentration for specificity studies.

The Surface Plasmon Resonance (SPR) studies

The Surface Plasmon Resonance (SPR) studies were carried out in a HORIBA instrument at 37 ºC. SPRi-Slides,™ were cleaned with cool Piranha solution *(warning: Piranha solution is very corrosive)* for 1 minutes, followed by thorough washing with water and finally treated with ozone using a PSD-UVT cleaning instrument (from Novascan, USA) for 9 min, rinsed with ethanol and dried under a filtered nitrogen stream. DCOOH was grafted a) by Zn-mediated method and b) allocating a drop of DCOOH sulphuric solution on slide, immersing the counter and reference electrodes in the drop, and doing the electrografting tacking the slide as working

electrode. The slide was properly washed as described above and after activation of DCOOH, 10 µM aminated-ssDNA was added and blocked with 1 mM ethanolamine-HCl pH 8 as previously described. An additional blocking was made by immersing in Denhardt´s solution during 15 min under stirring in the dark, washed with PBS during 15 min and then dried with nitrogen stream. Then the chip was allocated in the glass prism using 4 µL of oil. The conditions selected for the study were: Kinetics Angle: 58.20°, Flow rate: 50 µL/min, sample loop volume: 200 µL and 37 ºC. Firstly,12 mM of NaOH with 12 % of ethanol was passed at 50 µL/min, then washed with PBS (with 0.8 M NaCl) and 500 nM of specific or non-specific target was injected in 0.8 M NaCl (to achieve target saturation of the surface). After each step the surface was regenerated using NaOH and washed with PBS. Target surface coverage calculations were provided from the intrinsic software in pg/mm^2 of equipment and for Γ_{dsDNA} calculation the corresponding duplex molecular weights were taken (MW (ssDNA+Complementary Target) = 39837 g/mol and MW (ssDNA + Noncomplementary Target = 40759 g/mol)).

6.4. RESULTS AND DISCUSSION

DNA sensing gold and carbon platforms were prepared by linking the capture DNA to the already grafted surfaces with 5-bis(4-diazophenoxy)benzoic acid tetrafluoborate (DCOOH) by the new potentiostat-free method[21] or electrochemically (**Figure 6.1a**). After blocking the non-reacted carboxylates, the surfaces were used for capturing DNA target. The first approximation to evaluate the accessibility of target to the grafted capture probe was by Surface Plasmon Resonance (SPR) (**Figure 6.1b**). DNA target was allowed to interact at 37 ºC with the ssDNA surface at high concentration for ensuring surface saturation.

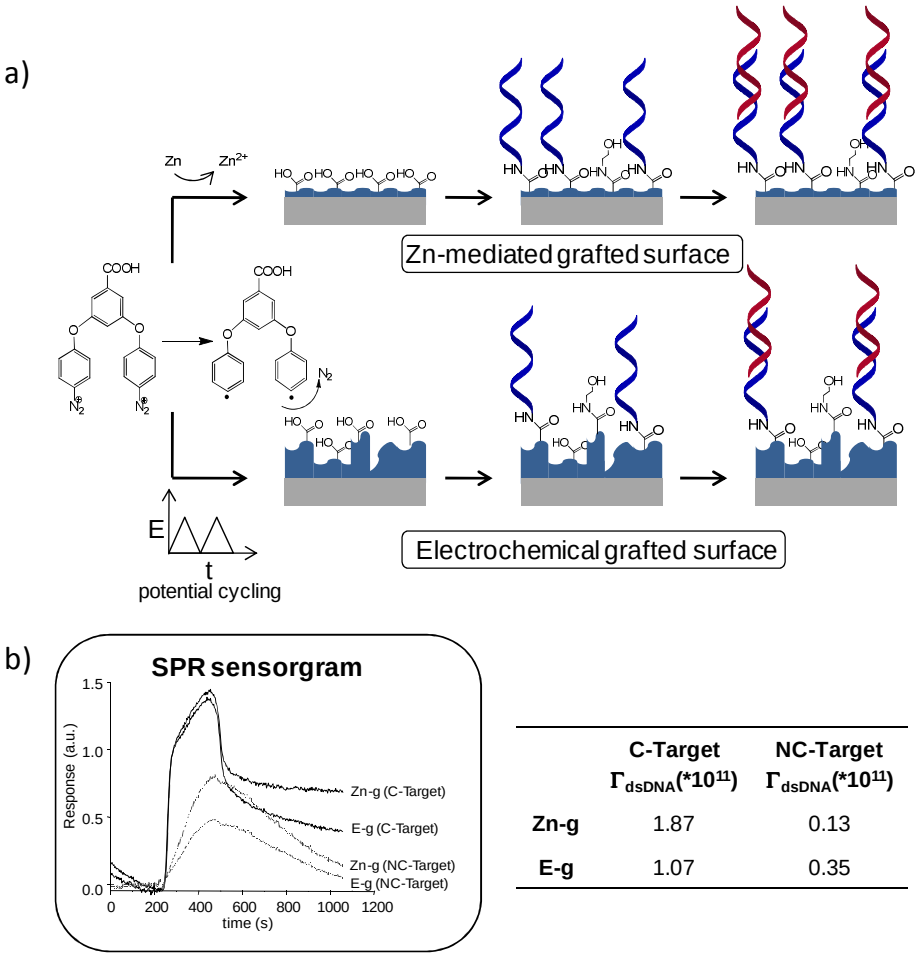

	C-Target Γ_{dsDNA}(*10^{11})	NC-Target Γ_{dsDNA}(*10^{11})
Zn-g	1.87	0.13
E-g	1.07	0.35

Figure 6.1. a) Schematics of diazonium salt grafted surfaces and accesibility of DNA for binding sites. b) SPR of the interaction of complementary (C-Target) and noncomplementary (NC-Target) DNA with Zn-mediated (Zn-g) and electrografted (E-g) DNA tethered surfaces. Γ_{sdDNA} in molecule/cm^2

Higher surface coverage by the DNA target (43%) was found for the spots where DCOOH was grafted following the Zn-mediated method. This could be explained attending to the thinner organic layer that can be achieved by the reduction of diazonium salt using Zn in comparison with electrografting,[21] avoiding multilayer formation that can block the access of the large DNA target to the small linker attached to organic surface. In addition, the surface prepared by electrografting showed around 4 times higher interaction with a non-complementary DNA target in comparison with the Zn-mediated approach, because of the lower accessibility of the blocking of the remaining carboxylic groups that can interact in electrostatic unspecific manner with DNA target.

Chronocoulometry (CC) was used to study the different surface modification steps in both gold and carbon substrates. CC allows to evaluate the surface coverage of the DNA after linking

with DCOOH and also the accessibility of the DNA target to the capture probes.[22,23] $[Ru(NH_3)_6]^{3+}$ cations act as counter ions to compensate the anionic phosphate backbone of DNA in 1 to 3 ratio, by replacing the natively entrapped monovalent Na^+ or K^+ in a low ionic strength solution. The pure electrostatic interaction of $[Ru(NH_3)_6]^{3+}$ without either intercalation or preference for specific base permits a calculation of DNA surface density (Γ_{DNA}) by determining the surface excess of the $[Ru(NH_3)_6]^{3+}$ entrapped in the DNA layer (Γ_{Ru}).[22-24] The values of Q_{dl} and $nFA\Gamma_{Ru}$ when $[Ru(NH_3)_6]^{3+}$ replaces native Na^+ from DNA, were determined by measuring the charge before and after immersing in the redox marker solution and extrapolating at time 0 in a Q vs time$^{1/2}$ plot (**Figure 6.2**). The results are in agreement with literature.[22-24]

As observed in **Figure 6.2**, the DNA surface coverage for Zn-mediated grafted substrates was increased in a 56% for gold and 34 % for carbon respect to the surfaces prepared by electrografting. In consequence, using the Zn-mediated approach, a significant increment of the amount of DNA target molecules captured (around 37 % for gold and 43 % for carbon) respect to electrografted surfaces was achieved. Lower interaction with a non-complementary DNA sequence was observed for the sensors prepared following the Zn-mediated grafting (for gold: 10% for Zn-mediated and 15% for electrografting; for carbon: 12% for Zn-mediated and 20% for electrografting, respect to the signal obtained with complementary target).

For the carbon surface prepared by Zn-mediated approach, the significant increment of the target entrapped is remarkable. The higher roughness and less conductivity of carbon comparing with gold enhance the differences between both approaches. They are more evident here, because the bigger size of DNA respect to the small ferrocene,[21] highlighting the importance of having a thin and organised layer, which can be obtained using Zn-mediated grafting.

The agreement of the results obtained from CC and SPR supports the viability of using Zn-mediated approach for grafting biosensing surfaces.

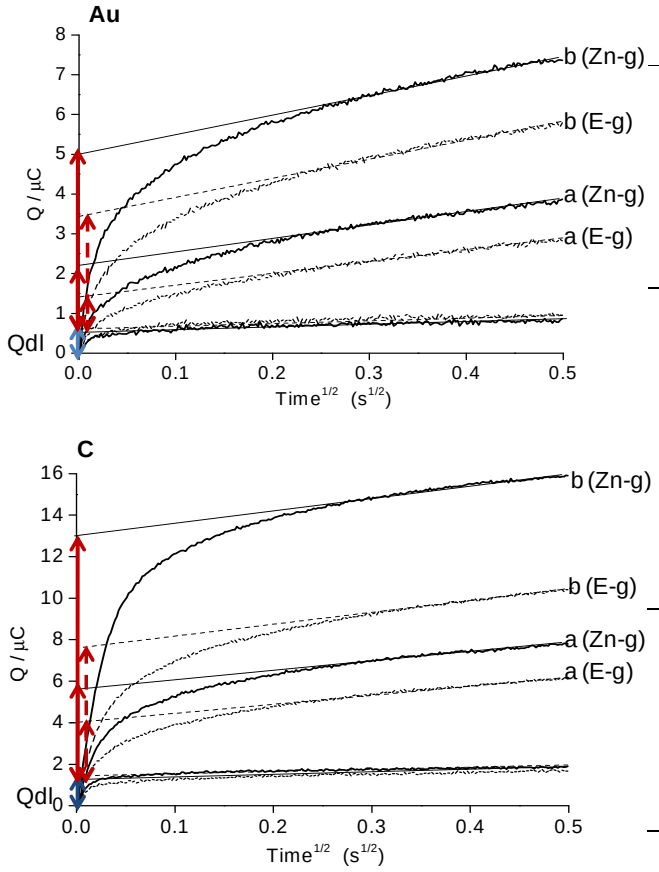

	ssDNA Γ_{Ru} (*10^{-10})	ssDNA Γ_{DNA} (*10^{12})	dsDNA Γ_{Ru} (*10^{-10})	dsDNA Γ_{DNA} (*10^{12})
Zn-g	1.39	6.8	3.67	5.2
E-g	0.75	3.7	2.36	3.3

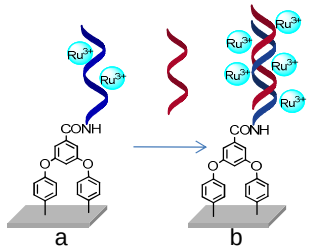

	ssDNA Γ_{Ru} (*10^{-10})	ssDNA Γ_{DNA} (*10^{12})	dsDNA Γ_{Ru} (*10^{-10})	dsDNA Γ_{DNA} (*10^{12})
Zn-g	3.18	15	8.62	12
E-g	2.19	11	4.82	6.8

Figure 6.2. Chronocoulometry study (Anson plot) of DNA surface coverage for gold and carbon substrates modified using both Zn-mediated (continuous trace) and electrografting (discontinuous trace) approaches. Blue arrows: CC in absence of $[Ru(NH_3)_6]Cl_3$ (Qdl); red arrows CC in presence of 150 µM $[Ru(NH_3)_6]Cl_3$ ($nFA\Gamma_{Ru}$) before (a) and after adding target (b). Γ_{DNA} in molecule/cm^2.

Finally, the surfaces were tested for developing amperometric calibration curves in a sandwich type assay using a HRP-modified secondary probe (**Figure 6.3**). As observed in **Figure 6.3**, in the case of the surfaces prepared using Zn-mediated approach, an increase in the sensitivity (around 5-6 times), a decrease in the LOD and lower non-specific interaction percent were observed. In addition, around 5% more of interaction with a non specific target was observed for electrochemical prepared surfaces in comparison with those grafted by Zn-mediated methodology. The higher roughness and less conductivity of carbon comparing with gold enhanced the differences between both approaches.

The better results obtained for Zn-mediated method can be due to the more controllable grafting which results in a thinner and more organised platform for attaching biomolecules. The less compact surface, in comparison with the electrografted surface, favours the electronic transferring from solution to the transducer. This also can be a justification of the increment of current on gold and carbon when the same concentrations are detected using surfaces modified by Zn-mediated grafting tethered DNA.

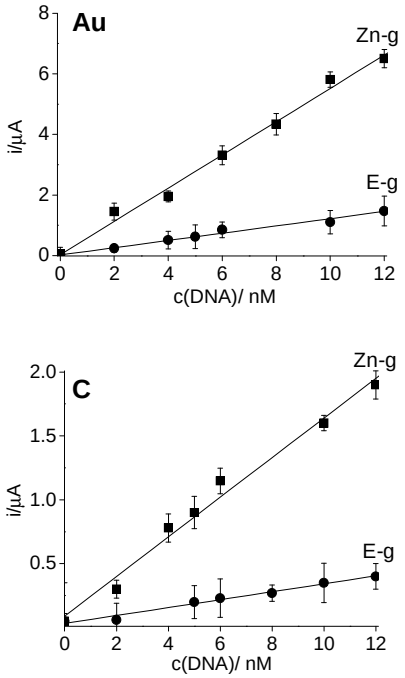

	Sensitivity (nA/nM)	LOD (nM)	non-specific signal (%)
Zn-g	550	0.5	4
E-g	115	1.2	10

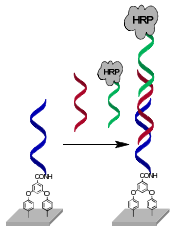

	Sensitivity (nA/nM)	LOD (nM)	non-specific signal (%)
Zn-g	151	0.9	7
E-g	25	1.4	15

Figure 6.3. Amperometric calibration curves for DNA detection using Zn mediated and electrochemical gold and carbon grafted surfaces.

6.5. CONCLUSIONS

The viability of using Zn mediated grafting for preparing DNA biosensing surfaces has been demonstrated for both carbon and gold surfaces. The potentiostat-free process is based on the reduction of diazonium salt by Zn, which combines the rapidness of electrografting and the simplicity of the spontaneous grafting in one single method. The usefulness of the method to improve the analytical performance of biosensors respect to the already reported methods has also been demonstrated.

6.6. REFERENCES

1. X. Luo and J. J. Davis, Chem. Soc. Rev., **2013**, 42, 5944.
2. Y. Liu, M. Luo, J. Yan, X. Xiang, X. Ji, G. Zhou, Z. He, Chem. Commun., **2013**, 49 7424.
3. N. Zhua, H. Gaoa, Q. Xua, Y. Linb, L. Sub, L. Mao, Biosens. Bioelectron., **2010**, 25, 1498.
4. a) A. Fragoso, N. Laboria, D. Latta, C. K. O'Sullivan, Anal. Chem. 80 (2008) 2556-2563. b) H. M. Nassef, M. C. Bermudo, P. J. Ciclitira, H. J. Ellis, A. Fragoso, C. K. O'Sullivan, Anal. Chem., **2008**, 80, 9265.
5. M. Nassef, L. Civit, A.Fragoso, C. K O'Sullivan, Anal. Chem. **2009**, 81, 5299.
6. P. R. Brasil de Oliveira Marques, A. Lermo, S. Campoy, H. Yamanaka, J. Barbé, S. Alegret, and M. I. Pividori, Anal. Chem., **2009**, 81, 1332.
7. D. M. Shewchuk and M.T. McDermott, Langmuir., **2009**, 25, 4556.
8. L. Civit, A. Fragoso and C. K. O'Sullivan, Electrochem. Commun., 2010, **12**, 1045.
9. W. R. Everett, T. L. Welch, L. Reed.and I. Fritsch-Fades, Anal. Chem., **1995**, 67, 292-298.
10. a) R. M. Lockett, M. L. Smith, Langmuir., **2009**, 25, 3340-3343.
11. M. Wang, M. R. Das, V. G. Praig, F. LeNormand, M. Li, R. Boukherroub, S. Szunerits, Chem. Commun., **2008**, 47, 6294-6296.
12. A. M. Debela, M. Ortiz, V. Beni, C. K. O'Sullivan, Chem. Eur. J., **2014**, 20, 7646-7654.
13. J. J. Gooding, Electroanal., **2008**, 6, 573-582.
14. D. Bélanger and J. Pinson, Chem Soc. Rev. ,**2011**, 40, 3995-4048.
15. J. Pinson, Wiley-VCH Verlag, Germany, **2012**, pp. 1–35.

16. R. T. Sanderson, Polar Covalence, Academic Press, New York, **1983**, Chapter 6.

17. A. Mesnage, X. Lefevre, P. Jégou, G. Deniau and S. Palacin, Langmuir., **2012**, 28, 11767-11778.

18. Z.-L. Cheng, R. Skouta, H. Vazquez, J. R. Widawsky, S. Schneebeli, W. Chen, M. S. Hybertsen, R. Breslow, L. Venkataraman, Nat. Nanotech., **2011**, 6, 353-357.

19. A. Girarda, F. Geneste, N. Coulona, C. Cardinaud, T. Mohammed-Brahim, Appl Surf Sci., **2013**, 282, 146-155.

20. S. Abdellaoui, B. C. Corgier, C. A. Mandon, B. Doumèche,C. A. Marquette and L. J Blum, Electroanal., **2013**, 25, 671-684.

21. M. Torrens, M. Ortiz, A. P. F. Turner, V. Beni and C. K. O'Sullivan, Chem. Eur. J., **2014**, 20, DOI: 10.1002/chem.201405121.

22. A. B Steel, T. M. Herne, M. J. Tarlov, Anal. Chem., **1998**, 70, 4670-4677.

23. J. Wang, Sh. Zhang, Y. Zhang, Anal. Biochem., **2010**, 396, 304-309.

24. H-Z. Yu, Ch-Y. Luo, C.G. Sankar, D. Sen. Anal. Chem., **2003**, 75, 3902- 3907.

CHAPTER 7

ELECTROCHEMILUMINESCENT DNA SESOR BASED ON CONTROLLED Zn-MEDIATED GRAFTING OF DIAZONIUM PRECURSORS

(Submitted, 2014)

CHAPTER 7

ELECTROCHEMILUMINESCENT DNA SENSOR BASED ON CONTROLLED Zn-MEDIATED GRAFTING OF DIAZONIUM PRECURSORS

7.1 ABSTRACT

Controlled Zn mediated grafting of a thin layer of a diazonium salt was used to functionalise a carbon electrode with a ruthenium(II)-tris-bipyridine-labelled DNA for use as a capture probe in an electrochemiluminescent genosensor. Secondary reporter probe was labelled with a ferrocene molecule, and in the presence of single-stranded DNA target, a genocomplex formed, where the Fc-label effectively quenched the ECL of the signal emitted from the Ru-label. The optimum spacing of the labels for maximum sensitivity and minimum detection limit was optimised, and the signal reproducibility and stability of the platform was demonstrated.

7.2 INTRODUCTION

Electrochemiluminescence (ECL) is a detection technique that combines both electrochemical and photochemical processes. It has long garnered a plethora of attention because it incorporates the advantages of both methods for biomolecule detection, resulting in high sensitivity and versatility.[1,2] In ECL, high-energy electron-transfer reactions are carried out on electrodes via the application of a specific potential to generate excited states that emit light.[3,4] Exploiting potential provides a more selective source of excitation than afforded optically,[5] and also simplifies the instrumentation for the construction of portable devices[6,7] The use of ECL transduction has been reported for the detection of DNA[8] and proteins[9] immobilised on different substrates such as carbon,[10] gold[11] and indium-tin oxide[12] using diverse ECL-active species as labels.[13,14] To date, the most commonly used ECL detection method is based on the co-reactant mechanism[15,16] and the coordination compounds formed by Ruthenium (II) and pyridinic derivatives as chelates, either as a single molecule or in combination with nanostructures,[2,17] have been reported as preferable luminophores, using tripropylamine (TPA) as co-reactant.[18,19] In this system the same

applied potential is able to oxidise both, the $Ru(bpy)_3^{2+}$ (luminophore) and the TPA (co-reactant), producing strong oxidative species. From the reaction of these two species the excited state $Ru(bpy)_3^{2+*}$ is formed which emits light.[20] ECL "on/off" strategies have recently been reported for clinical analytes[21] using immuno[22] and DNA[23] detection, where ferrocene derivatives are used to quench the ruthenium complex signal ("off"), as it has good quenching efficiency and stability in different chemical media.[1,24-26] Whilst ECL is a very sensitive method[27] one of its' limitations is the high potentials required to excite the active centre and this is particularly critical in the case of surface-immobilised ECL strategies. In order to solve this, a strong and stable covalent bond able to support the high applied potentials is required. The platforms based on diazonium derivatives immobilised on gold or carbon surfaces have been demonstrated to to be stable at the potential used in ECL detection.[28, 29]

In the present work an ECL genosensor for the detection of a *Francisella tularensis* DNA target was developed. The *Francisella* subspecies *tularensis* is one of the causative agents of the disease tularemia,[30] and current methods for the detection of the presence of this bacteria involves time-consuming culturing of suspect pathogens [31] or, alternatively, the detection of antibodies, which cannot be achieved until at least two weeks following infection.[32] These drawbacks render rapid DNA detection an attractive strategy and to this end, detection of the subspecies *tularensis* is the use of the specific sequences of tul4,[33] which was used as a model target for the present study.

7.3 EXPERIMENTAL SECTION

Materials

All reagents are commercially available and were used as received. Ruthenium (II) tris-bipyridine N-hydroxysuccinimide, N-ethyl-N`-(3-dimethylaminopropyl) carbodiimide hydrochloride (EDC), *N*-Hydroxysuccinimide (NHS), streptavidin, $NaH_2PO_4.H_2O$, Na_2HPO_4, 4-morpholineethanesulfonic acid hydrate (MES), 3-hydroxypicolinic acid (HPA), strontium nitrate, potassium ferricyanide (III), potassium ferrocyanide (II) and tetramethylbenzidine (TMB) liquid substrate system were purchased from Sigma-Aldrich (Barcelona, Spain). The sulphuric acid was purchased from Scharlau (Barcelona, Spain) and dimethyl sulfoxide from Abcam plc. The Sephadex G-25 size exclusion column were

received from Pierce, the magnetic beads from SIMAG and the 3,5-bis(4-aminophenoxy) benzoic acid was received from TCI. All solutions were prepared with Milli-Q water (18 MΩ.cm/ Millipore Inc.). All HPLC-grade oligonucleotides were provided by Biomers.net (Ulm, Germany). The sequences used in this work are listed below:

DNA model system designed for analysing the effect of the separation between the luminescent Ruthenium (II) tris-bipyridine (Rubpy) group attached to DNA and the quencher ferrocene (Fc) linked to the secondary probe

Probe for preparing the Rubpy-DNA: 5'- TGG GCG TTA AA CGT GAC A-3`-NH_2

Secondary probe: Fc-5'-ACC GAG ACG AAT AGG TAT-3'

Targets containing spacer T (n: 0,1,2,3,4,5 and 6):

5´-ATA CCT ATT CGT CTC GGT $(T)_n$ TGT CAC GTT TAA CGC CCA-3`

Francisella tularensis DNA model system

Target: 5'-ATT ACA ATG GCA GGC TCC AGA AGG TTC TAA GTG CCA TGA TAC AAG CTT CCC AAT TAC TAA GTA TGC TGA GAA GAA CGA TAA AAC TTG GGC A-3'

Capture probe: Biotin-TEG-5'-CTT AGT AAT TGG GAA GCT TGT ATC ATG GCA CTT AGA A-3'

Probe for preparing the Rubpy-DNA: (same capture probe + NH_2 in 3`- position)

HRP-labeled secondary probe: 5'-TTC TGG AGC CTG CCA TTG TAA T-3'-HRP

Fc-labeled secondary probe: Fc-5'-TTC TGG AGC CTG CCA TTG TAA T-3`

Instrumentation and methods

Optical instrumentation

UV–Vis spectra were recorded in a temperature controlled Cary 100 Bio spectrophotometer (Varian) in 1 cm quartz cells. Plate optical densities were recorded in a Wallac Victor2 1420 Multilabel counter from Perkin Elmer. The fluorescence experiments were performed in a Cary Eclipse spectrofluorimeter. The excitation wavelength was set at 460 nm. The

fluorescence spectra were recorded in the wavelength interval of 540-700 nm with excitation and emission slits of 10 nm and a scan rate of 240 nm/min.

All experiments were carried out in triplicate and the average value was used.

Electrochemical and electrochemiluminescence instrumentation

Electrochemical (EC) measurements were performed on a PC controlled PGSTAT12 Autolab potentiostat (EcoChemie, The Netherlands). The electrochemiluminescence (ECL) experiments were carried out using a device assembled at Institut für Mikrotechnik Mainz GmbH (IMM), Germany. The ECL equipment contains a photomultiplier (Hamamatsu H10682-01) connected to a potentiostat manufactured by PALM INSTRUMENTS BV to supply the voltage to the working electrode. Screen printed carbon electrodes configuration (DRP-110): working electrode: carbon disk (φ = 4 mm), reference electrode: silver, counter electrode: carbon, were used in both EC and ECL experiments. The carbon electrodes were activated by cycling 3 times from 0 to -1.2 V in 0.5 M KOH at of 50 mV/s scan rate. The quality of the cleaning step was checked using cyclic voltammetry in 1 mM of $K_4[Fe(CN)_6]$ /$K_3[Fe(CN)_6]$ + 50 mM of $Sn(NO_3)_2$ as supporting electrolyte. The CV was recorded from -0.2 to 0.4 V at 100 mV/s.

MALDI-TOF analysis of the DNA conjugates

The analysis of the conjugates were carried out in an Applied Biosystems Voyager STR MALDI-TOF spectrometer. Samples were prepared using 3-hydroxypicolinic acid in 50:50 (v/v) acetonitrile/water buffered with 0.05 M diammonium acetate as matrix. Linear positive mode was used for detection.

Synthesis of the conjugates Rubpy-DNA

Ruthenium (II) tris-bipyridine N-hydroxysuccinimide was previously dissolved in DMSO and then water was slowly dropped for avoiding precipitation (important: % (v:v) of DMSO respect the final volume of water was less than 10 %). Then Rubpy solution was mixed with a 25 μM solution of biotin-TEG-DNA-NH_2 probe in PBS (pH=7.8) in a 1:8 DNA:Rubpy molar ratio. The reaction was carried out by shaking at room temperature. Since the Rubpy is very sensitive to light, the conjugation was carried out in light shielded containers. After 1 hour, the product obtained was purified using NAP G-25 size exclusion

column DNA quality to separate the uncoupled Rubpy. This step was achieved following the step 7 of the procedure *MSD® TAG-NHS-Ester, MSD Labeling method*. The column was pre-equilibrated with PBS and the absorbance of the fractions obtained was measured. Finally the non-labeled DNA was isolated from the conjugate using carboxyl magnetic beads. 500 μL of the particles were washed with 1 mL of MES two times and the carboxyl groups were activated adding EDC and NHS at 80 and 40 mg/mL respectively during 20 minutes. The activated particles were separated using magnet and washed with PBS. Then the DNA conjugate were mixed with the magnetic beads and shaken during 2 hours. The beads containing the non-labeled DNA were separated by magnet and the supernatant was characterised by mass spectroscopy and UV-Vis.

TGG GCG TTA AAC GTG ACA-Rubpy m/z = 6370.69

Biotin-TEG-CTT AGT AAT TGG GAA GCT TGT ATC ATG GCA CTT AGA A-NH-Rubpy m/z = 12815.74

UV-Vis spectra were very similar for both conjugates: 260 nm (DNA band) and also the characteristic bands of Rubpy MLCT at 460 nm and the $\pi \rightarrow \pi^*$ ligand charge transfer transition at 277 nm.

Optimisation of Rubpy-DNA and quencher distance in fluorescence and ECL detection

The fluorescence spectrum of Rubpy-DNA dissolved in PB buffer with 0.8 M NaCl was recorded (λ_{exc} = 460 nm) at 25 ºC. In order to elucidate the optimum quencher distance, targets containing spacer (from 0 to 6 bases) with consecutive numbers of bases were incubated with Rubpy-DNA during 1 hour at 25 ºC in light shielded fluorescence cell (on carbon electrode). Finally, Fc-DNA was added and the same reaction conditions than for target hybridisation were used. In all the steps the molar ratio was 1:1:1. Control experiment was performed by mixing Fc-DNA and Rubpy-DNA in molar ratio 1:1, without target. The ECL study was carried out using the same system described for fluorescence. A potential pulse of +1 V was applied for 5 s and 100 mM TPA as coreactant in PBS pH 7.8.

ELONA study to optimise the pH evaluate the non-specific interaction between probes

Streptavidin Coated Plates were washed three times with 100 µL of PBS. Secondly, biotin-TEG-DNA (40 nM in PBS buffer pH 7.4) was immobilised on streptavidin coated plate during 30 min. After washing, the target (10 nM) was added and incubated during 1 hour. Then the secondary HRP-DNA probe (10 nM) was incubated for 1 hour. Subsequently, to elucidate the optimum working pH, different solutions of 100 mM TPA in PBS at pH from 7 to 12 were incubated in different strips. After each immobilisation step, the wells were three times washed with 100 µL of PBS. Finally after adding TMB as substrate, the absorbance was measured.

ELONA study to evaluate the non-specific interaction between probes

Streptavidin Coated Plates were washed three times with 100 µL of PBS. Then biotin-TEG-DNA (40 nM in PBS at pH 7.4) was immobilised on streptavidin coated plate during 30 min. After washing, the target was added at different concentrations (0, 5, 25, 45, 100 nM) and incubated during 1 hour. The secondary DNA probe labeled with HRP (10, 40, 100 nM) was added at different concentrations. After each immobilisation step, the wells were three times washed with 100 µL of PBS. Finally after adding TMB as substrate, the absorbance was measured.

ECL detection in solution

Protected from light, DNA target and Rubpy-DNA were pre-incubated for 1 hour at 25 ºC and then a solution of Fc-DNA was added and mixed during 1 hour more. The DNA sandwich system was prepared in 0.5:0.15:0.5 and 0.5:0.5:0.5 µM (Rubpy-DNA:target:Fc-DNA) in PB + 0.8 M NaCl. ECL measurements were carried out before and after mixing with Fc-DNA. In addition, the ECL signal of Rubpy-DNA, Fc-DNA and 100 mM TPA in 0.1 M of PB at pH 7.8 used for experiment were recorded as controls.

Preparation of the surface for ECL measurements

The details of the synthesis of 3,5-bis(4-diazophenoxy) benzoic acid tetrafluoroborate and its immobilisation on carbon electrodes via Zn-mediated grafting were reported in previous work.[29]

After activation of the carboxylate group of the diazonium salt-coated surface using 20 µL

EDC/NHS (2:1 molar ratio), 1 µM streptavidin; was linked via amide bond formation. Then, after washing, the biotin-Rubpy-DNA capture probe at 1 µM, previously dissolved in PBS buffer at pH 7.4 was immobilised on the modified carbon surfaces during 1 hour at 25 ºC. After rinsing the electrode, ECL signal was recorded using the same parameters described above. The measurement was recorded 10 times to check the reproducibility of the signal

Differential Pulse Voltammetry (DPV) to check the presence of Rubpy and ferrocene linked to DNA probe and secondary probe respectively on the sandwich after detection

After the modification of the electrode with Rubpy-DNA, a DPV was recorded in 0.1 M PB pH 7.4, at potential range from 0.1 to 1.1 V and the scan rate was 50 mV/s. Consequently the target and secondary Fc-DNA was hybridised and once more DPV was recorded but in the potential range from 0.1 to 0.4 V to detect the ferrocene on surface. In the absence of target, the signal from ferrocene was not observed as expected.

Calibration curve for DNA detection

After the immobilisation of the Rubpy-DNA capture probe to the surface following the same procedure mentioned in session 3.7, the target sequence (0; 0.1; 0.5; 0.7; 0.8; 1; 2; 3; 4; 5 nM) was dissolved in PBS buffer (pH 7.4 + 0.8 M NaCl) and hybridised to the capture element during 1 hour. Finally the secondary Fc-DNA probe was hybridised to the target in a molar ratio 1:1 respect the Rubpy-DNA and the detection was carried out using the same parameters described in section 3.2.

7.4 RESULTS AND DISCUSSION

In the work reported here, an “on/off” approach was developed based on a sandwich type detection of DNA by using two DNA sequences complementary to almost consecutive regions of the DNA target: a capture DNA probe labeled with ruthenium (II) tris-bipyridine (Rubpy), and a secondary DNA reporter probe labeled. In the presence of single stranded target DNA, the probes hybridise to their complementary sequences on the target, bringing them into close proximity, permitting energy transfer and thus facilitating the quenching effect of the ferrocene on the Ru(bpy) signal. This on/off sandwich approach also increases the specificity as two regions of the target hybridise with two different probes. The system

was optimised in solution-phase and then, using the optimised experimental conditions, a solid-phase system exploiting stable diazonium grafting was explored .[29]

Firstly, a model system based on short sequences, specifically designed not to have self-complementarity leading to secondary structures, was used to study the effect of the separation between the luminescent Rubpy and the quencher ferrocene (**Figure 7.1**). Rubpy was linked to DNA via amide bond formation between the activated carboxylic group of a Rubpy derivative and aminated DNA, and the bioconjugate was purified using column chromatography. It was then evaluated using UV-Vis at 260 nm to detect DNA and at 460 nm to measure the characteristic bands of Rubpy MLCT, as well as at 277 nm

to measure the the $\pi \rightarrow \pi^*$ ligand charge transfer transition, which appears 10 nm shifted to blue respect to the starting Rubpy. Additionally, the expected m/z = 12815.74 of the bioconjugate was observed using MALDI-TOF.

Rubpy-DNA and Fc-DNA were added in 1:1 molar ratio to target DNA sequences that separate them by 0 to 6 bases, and the genocomplex incubated protected from light. A control was carried out in the absence of any target DNA and no quenching was observed. The same procedure was followed to study the system using fluorescence detection and the results were compared considering the control response as a 100% signal (**Figure 7.1**).

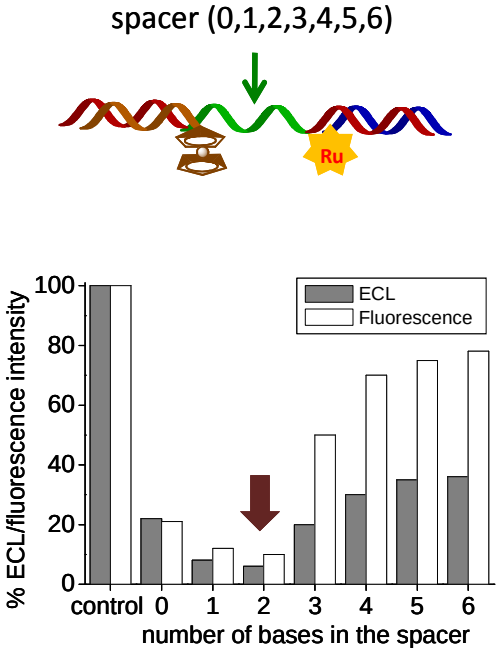

Figure 7.1. ECL (grey) and fluorescence (white) study of the effect of the distance on the quenching of the luminescent $Ru(bpy)_3^{2+}$ group.

Comparing both methods, two bases in the spacer of target was found as the optimum compromise between the proximity (needed for energy transfer) and the steric hindrance (which could affect the hybridisation of strands) to obtain the highest quenching effect, giving a decrease in signal of 85% and 95% for ECL and fluorescence, respectively (**Figure 7.1**). It should be noted that the concentration of the probes used for ECL analysis was four orders of magnitude lower than in case of fluorescence analysis, highlighting the increased sensitivity achievable using ECL detection. Once the spacing of Fc to Rubpy labels had been optimised, the target system of *Francisella tularensis* was studied. Any potential cross-reactivity between the two probes to be used was evaluated and no interaction was observed (**Figure SI 7.2a**). The pH for maximal ECL (basic)[34] whilst not inhibiting hybridisation was evaluated by immobilising the capture probe on a streptavidin plate and the secondary probe labeled with HRP was used for detection by colorimetric enzyme-linked oligonucleotide assay, and pH 7.8 was chosen as an optimum compromise between efficient DNA hybridisation and TPA deprotonation[12]. Finally, using optimised conditions of two base spacing between labels and a pH of 7.8, a 22-mer-Fc-DNA probe and a 37-mer-Rubpy probe were hybridised with 91-mer-*Francisella tularensis* target in solution phase as a proof-of-concept with a real system. The evaluation was carried out using two concentrations of target DNA (0.15 and 0.5 μM). The controls of Rubpy-DNA and Fc-DNA in the absence of DNA target were observed, as expected, to be maximal and minimal, respectively. When DNA target was introduced in a quantity of 0.5: 0.15: 0.5 μM, a notable quenching of about 60 % was observed, and when the concentration of DNA target was increased, the ECL signal was further reduced, indicating that the quenching effect is proportional to the target concentration.

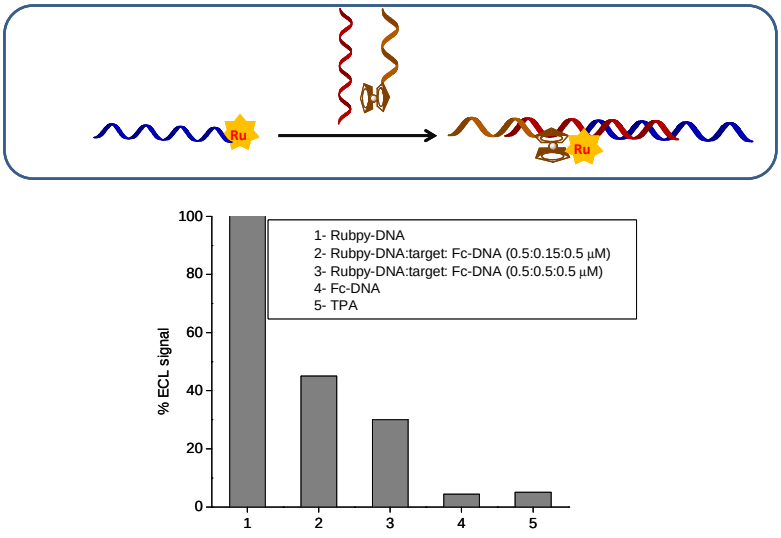

Figure 7.2. ECL study of system Rubpy-DNA/target/Fc-DNA in solution and using TPA as co-reactant (Column 2 and 3). Controls: Rubpy-DNA, Fc- DNA or TPA alone (Column 1, 4, 5). All signals were referenced with respect to the initial Rubpy-DNA ECL signal.

Having demonstrated a proof-of-concept in the homogenous solution phase, the possibility of transferring the system to an immobilised, heterogenous phase was pursued. This is highly attractive in terms of simplicity and potentially increased sensitivity and multiplexing capability. However, it is known that thiolated DNA desorbs from gold electrodes at potentials of > ca. 1V vs Ag/AgCl, and thus grafting of a bipodal diazonium salt on carbon electrodes was exploited. This diazonium salt 3,5-bis(4-diazophenoxy)benzoic acid tetrafluoroborate (DCOOH) has recently been demonstrated to be stable at high positive potential due to the formation of covalent bonds with carbon. Furthermore the immobilisation strategy involves a simple 5-minute Zn-mediated grafting without the necessity of using a potentiostat resulting in an almost monolayer formation due to a lack of radicals.[29]

In the approach studied here this organic platform was linked to streptavidin and used to anchor the labeled biotin- Rubpy-DNA capture probe. Stability of immobilisation was tested by applying a potential of +1 V vs Ag/AgCl The stability and reproducibility of the signal was recorded and remained unaffected during at least ten cycles of application of potential (SD 3%) (**Figure 7.3a**, inset).

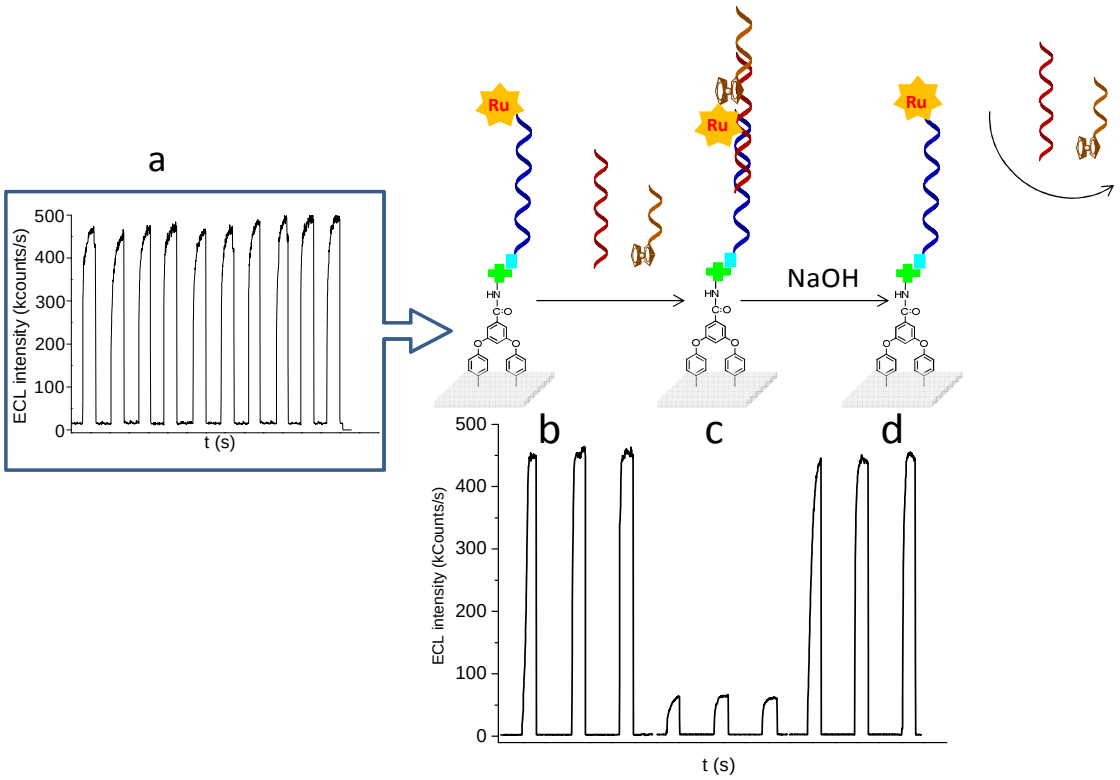

Figure 7.3. a) The ECL signal from carbon modified Rubpy-DNA for ten consecutive pulses of potential application. b) Initial ECL signal from immobilised Rubpy-DNA, c) Following hybridisation with target DNA and Fc-DNA and d) Following denaturation of genocomplex with 0.1 M NaOH. ECL conditions: potential pulse of +1 V during 5 s and 100 mM TPA in PB pH 7.8

Figure 7.3 shows the switch on/off process used for detection of DNA target. Firstly, the baseline ECL signal from the immobilised Rubpy-DNA was recorded (**Figure 7.3b**) and then following addition of target DNA and the reporter Fc-DNA probe (**Figure 7.3c**). To demonstrate that the quenching of the Rubpy signal is due to the effect of ferrocene and not due to damage to platform, alkaline conditions were used to denature the genocomplex and reverting to the Rubpy-DNA probe. The ECL signal was successfully recovered (**Figure 7.3d**), clearly demonstrating the quenching effect of ferrocene as well as the possibility to re-use the platform for repeated measurements of target DNA. The presence of the Rubpy and ferrocene labeled probes was further demonstrated by recording the differential pulse voltammograms (**Figure 7.4a** and **b**). The significant difference in current intensity between Rubpy and ferrocene can be attributed to the dependence of the amount of

ferrocene present on the target DNA concentration, whilst a monolayer of the immobilised labelled DNA probe would result in a higher amount of Rubpy being present. The surface confinement of the ferrocene group was also confirmed using cyclic voltammetry by obtaining a linear behavior of cathodic and anodic peak currents *vs*. scan rate (**Figure 7.4c**.).

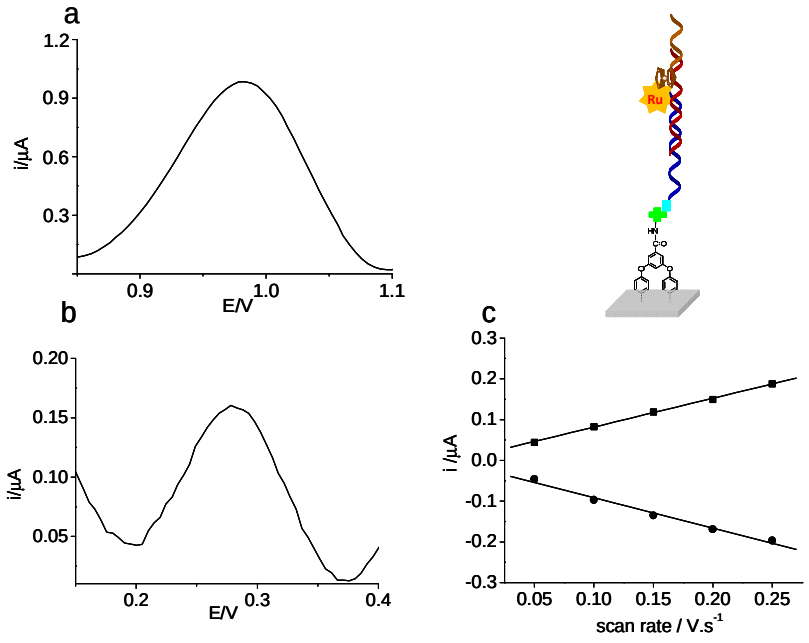

Figure 7.4. Evidence of the presence of Rubpy (a) and ferrocene (b) in the system (DCOOH/streptavidin/ Rubpy-DNA /target/ Fc-DNA) on carbon surface. c): Dependence of peak current with scan rate of immobilised Fc-DNA.

Finally, this platform was tested to quantitatively detect the *Francisella tularensis* target DNA. A calibration curve was constructed with different target concentrations (**Figure 7.5**) using the optimised experimental parameters. As can be seen in **Figure 7.5**, the quenching of the signal was proportional to the concentration of the DNA target in the range from 0 to 1 nM with a limit of detection of 0.1 nM.

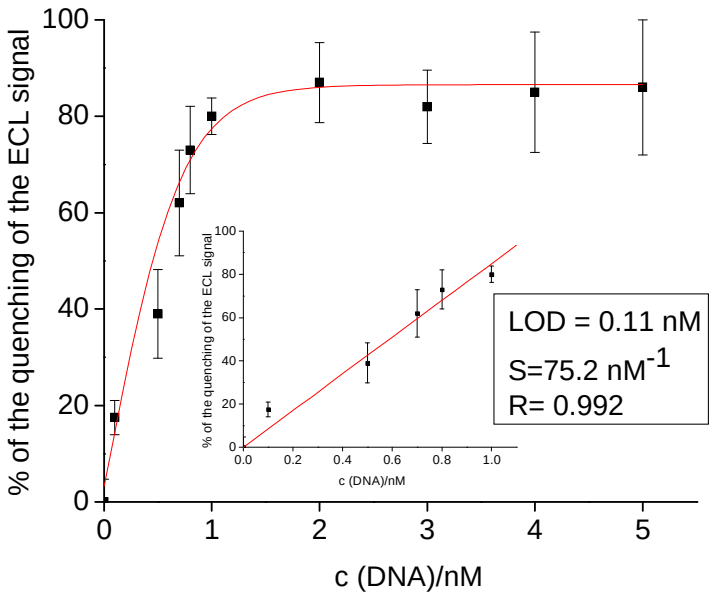

Figure 7.5. Calibration curve for DNA target detection based on the percentage of Rubpy ECL signal following quenching by the Fc-DNA via target DNA hybridisation. Inset: Linear range from 0 to 1.0 nM of target. ECL conditions: potential pulse of +1 V for 5 s and 100 mM TPA in PB pH 7.8

7.5 CONCLUSIONS

A platform based on the Zn-mediated immobilised 3,5-bis(4-diazophenoxy)benzoic acid tetrafluoroborate (DCOOH) to demonstrated to be efficient for the surface confinement of capture Rubpy labeled DNA probe and its subsequent use for DNA target detection by ECL quenching by a Fc-labeled reporter probe. As a result of the robustness of the thin layer of covalent linker, a stable and reproducible ECL signal from Rubpy-DNA was recorded during ten cycles after applying + 1 V. Experimental parameters were optimised and a subnanomolar concentration of DNA target was achieved.

7.6 REFERENCES

1. L. Meng, Y. Hongmei, M. Chao, Z. Yan, G. Shenguang, Y. Jinghua, Y. Mei, Sens. Actuators B: Chem., **2014,** 191, 377.

2. H. Wang, G. Xu, S. Dong, Anal. Chim. Acta, **2003**, 480, 285.

3. M. M. Richter, Chem. Rev., **2004**, 104, 3003.

4. Electrogenerated Chemiluminescence. Edited by A. J. Bard. Copyright, **2004** by Marcel Dekker, Inc. Introduction, A. J. Bard.

5. L. Hu and G. Xu, Chem. Soc. Rev., **2010**, 39, 3275.

6. N. Hao, M. Xiong , J. D. Zhang, J. J. Xu, H. Y. Chen, Anal. Chem., **2013**, 85, 11715.

7. W. J. Cao, X. Liu, E. Yang, E. Wang, Electrophoresis, **2002**, 23, 3683.

8. M. S. Wu, L. J. He, J.-J.Xu, and H.-Y. Chen, Anal. Chem., **2014**, 86, 4559.

9. Y. He, Y. Chai, R. Yuan, H. Wang, L. Bai, N. Liao, Analyst, **2014**, 139, 5209.

10. J. Wang, Y. Shan, W. W. Zhao, J. J. Xu, H. Y. Chen, Anal. Chem., **2011**, 83, 4004.

11. H. F. Zhao, R. P. Liang, J. W. Wang, J. D. Qiu, Biosens. Bioelectron., **2014**, 63, 458.

12. Y. Chen, B. Qiu, Y. Jiang, Z. Lin, J. Sun, L. Zhang, G. Chen, Electrochem. Comm., **2009**, 11, 2093.

13. C. Yuanyuan, T. Yifeng, Electrochim. Acta, **2014**, 135, 187.

14. L. Liu, Q. Ma , Y. Li, Z. Liu, X. Su, Biosens. Bioelectron, **2014**, 63, 519.

15. Y. He, Y. Chai, R. Yuan, H. Wang, L. Bai, Y. Cao, Y. Yuan, Biosens. Bioelectron., **2013**, 50, 294.

16. W. Gu, Y. Xu, B. Lou, Z. Lyu, E. Wang, Electrochem. Comm., **2014**, 38, 57.

17. Q. Sun, G. Zou, X. Zhang, Electroanalysis, **2011**, 23, 2693.

18. X. B. Yin, S. Dong, E. Wang, Trends in Anal. Chem., **2004**, 23, 432.

19. X. Zhou, D. Zhu, Y. Liao, W. G. Liu, H. Liu, Z. Ma and D. Xing, Nature Protocols, **2014**, 9,1146.

20. M. Su, S. Liu, Anal. Biochem., **2010**, 402, 1.

21. W. Gao, A. Zhang, Y. Chen, Z. Chen, Y. Chen, F. Lu, Z. Chen, Biosens. Bioelectron., **2013**, 49, 139.

22. M. Zhang, S. Ge, W. Li, M. Yan, X. Song, J. Yu, W. Xua and J. Huang, Analyst, **2012**, 137, 680.

23. W. Yao, L. Wang , H. Wang, L. Li, N. Zhangb, L. Pan, N. Xing, Biosens. Bioelectron., **2013**, 40, 356.

24. W. Cao, J. P. Ferrance, J. Demas, J. P. Landers, J. Am. Chem. Soc., **2006**, 128, 7572.

25. L. Chen, Q. Cai, F. Luo, X. Chen, X. Zhu, B. Qiu, Z. Lin and G. Chen, Chem.Comm., **2010**, 46, 7751.

26. Y. Liao, R. Yuan, Y. Chai, L. Mao, Y. Zhuo, Y. Yuan, L. Bai, S. Yuan, Sens. Actuators B: Chem., **2001**, 158, 393.

27. H. Wei and E. Wang, Luminescence, **2011**, 26, 77.

28. D. J. E. Piper, G. J. Barbante, N. Brack, P. J. Pigram, C. F. Hogan. Langmuir, **2011**, 27, 474.

29. M. Torréns, M. Ortiz, A. P. F. Turner, V. Beni and C. K. O'Sullivan, Chem. Eur. J.l, **2014**. 20, 1-12 DOI: 10.1002/chem.201405121.

30. R. M. Jones, M. Nicas, A. Hubbard, M. D. Sylvester and A. Reingold, Applied Biosafety, **2005**, 10, 227.

31. X. Haristoy, A. Lozniewski, C. Tram, D. Simeon, L. Bevanger and C. Lion, Journal of Clinical Cicrobiology, **2003**, 41, 2774.

32. H. E. Carlsson, A. A. Lindberg, G. Lindberg, B. Hederstedt, K. A. Karlsson and B. O. Agell, Journal of Clinical Microbiology,**1979**, 10, 615.

33. B. Celebi, S. Kilic, M. Yesilyurt, B. Acar, MikrobiyolojiBulteni, **2014**, 48, 135.

34. W. Gao, X. H. Xia, J. J. Xu and H. Y. Chen, J. Phys. Chem. C, **2007**, 33, 12213.

7.7 SUPPORTING INFORMATION

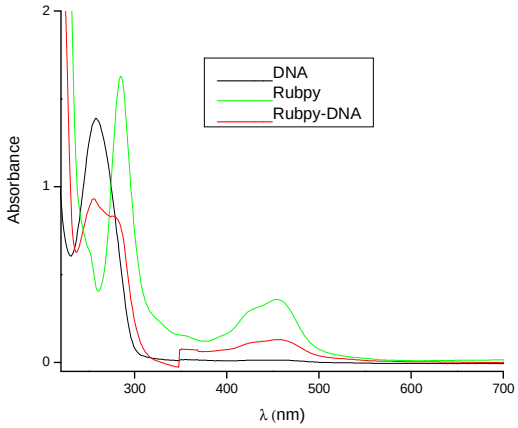

Figure SI 7.1. UV-vis spectra of DNA (black), Rubpy (green) and Rubpy-DNA (red). The spectra were registered in water in a quartz cell.

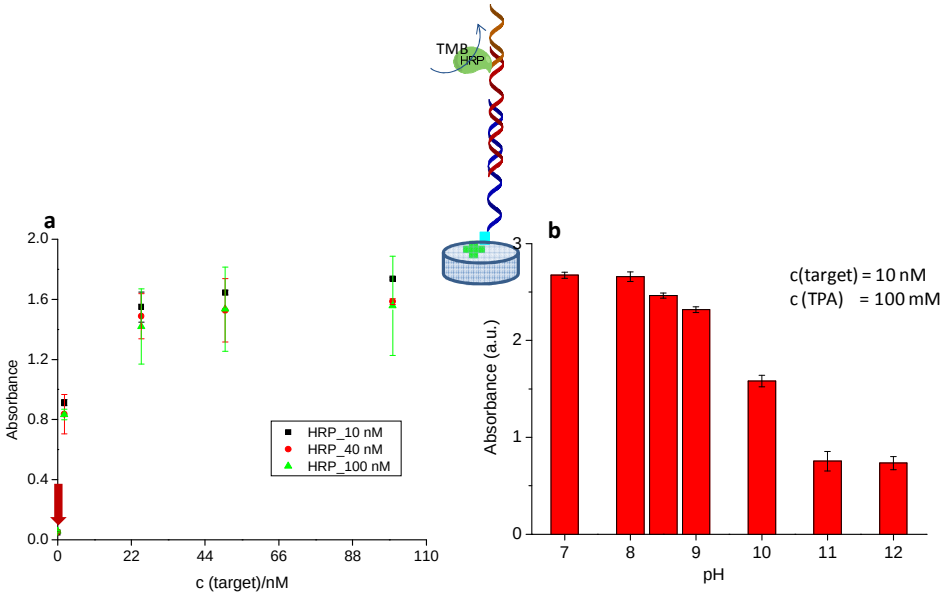

Figure SI 7.2. ELONA studies to evaluate: (a) the non-specific interaction between the surface tethered and labelled reporter probe and (b) evaluation of optimum pH for ECL detection without affecting the hybridisation between DNA sequences.

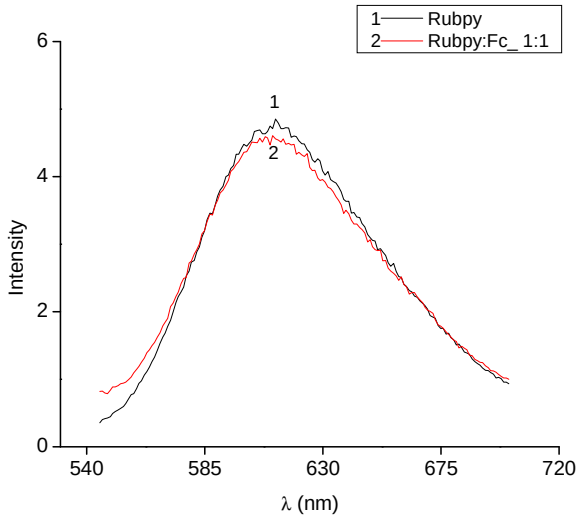

Figure SI 7.3. Fluorescence study of interaction between fluorophore Rubpy and quencher Fc-NH_2 in solution. λ_{exc} = 460 nm, E_{xc}/ E_m slit = 10 nm.

GENERAL CONCLUSIONS AND FUTURE WORK.

GENERAL CONCLUSIONS

The feasibility of applying the host-guest interactions for building supramolecular platforms to create versatile platforms with biosensor purposes has been demonstrated along the Chapters 2-4. These platforms were based on bifunctionalised carboxymethylcellulose (CMC) polymer backbone bearing adamantane/ferrocene units and a DNA probe on a cyclodextrin surface linked to the gold surface. In these approaches, the presences of CMC backbone allowed the improvement in the spatial orientation of the DNA probes on the surface and decrease the non-specific interactions.

In Chapter 2, the applicability of supramolecular host–guest interactions in the development of colorimetric DNA tests based on the self-assembly of bifunctionalised CMC polymers on cyclodextrin-modified microtitre plates was demonstrated. A real PCR amplified sample of a celiac patient, demonstrated to carry the HLA-DQA1*0201 allele using Luminex-based HLA typing, was tested using the supramolecularly coated plates and compared with the thiolated probe-coated plates. The results obtained using supramolecular plates were in subnanomolar ranges and lower than those obtained using a thiolated DNA capture probe, clearly demonstrating that the supramolecular chemistry is not affected by the sample matrix and does not need to be pre-treated.

In Chapter 3, the platform based on the self-assembly of bi-functionalized polymer bearing adamantane and DNA onto cyclodextrin surface was successfully tested in an amperometric genosensor Using this platform an excellent LOD of 0.08 nM as well as high selectivity were achieved. It was also applied to the detection of DNA in a real patient's sample.

In Chapter 4, a novel route for the immobilisation of electron transfer mediators on electrode surfaces based on the interfacial complexation of a polymer backbone bearing ferrocene units on a cyclodextrin surface was successfully established. This strategy only requires the addition of an enzyme substrate and could be an attractive alternative to the development of packaged genosensors avoiding the use of unstable redox mediators. The confinement of the ferrocene (mediator) to the electrode surface greatly decreased the detection limits attained with respect to a similar supramolecular system based on electrochemically inactive adamantane/CD inclusion complexes and requiring addition of the mediator in solution.

- For both supramolecular systems and in both colorimetric and amperometric detection techniques the combination of a hydrophilic support layer (βCDPSH) with the controlled

attachment of the capture probe to a polymeric backbone minimises non-specific interactions and provides an optimal probe separation to avoid electrostatic repulsions, which is essential in the development of DNA biosensors. The CMC backbone allows an optimal spacing of the DNA probes to avoid steric hindrance for target binding due to an excessively dense layer of probe DNA, with the negative charge of the CMC vertically orienting the probe, and the combination of the CD and the CMC facilitate maximal binding of the target DNA.

The second alternative of surface modification studied was based on a covalent organic linker to expand the frontier of the surface functionalisation from the gently potential window techniques like amperometry to a harsh electrochemiluminiscence, where extreme potentials could be applied.

In Chapter 5, a new approach based on Zn-mediated grafting of a bipodal diazonium salt (3,5-bis(4-diazophenoxy)benzoic acid tetrafluoroborate (DCOOH)) was developed. This strategy successfully combines the principal advantage of potentiostat-free spontaneous grafting with the rapidness of electrografting. In this method, by exploiting zinc as a reducing agent for the formation of aryl radicals, the grafting in few minutes of a very thin organic layer with no instrumentation required was accomplished. The surface was characterised by Raman, XPS, AFM and voltammetric techniques. The feasibility of linking a ferrocene derivative was demonstrated using cyclic voltammetry and XPS. This work opened the doors for the applicability of this surface on biosensors, which were demonstrated in the following chapters.

In Chapter 6 the efficiency of Zn-mediated grafted diazonium salt surfaces for tethering DNA in both gold and carbon substrates was demonstrated. Higher sensitivity and lower limit of detection were achieved when these surfaces were used for detecting a *Francisella tularensis* DNA target in comparison with those prepared by traditional electrografting. The systems were studied by surface plasmon resonance, choronocoulometry and AFM. It is important to remark that although similar amounts of small ferrocene molecules were linked to the surfaces modified for both methods; in the case of large DNA molecule the case is different. Probably, the DNA is more dependent on the effect of thinner organic layer grafted our approach, which achieves better organisation of the probe on surfaces leading the better results in amperometric measurements.

The robustness of diazonium grafted carbon surface demosntrated in Chapter 5, made posible to explore its applicability in electrochemiluminiscence in Chapter 7. The platform based on the Zn-mediated immobilised 3,5-bis(4-diazophenoxy)benzoic acid tetrafluoroborate (DCOOH) demonstrated to be efficient for the confinement of luminescent Rubpy labeled DNA probe and its subsequent use for DNA target detection by ECL. As a result of the robustness of this thin layer of covalent linker, a stable and reproducible ECL signal from Rubpy-DNA was recorded during ten cycles after applying +1 V vs Ag/AgCl. Finally, a subnanomolar concentration of DNA target was detected by the quenching of the fluorescent Rubpy by the ferrocene labeled DNA which can be in contact through the target DNA.

In summary, the approaches reported here, constitute alternatives to apply in the biosensors where the detection of biomolecules or pathogen are required with high sensitivity and low limit of detection.

FUTURE WORK

The present Thesis highlights the feasibility of using two types of platforms: cyclodextrin based supramolecular and diazonium grafted surface chemistries for the detection of DNA and the work will be extended to multiplexed, microsystem packaged, genosensor arrays with a focus on reducing hybridisation time and the number of PCR cycles required.